CO_2 Capture from Coal Fired Power Plants

Jostein Gabrielsen

2007

Ph.D. Thesis

TECHNICAL UNIVERSITY OF DENMARK
DEPARTMENT OF CHEMICAL ENGINEERING

CO_2 Capture from Coal Fired Power Plants

Ph.D. Thesis

by

Jostein Gabrielsen

2007

IVC-SEP

Department of Chemical Engineering

Technical University of Denmark

DK-2800 Kgs. Lyngby

Printed by Book Partner, Nørhaven Digital, Copenhagen, Denmark

ISBN 978-87-91435-46-3

Preface

The thesis is submitted in partial fulfillment of the requirements for the Ph.D. degree at the Technical University of Denmark (Danmarks Tekniske Universitet). The work has been carried out from May 2003 to October 2006 at the Department of Chemical Engineering (Institut for Kemiteknik) under the supervision of Associate Professor Georgios M. Kontogeorgis, Reader Michael L. Michelsen and Professor Erling H. Stenby. The project has been financed by Nordic Energy Research in the framework of the Nordic project: Nordic CO_2 Sequestration Project. The facilities for and financial support of the experimental part of the project was provided by the NTNU/SINTEF ENGAS research infrastructure.

I want to thank a group of people whom without this thesis would have been impossible:

I want to thank Georgios M. Kontogeorgis for the continuous support, valuable comments and suggestions and excellent guidance he has given me throughout my work on this thesis. Furthermore, I want to thank him for the enormous enthusiasm he has shown every time we have discussed something scientific, I hope some of it rubbed off on me. I am grateful to Michael L. Michelsen for putting his foot down at an early stage of the project and giving my work the direction it has, and for sharing his vast knowledge and insight in scientific questions through comments and suggestions to my work. It has been inspiring to work with both of you. I would like to thank Erling H. Stenby for giving me the opportunity to be a member of the IVC-SEP group, for bringing CO_2 capture on the agenda of the group and ensuring the industrial contact in the field of CO_2 capture.

I want to thank Professor Hallvard F. Svendsen at NTNU and the other members of the CO_2 capture group at NTNU/SINTEF for the good collaboration, interesting discussions and their willingness to share their vast knowledge in the field of CO_2 capture during period I spent there.

I want to thank my colleagues at IVC-SEP for all the good times and especially Georgios Folas for all the fruitful discussions and for being an excellent office mate (whenever he was present at the office).

I want to thank Associate Professor Ole Kristian Førrisdahl at Østfold University College for inspiring me to pursue further education after my bachelor's degree.

I want to thank my parents for always supporting me and backing me up no matter what I have decided to do with my life.

Louise thanks for helping me with the Danish Resumé, but most important thank you for everything. Without you I would never have gotten this far.

Jostein Gabrielsen

Summary

The purpose of this thesis is to contribute to the development of efficient carbon dioxide (CO_2) capture technology useful for coal fired power plants. This has been done through modeling, theoretical and experimental work.

After a short introduction, given in chapter 1, the thesis is divided into the following chapters:

Chapter 2 gives an introduction to different post combustion CO_2 capture technologies with an emphasis on reactive absorption using aqueous solutions of alkanolamines.

In chapter 3 a rate-based absorber model is developed and presented along with the theory needed to develop a model for reactive absorption in a packed column.

In chapter 4 a thermodynamic model capable of presenting the CO_2 solubility in aqueous solutions containing one alkanolamine (MEA, DEA, MDEA, AMP, Piperazine) and one mixture (Piperazine/MDEA) is presented. From the proposed model an expression for the heat of absorption of CO_2 in the same solutions is derived. The model is developed specifically to be valid under the conditions encountered during CO_2 capture from coal fired power plants.

In chapter 5 experimental data and calculated values of the rate constants for the reaction of CO_2 with AMP in an aqueous solution using a string of discs absorber are presented. Furthermore, experiments were carried out in order to define the mass-transfer area of the string of discs desorber.

In chapter 6 detailed experimental pilot plant data at 11 different process conditions are presented for a complete CO_2 absorption/desorption unit in an integrated laboratory pilot plant using an aqueous AMP solution. Temperature profiles over the absorber and desorber are included in the experimental data.

In chapter 7 validation of the proposed rate-based absorber model is carried out for CO_2 absorption using solutions of both MEA and AMP. This is done using both the experimental data presented in chapter 6 and experimental data found in the literature.

Chapter 8 presents the main conclusions from this work and suggestions for further investigations based on the work presented in this thesis are given.

Dansk Resumé

Formålet med denne afhandling er at bidrage til udviklingen af en effektiv CO_2 capture-teknologi, som kan bruges på kulfyrede kraftværker. For at opnå dette mål er der både udført teoretisk og eksperimentelt arbejde. Efter en kort introduktion i kapitel 1 er afhandlingen inddelt i følgende kapitler:

I kapitel 2 bliver forskellige CO_2 capture-teknologier, som kan bruges efter forbrænding, beskrevet med en hovedvægt på kemisk absorption i vandige alkanolaminopløsninger.

I kapitel 3 præsenteres en hastighedsbaseret model, som beskriver kemisk absorption af CO_2 i vandige alkanolaminopløsninger i fyldte kolonner. Derudover præsenteres teorien, der er nødvendig for at kunne udvikle den pågældende model.

I kapitel 4 præsenteres en model for opløseligheden af CO_2 i vandige opløsninger med en enkelt alkanolamin (MEA, DEA, MDEA, AMP eller Piperazine) og med en blanding (Piperazine/MDEA). Modellen er specielt udviklet med henblik på at kunne beskrive de pågældende opløsninger under forhold, som er relevante for CO_2 capture fra affaldsgasser fra kulfyrede kraftværker. Et udtryk for absorptionsvarmen for CO_2 i disse opløsninger er udledet fra opløselighedsmodellen, og de beregnede værdier er verificeret med eksperimentelle data fra litteraturen.

I kapitel 5 præsenteres eksperimentelle data og beregnede værdier af hastighedskonstanten for reaktionen mellem CO_2 og AMP i en vandig opløsning. Eksperimenterne er udført med en string of discs absorber. Der er også udført eksperimenter for at bestemme det effektive masseoverføringsareal for apparaturet.

I kapitel 6 præsenteres pilotanlægsstudier af CO_2 capture med en vandig AMP opløsning. Der rapporteres detaljerede eksperimentelle procesdata for 11 forskellige procestilstande både for absorber- og stripper delen. Der vises desuden temperaturprofiler for begge kolonner.

I kapitel 7 valideres den hastighedsbaserede absorptionskolonnemodel, som blev præsenteret i kapitel 3. Modellen valideres for vandige opløsninger af både MEA og AMP. Dette gøres ved hjælp af de eksperimentelle data, præsenteret i kapitel 6, og eksperimentelle data fra litteraturen.

I kapitel 8 gives slutteligt en kort præsentation af afhandlingens hovedkonklusioner sammen med foreløbige resultater/forslag, der kan betragtes som fremtidige udfordringer.

Contents

Nomenclature

a = specific wetted area for mass transfer, m^2 / m^3

a_0 = initial molefraction of amine

A_C = cross sectional area of the column, m^2

C_i^0 = concentration of i in the bulk liquid, mol/m^3

$C_{CO_2}^{inf}$ = concentration of molecular CO_2 at the liquid interphase, mol/m^3

$\hat{c}_p$ = mass based heat capacity of component i in the gas phase, $J/kg \cdot K$

$c_{p,i}$ = molar heat capacity of component i in the gas phase, $J/mol \cdot K$

$c_{p,L}$ = molar heat capacity of the liquid, $J/mol \cdot K$

$D_{i,L}$ = diffusivity of component i in the liquid, m^2/s

E = Enhancment factor

E_∞ = Enhancment factor for instantaneous reaction

G = molar gas flow, mol/s

h = heat transfer coefficient in gas, $J/s \cdot K \cdot m^2$

H_{CO_2} = Henry's Law Constant for CO_2, $Pa \cdot m^3/mol$

ΔH_{H_2O} = heat if condensation of H_2O, J/mol

ΔH_{CO_2} = heat if absorption of CO_2, J/mol CO_2

j_D = chilton-colburne j-factor for mass transfer, dimensionless

j_H = chilton-colburne j-factor for heat transfer, dimensionless

$k_{G,i}$ = gas-side mass-transfer coefficient of component i, $mol/m^2 \cdot s \cdot Pa$

$k_{L,i}$ = liquid-side mass-transfer coefficient of component i, m/s

$k_{L,i}^{chem}$ = liquid-side mass-transfer coefficient includinc chemical reaction of component i, m/s

k_2 = rate constant, $m^3/mol \cdot s$

$K_{G,i}$ = overall mass-transfer coefficient of component i, $mol/m^2 \cdot s \cdot Pa$

K_{CO_2} = combined Henry's law and chemical equilibrium constant for CO_2 partial pressure, kPa

L = molar liquid flow, mol/s

M = Dimensionless number used in the enhancment factor

N_i = Molar flux of component i, $mol/m^2 \cdot s$

p_i = partial pressure of component i in the bulk gas phase, Pa (kPa)

p_i^* = partial pressure of component i gas phase if it were in equilibrium with the liquid phase, Pa

q = heat flux, $J/m^2 \cdot s$

T_L = liquid phase temperature, K

T_G = gas phase temperature, K

x_i = liquid phase mole fraction of component i, mol/mol

X_{CO_2} = liquid phase mole fraction of CO_2 in both reacted and unreacted form, mol/mol

y_i = gas phase mole fraction of component *i*, mol/mol

z = height of packing, m

Greek Symbols

δ = film thickness, m

θ = loading, mole CO_2/mole initial amine

λ = Thermal conductivity $W/m \cdot K$

μ = viscosity, $Pa \cdot s$

ν_0 = kinematic viscosity, $m^2 \cdot s$

ρ = density, kg/m^3

1 Introduction

Numquam ponenda est pluralitas sine necessitate.
William Ockham (1495)

1.1 Motivation and Purpose of the Thesis

CO_2 capture from process streams is an established concept which has achieved industrial practice, but usually for applications on a much smaller scale than power plant flue gas cleaning. Approximately one third of all CO_2 emission from human activity comes from generating electricity. Therefore CO_2 capture and storage from fossil fuel power plants presents an opportunity to achieve large reductions in greenhouse gas emissions without having to change the energy supply infrastructure and also without having to make large changes to the basic process of producing electricity.

The idea of capturing CO_2 from the flue gas of power plants did not start with the concern of the increasing greenhouse effect, the idea gained attention because of the possible economical benefits through enhanced oil recovery (EOR). During EOR CO_2 is injected into oil reservoirs to increase the mobility of the oil and, thus the productivity of the reservoir. Several commercial CO_2 capture plants were constructed in the United States of America in the late 1970s and the early 1980s, but when the oil price dropped in the middle of the 1980s the recovered CO_2 was too expensive for EOR operations and the plants were closed.

The largest problems concerning the use of alkanolamines as chemical absorbents for CO_2 are the amount of energy needed to regenerate the CO_2 rich solvent and to a certain extent the size of the CO_2 capture plant. The capture of CO_2, specifically the regeneration of solvent has significant energy requirements thereby reducing the plant's conversion efficiency and net power output which in turn increases the amount of CO_2 produced per net kWh produced.

The purpose of this work is to contribute to the development of efficient CO_2 capture technology in relation to coal fired power plants. The main aim of this thesis is to contribute to the modeling and simulation of CO_2 capture in aqueous solutions of alkanolamines. The philosophy behind the modeling approaches in this work has been to describe the natural phenomena occurring with a simple model, but without sacrificing the accuracy at the conditions relevant for flue gas cleaning.

1.2 Main Contributions of the Thesis

In this thesis results from modeling, theoretical and experimental work are presented.

- A simple model for CO_2 solubility in aqueous solutions of several single alkanolamines and one alkanolamine mixture has been proposed and an expression for the heat of absorption of CO_2 has been developed.
- A predictive rate-based steady-state model for CO_2 absorption into an AMP and an MEA solution has been proposed, implemented and validated, utilizing both the proposed expression for the CO_2 solubility and the expression for the heat of absorption.
- Experimental pilot plant work has been carried out and detailed experimental data, including temperature profiles over the absorber and desorber, for an integrated laboratory pilot plant using an aqueous AMP solution and structured packing. A predictive rate-based steady-state model for CO_2 absorption into an AMP solution, using an implicit expression for the enhancement factor, has been validated against the presented pilot plant data.
- Experimental work has been carried out to find the chemical rate constants for the reaction of CO_2 with AMP in an aqueous solution using a string of discs absorber.

2 Post Combustion CO_2 Capture

This work is concentrated on post combustion CO_2 capture using aqueous alkanolamines because it is the technology closest to be ready to implement on a large scale for CO_2 capture from flue gases, and it can be used to retrofit already existing power plants. The technology is currently being used in CO_2 production plants, and for the capture of CO_2 from natural gas[1]. But all existing plants are much smaller than what is needed for CO_2 capture from power plants. The largest problems concerning the use of alkanolamines as chemical absorbents for CO_2 are the amount of energy needed to regenerate the CO_2 rich solvent and to a certain extent the size of the CO_2 capture plant. The capture of CO_2, specifically the regeneration of solvent has significant energy requirements thereby reducing the plant's conversion efficiency and net power output which in turn increases the amount of CO_2 produced per net kWh produced. The most commonly used alkanolamine for low partial pressures of CO_2, as would be encountered in post combustion CO_2 capture, is monoethanolamine (MEA)[2]. MEA has good CO_2 absorption capacity and a high absorption rate, but requires a large amount of energy to regenerate due to its high heat of reaction. A common estimate for absolute efficiency reduction for modern coal fired power plants using 30 weight percent MEA as solvent and 90 percent CO_2 removal and liquefaction is approximately 10 percent, which gives a relative decrease in efficiency of approximately 25 percent[3,4]. The largest fraction of the efficiency reduction comes from the energy needed to regenerate the solvent[5], thus it is evident that alternative solvents exhibiting lower heat of reaction may reduce energy consumption significantly. Furthermore, a significant amount of work needed to push the flue gas through the CO_2 absorption tower, thus a packing giving a small pressure drop over the tower is of high importance. Work on efficient structured packing is being done by e.g. Aroonwilas et al.[6] and Mimura et al.[7].

2.1 CO_2 Capture Using Aqueous Alkanolamines

CO_2 absorption with aqueous alkanolamines has been used commercially since the early 1930's[1] and is based on a reaction of a weak base (alkanolamine) with a weak acid (CO_2) to produce a water soluble salt. The reaction is reversible and the equilibrium is temperature dependent and the process is usually operated as a temperature swing with absorption at a low temperature and desorption at a high temperature. CO_2 absorption using alkanolamines falls in the general category of chemical absorption. In Figure 2-1 a simplified flow sheet of a CO_2 capture plant using e.g. MEA is presented. The two main units in the capture plant are two packed towers; the absorber and the stripper. Both columns are packed with either random or structured packing. Before the flue gas is introduced in the absorber it is important to remove

SO_2 and NO_X in order to prevent formation of unwanted by-products such as sulfates and nitrates. The flue gas is cooled and fed to the bottom of the absorption tower at approximately 40°C and atmospheric pressure. If the gas is not cooled prior to the introduction into the absorber the inlet temperature is approximately 50°C. The flue gas then rises through the tower and is contacted counter currently with the absorption liquid alkanolamine fed at the top of the column labeled "lean amine" in Figure 2-1. Along the absorption tower CO_2 is absorbed by the liquid. When CO_2 is absorbed the temperature in the absorber increases due to the strongly exothermic reaction between alkanolamine and CO_2. At the top of the absorption tower flue gas with low content of CO_2 is released into the atmosphere. When using volatile solvents such as MEA a recirculating water wash should be included in the absorber to prevent loss of alkanolamine to the surroundings, this is of importance both economically and environmentally.

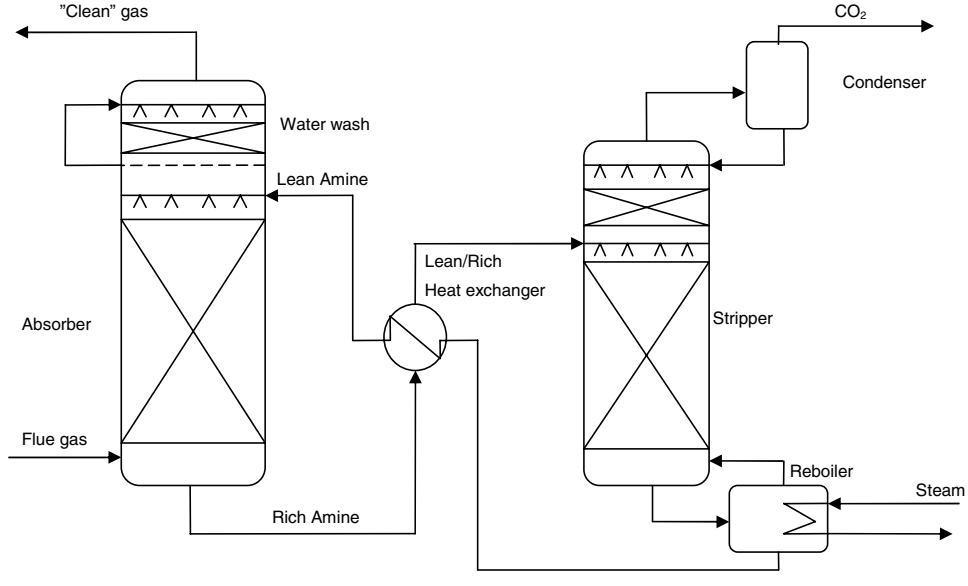

Figure 2-1. Simplified flow sheet for a CO_2 capture plant using aqueous alkanolamines.

Flue gas from coal fired power plants contains approximately 12-13 %-vol. CO_2 and a commonly seen specification is to capture 90% of the CO_2 in the flue gas. The absorption liquid leaving the bottom of the column, labeled "rich amine" in Figure 2-1 is heat exchanged with the lean amine leaving the reboiler. The pinch side of the lean/rich heat exchanger is the cold side since the lean solution has a slightly lower heat capacity than the rich. Normally the temperature approach at the cold side is set to approximately 10-15°C, but using a modern heat exchanger the temperature approach can be below 5°C according to Tobiesen et al.[8]. A standard stripper in a CO_2 capture plant consists of three different units: condenser, stripper column, and reboiler. The rich amine is fed to the top of the stripper column with a temperature of approximately 100°C. The pressure in the stripper is typically 1.6-1.7 bar. In the column the amine solution is

stripped for CO_2 with a gas mainly consisting of water and some CO_2. The stripping gas comes from a reboiler operated at about 120°C, where the amine solution leaving the desorption tower is heated using low pressure steam from the power plant. The energy supplied by the steam is used for three main purposes, (1) to break the chemical bond between the CO_2 and the amine, (2) evaporate enough water to dilute the CO_2 gas in the column in order to have a driving force for CO_2 to leave the liquid phase and (3) to provide sensible heat to warm the rich amine liquid feed. The gas leaving the top of the column is mainly a mixture of CO_2 and water. The gas is cooled and liquid water is condensed in a flash drum and recycled to the column as wash water and pure CO_2 leaves the condenser. The lean amine leaves bottom of the reboiler and is recycled through the lean/rich heat exchanger to the absorber. A reclaimer used to concentrate and remove heat stable salts is usually installed in the plant.

The ability of a solvent to remove carbon dioxide is dependent on its equilibrium solubility as well as mass transfer and chemical kinetics characteristics. Alkanolamines are commonly referred to as primary, secondary or tertiary depending on the number of groups containing carbon which are attached to the nitrogen atom e.g. MEA (primary), diethanolamine (DEA) (secondary), and methyldiethanolamine (MDEA) (tertiary) for structures and abbreviations of the different compounds in the text see appendix A.

2.1.1 Equilibrium Chemistry

As stated earlier the absorption of CO_2 into an alkanolamine solution is a reaction between a weak acid and a weak base, where both are weak electrolytes. The weak electrolytes partially dissociate in aqueous solution. The chemical equilibrium taking place in the liquid phase when CO_2 is absorbed in an aqueous solution of primary or secondary alkanolamines can be written with the following equilibrium equations where the alkanolamine is R_3N and R can represent an alkyl group, alkanol group, or hydrogen:

$$2H_2O \rightleftharpoons H_3O^+ + OH^- \tag{2.1}$$

$$CO_2 + 2H_2O \rightleftharpoons H_3O^+ + HCO_3^- \tag{2.2}$$

$$HCO_3^- + H_2O \rightleftharpoons H_3O^+ + CO_3^{2-} \tag{2.3}$$

$$R_3NH^+ + H_2O \rightleftharpoons H_3O^+ + R_3N \tag{2.4}$$

$$R_2NCOO^- + H_2O \rightleftharpoons R_3N + HCO_3^- \tag{2.5}$$

The reaction of CO_2 with aqueous MEA can, given that the loading is in the region between 0.02 and 0.48, be approximated by a single chemical equilibrium reaction, Astarita[9]:

$$R_2NH_2^+ + R_2NCOO^- \rightleftharpoons 2R_2NH + CO_2\,(aq.) \tag{2.6}$$

implying that all absorbed CO_2 reacts with the alkanolamine to form carbamate. The equation (2.6) neglects the presence of bicarbonate (HCO_3^-), hydroxide (OH^-), and carbonate (CO_3^{2-}) ions. The concentration of these ions will be very small in the region of loading which is of interest to CO_2 capture from power plants fired with fossil fuels using a primary or secondary alkanolamine since the area of interest is where the fast carbamate reaction dominates.

For aqueous solutions of tertiary or sterically hindered alkanolamines such as MDEA and 2-amino-2-methyl-1-propanol (AMP) respectively equation (2.5) can be neglected since no stable carbamates are formed, Sartori et al.[10], thus the main reaction is:

$$R_3NH^+ + HCO_3^- \rightleftharpoons R_3N + CO_2\left(aq.\right) + H_2O \qquad (2.7)$$

Equation (2.7) is valid to the limit of chemical absorption.

In reactions of CO_2 with conventional primary and secondary alkanolamines in aqueous solutions carbamate is the main product, whereas aqueous solutions of the sterically hindered primary alkanolamine AMP, or a tertiary alkanolamine, exhibiting low carbamate stability the main reaction product is bicarbonate as seen in equation (2.7). The maximum chemical absorption capacity for a mono amine is one mole of CO_2 per mole amine, but higher loadings are possible due to physical absorption at very high partial pressures of CO_2.

2.1.2 Alkanolamines Used for Absorption

Important factors when considering solvents for CO_2 capture are[5];

1. Absorption rate, a high absorption rate reduces the height of the absorption tower and thus the capital investment cost.
2. Absorption capacity, a high cyclic capacity reduces the volume of solvent circulating in the system and is achieved with a solvent with high CO_2 solubility.
3. Solvent heat of absorption, a low heat of absorption is important to reduce the amount of stripping steam needed.
4. Solvent volatility, vapor pressure of the solvent should be low to avoid loss of solvent with the clean flue gas. This point is important both from an economical and environmental point of view.
5. Solvent stability, the solvent should be resistant to carbamate polymerization, thermal degradation and oxidative degeneration.
6. Solvent price, the price of the solvent should of course be as low as possible.
7. Solvent toxicity, if a solvent is classified as toxic it will prohibit the use.

Most of these properties are directly related to the operating and investment cost of the capture plant, but the environmental properties of the solvent are also of high importance.

MEA is considered an attractive solvent at low partial pressures of CO_2 in the flue gas because it reacts at a rapid rate and the cost of the raw materials is low compared to secondary, tertiary, and sterically hindered amines. However the costs of absorption processes using MEA are high due to high energy consumption during regeneration and operational problems such as corrosion, solvent loss, and solvent degradation[11]. In general two different approaches are being explored to overcome the problems formerly mentioned. One is to use sterically hindered amines; the other is to use blends of primary/secondary amines with tertiary amines. Both of the approaches are commercialized, A solvent called KS-1 is sold by Mitsubishi and is pure amine or mixture of amines where at least one is sterically hindered. BASF is selling a product they call aMDEA (activated MDEA) which is a blend of piperazine and MDEA. Further at the University of Texas at Austin a research group is investigating the use of aqueous solutions of potassium carbonate and piperazine.

Among the most active groups in developing new improved chemical CO_2 absorbents are Kansai Electric Power Co. and Mitsubishi Heavy Industries, Ltd. and Professor Amit Chakma's group at the University of Regina. KS-1, KS-2, and KS-3 (KS is short for Kansai Solvent) are proprietary sterically hindered alkanolamine absorbents developed by Kansai Electric Power Co. and Mitsubishi Heavy Industries, Ltd. According to their own testing they have outstanding properties regarding absorption capacity, stability, corrosion, and amount of energy needed to regenerate (approximately 20% less than MEA[7]). KS-1 also is hardly corrosive towards carbon steel. The cost of KS-1 is three times as high as MEA, but it is said that KS-1 solvent consumption is 1/6 of MEA solvent consumption[12]. The first commercial installation using KS-1 for CO_2 capture is a natural gas fired power plant in Malaysia, which came in operation in late 2000. The lowest energy penalty associated with CO_2 capture from flue gas streams is 7.7% by using a patented solvent developed by Kansai Electric Power Co. and Mitsubishi Heavy Industries, Ltd and proprietary structured packing called KP-1.

Solvents containing blended amines are believed to be a possible solution to the problematic trade off between capture rate and energy consumption during regeneration. The idea is based on having a slow amine with high CO_2 capacity and then adding a relatively small amount of fast amine that reacts quickly with the CO_2 in the gas. The fast amine added is often called a promoter. One solvent that is being investigated and used is MDEA activated with piperazine. Erga et al.[18] studied absorption rates of CO_2 and energy requirements for stripping of CO_2 rich solvent for aqueous amine systems. According to Erga et al.[18] the energy required for regeneration of a mixture of 50% MDEA and 5% piperazine compared to MEA is around 20% lower when the CO_2 concentration in the flue gas is 6%vol, and probably even lower for a higher CO_2 concentration in the flue gas. The PZ/MDEA blend is utilized in sour gas

sweetening with intent to use PZ as a kinetic promoter for the slowly reacting MDEA following a mechanism described in Astarita [13]. Studies carried out by Bishnoi et al. [14] suggests that the effect of PZ on the partial pressure of CO_2 over a PZ/MDEA/H_2O solution with a relatively small amount of PZ compared to MDEA on a mol basis (1:10) is only significant for loadings less than 0.2. At higher loading the solution behaves as a "pure" aqueous MDEA solution with respect to CO_2 partial pressure. BASF is making a solvent called aMDEA which is a mixture of piperazine and MDEA, and possibly other alkanolamines. They claim great performance, capacity and stability, but the flue gas needs to have a total pressure of at least 3.5 bars when it is fed to the absorber (BASF's product sheet for aMDEA[15]). However pure MDEA is commonly used for selective H_2S removal when a gas contains both CO_2 and H_2S because it reacts at a fast rate with H_2S but slowly with CO_2.

Other non-patented alkanolamines include; AMP, diisopropanolamine, diglycolamine (DGA), and triethanolamine (TEA). Bonenfant et al.[22] conducted experimental studies of the absorption and regeneration characteristics of several amines in aqueous solution. Among the tested solutions were 5 wt percent ammonia, MEA, TEA, pyridine, and N-(2-aminoethyl)-1,3propanediamine (AEPDNH_2). The solvents had different structural features such as aromatic rings, non aromatic rings, several amine groups, sterical hindrance, and primary, secondary and tertiary amines were tested. And in the article they conclude that AEPDNH_2 a polyamine with three amine groups, 2-(2-aminoethylamino) ethanol (AEE) an alkanolamine with two amine groups, and TEA (a tertiary alkanolamine) possessed the greatest CO_2 loading and recovery capacity, and were among the solvents with the best regeneration capacity. Their conclusion is that AEE and AEPDNH_2 represent interesting compounds for further investigation as CO_2 absorption solvents. No estimation of the absorption rate of these solvents was shown, but they require low regeneration energy which indicates slow absorption capacity so a mixture with a primary amine to activate might be an interesting solution. Further, the stability and corrosiveness of the solvents was not discussed in the article. The cost of the solvents is not mentioned either.

2.2 Alternative Solvents and Contact Apparatuses

There are several different techniques for CO_2 capture from process gas streams, where chemical absorption using alkanolamines in a packed absorption tower, as described earlier, is the most commonly used. This work concentrates on chemical absorption using aqueous alkanolamines in packed towers, but in this review other chemical absorption methods such as absorption with alkaline salts of amino acids, ammonia scrubbing, absorption with lithium oxides, and a dual alkali process are presented along with alternative absorption equipment.

2.2.1 Alkaline Salts of Amino Acids

Aqueous alkaline salts of amino acids can be an alternative to aqueous solutions of alkanolamines, particularly in membrane gas absorption. The ionic nature makes them more stable to oxidative degradation, gives them lower volatility consequently leading to negligible loss of solvent in the stripper, and higher surface tension than solutions of alkanolamines. They have similar CO_2 absorption kinetics and capacity as primary alkanolamines; this gives the drawback of high heat of reaction leading to energy intensive solvent regeneration. On the negative side Kumar et al.[16] show they are more expensive than alkanolamines and crystallization during absorption can happen, especially for solutions of high amino acid salt concentration at high CO_2 loading. Drawbacks related to crystallization are plugging, and fouling of the gas-liquid contactors and heat transfer surfaces. Moreover, the presence of particles in the liquid phase can influence the characteristics of the gas–liquid contactors. On the positive side crystallization of the reaction product in this equilibrium limited liquid-phase reaction leads to an increase of CO_2 loading capacity. In the works of Kumar et al.[16,17] potassium salt of taurine has been investigated as an absorbent, while the company TNO uses a wide range of alkaline salts of amino acids for their proprietary absorbents called CORAL (CO_2 Removal Absorption Liquid).

According to experiments and calculations done by Erga et al.[18] approximately 2.7 kg steam at 140°C and 3.4 atm is needed per kg CO_2 for regeneration of solvent when the flue gas contains 6.0 vol% CO_2 with a removal efficiency of 90%. The solvents considered were 4.0 M solutions of potassium glycine (KGl) and 4.0 M potassium sarcosine (KSar). The amount of steam is similar to the amount of steam needed to regenerate MEA.

The following description of the chemistry of CO_2 absorption in aqueous amino acid salt solutions is from the work of Kumar et al.[19]. Amino acids in water, when no other solute is present, exist as zwitterions and the pH of the solution is equal to the isoelectric point of the given amino acid.

$$\underset{I}{HOOC-R-NH_3^+} \overset{-H^+}{\rightleftharpoons} \underset{II}{^-OOC-R-NH_3^+} \overset{-H^+}{\rightleftharpoons} \underset{III}{^-OOC-R-NH_2} \qquad (2.8)$$

The amino group should be deprotonated before it can react with CO_2, hence in the form of *III* in equation (2.8). This is usually done by adding an equimolar amount of base, e.g. potassium hydroxide. Alkaline salts of amino acids reacts with CO_2 and the reactions in the liquid phase are as follows:

$$2RNH_2 + CO_2 \rightleftharpoons RNHCOO^- + RNH_3^+ \qquad (2.9)$$

$$RNHCOO^- + H_2O \rightleftharpoons RNH_2 + HCO_3^- \qquad (2.10)$$

$$HCO_3^- \rightleftharpoons CO_3^{2-} + H^+ \quad (2.11)$$

$$RNH_3^+ \rightleftharpoons RNH_2 + H^+ \quad (2.12)$$

$$H_2O \rightleftharpoons H^+ + OH^- \quad (2.13)$$

An amino acid salt (represented with RNH_2) reacts with carbon dioxide yielding the primary products carbamate and protonated amine. In aqueous solutions the carbamate undergoes hydrolysis and forms carbonate or bicarbonate, depending on the pH of the solution, and an amine.

2.2.2 Ammonia Scrubbing

Injection of NH_3 or aqueous NH_3 for removing NOx form flue gas in power plants is a common process. Therefore it might be economical to use ammonia scrubbing to remove CO_2 since less space and new equipment will be required compared to competing technologies. Further there are lower material costs and the corrosion in the absorber is lower.

Under very specific conditions Zheng et al.[20] show that removal efficiencies as high as 95% to 99% percent are achieved after one minute. Figure 2-2 gives a description of removal efficiency as a function of time and temperature. During the scrubbing process carbon dioxide reacts with ammonia in several steps to form ammonium bicarbonate, a widely used fertilizer in

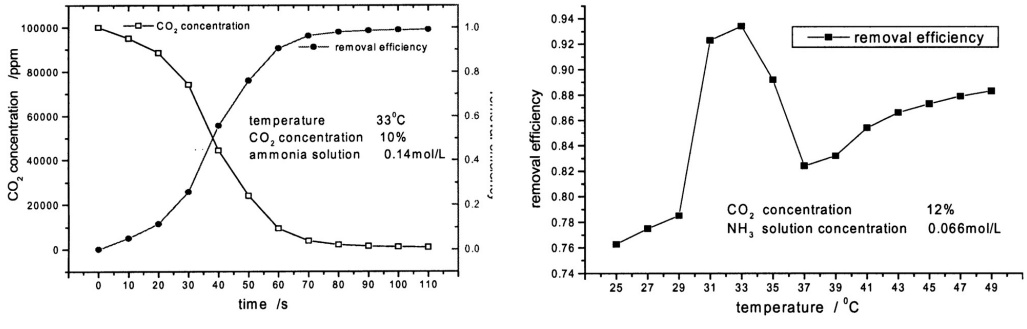

Figure 2-2. CO_2 removal efficiency as a function of time and temperature figures from ref. [20]

China. The crystalline ammonia bicarbonate can also be heated to release the carbon dioxide and regenerate ammonia.

During ammonia scrubbing of flue gases to capture carbon dioxide the probable reactions taking place are the formation of ammonium carbonate, equation (2.14), and ammonium bicarbonate[21], equation (2.15), with ammonium bicarbonate as the main product of the reaction:

$$2NH_3(l) + CO_2(g) + H_2O(l) \leftrightarrow (NH_4)_2CO_3(s) \quad (2.14)$$

$$NH_3(l) + CO_2(g) + H_2O(l) \leftrightarrow NH_4HCO_3(s) \quad (2.15)$$

Experiments carried out by Zheng et al.[20] show that the CO_2 removal efficiency is strongly temperature dependent as shown in Figure 2-2, the graph to the right in Figure 2-2 is a plot of CO_2 capture efficiency after 80 s; According to Zheng et al.[20] removal rate is dependent on CO_2 concentration, as the removal efficiency decreases with increasing CO_2 inlet concentration, but according to Hsunling et al.[21] the effect of changing the CO_2 inlet concentration is minimal. CO_2 removal efficiency increases with increasing NH_3 concentration in the scrubber solution.

The technique looks promising, but the energy needed to regenerate is considerably higher than e.g. for MEA[22] and there is also the concern with the highly volatile nature of ammonia. But a novel approach for regenerating the ammonia has been suggested by Huang et al.[23]. The approach involves a weakly basic ion-exchange resin containing amine functional groups which is used to regenerate ammonia through absorbing carbonic acid at ambient temperatures from ammonium bicarbonate. The resin can be regenerated when it is heated with water to temperatures equal or greater than 50°C. A 50 % energy saving is expected by Huang et al.[23] and is based on an expected enthalpy of dissociation of CO_2 from the resin which is half of the enthalpy of dissociation of CO_2 from MEA. This method of regenerating ammonia seems very cumbersome, but the removal efficiency looks very promising compared to the more common technique involving MEA as a solvent.

2.2.3 Lithium Containing Absorbents

Nakagawa et al.[24] showed that during investigation of lithium zirconate as an additive for molten carbonate fuel cell electrode plates, a durability test of the material showed that the lithium zirconate which had been synthesized by heat treatment of zirconia and lithium carbonate returned to the starting materials in the presence of CO_2 see reaction (2.16).

$$Li_2ZrO_3 + CO_2 \rightleftarrows Li_2CO_3 + ZrO_2 \quad (2.16)$$

Nakagawa et al.[24] then investigated the possibilities of using Li_2ZrO_3 to capture CO_2 in the fuel reforming process. And found that CO_2 was absorbed at temperatures between 450°C and 550°C and released at temperatures above 650°C. Moreover, they found that the reaction is independent of gas species other than CO_2. Kato et al.[25] further investigated the use of various lithium-containing oxides to absorb CO_2, and found lithium orthosilicate, equation (2.17), to have a the highest reactivity, approximately 30 times faster than lithium zirconate at 500°C and at a concentration of 20% CO_2.

$$Li_4SiO_4 + CO_2 \rightleftarrows Li_2SiO_3 + Li_2CO_3 \quad (2.17)$$

The model of CO_2 reaction with Li_4SiO_4 is illustrated in Figure 2-3.

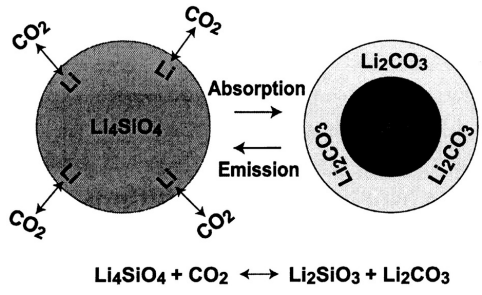

Figure 2-3. Reaction model of Li_4SiO_4 with CO_2 from ref.[25]

Since lithium orthosilicate is synthesized from silicon dioxide it has lower weight, and lower cost than lithium zirconate. Kato et al. [25] carried out experiments to examine the cyclic behavior of Li_4SiO_4 and found out that after five absorption/emission cycles the absorption behavior was almost the same as the initial.

2.2.4 Dual Alkali Approaches

The dual alkali process is described by Huang et al.[26]. The Solvay process uses two alkalis, ammonia and lime; in sequential order to convert carbon dioxide to sodium carbonate for commercial use, the secondary alkali is used to regenerate the first. A new process called the "Dual Alkali Approach" is a modification of the Solvay process to make it applicable in capture of CO_2 from flue gases from coal fired power plants. It attempts to replace both or either one of the bases used in the Solvay process to make the CO_2 capture and separation efficient. Ammonia was replaced with alkanolamines, MEA or methylaminoethanol (MAE), in aqueous solutions of salts, and bicarbonate precipitation occurred. A method to regenerate the alkanolamine in the second step has not been implemented. The second step of Solvay process has been implemented with ammonia regenerated from an ammonium chloride solution using activated carbon.

Experiments with both MEA and MAE were carried out both with and without sodium chloride added. For MEA there was no difference in the CO_2 removal efficiency with added sodium chloride, whereas the removal capacity increased for MAE with added sodium chloride.

The main reaction product of MEA with CO_2 is carbamate. Therefore the addition of sodium chloride does not change the amount of carbon dioxide absorbed by the MEA solutions. MAE has a greater carbon dioxide absorption capacity than MEA, indicating that the reaction products are shifted towards bicarbonate. It looks promising to introduce sodium chloride into the aqueous MAE solution in the scrubbing process, since it increases the solvents capacity to

absorb CO_2 considerably. There is no estimation of energy needed to regenerate the ammonia. I assume that regeneration of MAE is as energy demanding as in the standard MAE procedure. Huang et al.[26] are stating that returning CO_2 to nature after converting it to carbonate salts is safe since weathering of alkaline rocks is a natural method of CO_2 sequestration. For further explanation see Kojima et al.[27].

2.3 Alternative Absorption Equipment

The development of new and efficient absorption equipment is very important since low pressure drop is an important factor in keeping the CO_2 capture process economically viable, the size of the equipment is also important considering that space often is limited in existing power plants. Absorption columns with conventional packing gives a surface area between 100–800 m^2m^{-3} in comparison a membrane gas absorber (MGA) gives between 1500–3000 m^2m^{-3} of surface area[19]. A rotating packed bed (RPB)/high-gravity contactor (HIGEE) gives a surface area between 2000–5000 m^2m^{-3} ref.[28]. From these comparisons it is clear that there might be great advantages in using alternative absorption equipment.

2.3.1 Membrane Gas Absorption

Membrane processes are expected to have the potential to be less energy demanding and smaller in size than conventional CO_2 capture units used today, but Feron et al.[29] showed that commercially available gas separation membranes are not capable of pressure driven CO_2 from power plants. A hybrid membrane gas absorption process is worth considering, since it can combine the strong points of the two different technologies. The strong points are small size and modularity from membranes and high selectivity from chemical absorption. Currently two different MGAs are being developed one by TNO in the Netherlands and one by Kværner/Gore in Norway and Germany. TNO are using common, cheap polyolefin membranes which are limited in chemical stability making it impossible to use alkanolamine solutions as absorbents due to the low surface tension of water/alkanolamine solutions since this will give wetting of the membrane. TNO are using proprietary inorganic solvents CORAL which are based on aqueous solutions of amino acid salts and having a surface tension higher than or close to pure water[16] making it possible to use polyolefin membranes, moreover the vapour pressure of the active components in CORAL are close to zero hence the solvent is not lost through evaporation. Kværner/Gore is using PFTE (Teflon) membranes which are expensive, but chemically stable and can be used with every available, interesting solvent and solvent group.

The essential element in a membrane absorber is a porous, hydrophobic, polymeric membrane Svendsen et al.[2]. The gas is kept separate from the solvent by the membrane and the component to be removed, in this case CO_2, will diffuse through the membrane and react with

the solvent. Ideally, the micro pores of the membrane should be completely gas filled, to minimize any mass transfer resistance due to the presence of the membrane Kumar et al.[19]. A principal sketch is shown in Figure 2-4. The membrane itself does not offer any selectivity for the separation of the gases, which is left to the absorption liquid. Chemically reactive absorption liquids are preferred over physical absorption liquids due to faster absorption rate and higher capacity. Advantages of MGA over packed absorption towers are:

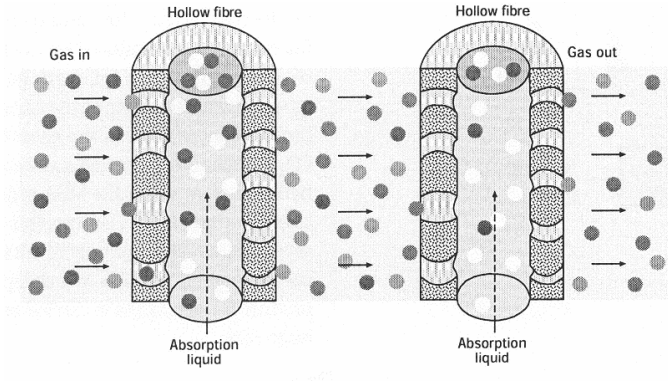

Figure 2-4. Membrane gas absorption principle form ref.[19]

- Gas and liquid flows are separate avoiding problems as flooding, foaming, channeling, and entrainment. This also means that the gas and liquid flow rates can be varied independently of each other almost without limits.
- The solvent is not carried out of the absorber, thus there is no need for a wash section after the absorber.
- Operation is not dependent on the orientation of the absorber.
- Equipment will be compact (theoretically based performance comparisons have showed that a membrane absorber can lead to a tenfold reduction in size).

The membrane absorber design can not be based on conventional membrane module design, since these designs traditionally have been based on the use of hollow fibre membranes for filtration duties with ill-defined flow conditions on the shell side of the membrane. When membranes are used for contacting duties it is important that flow conditions are well defined on both sides of the membrane in order to achieve good mass transfer.

2.3.2 Rotating Packed Bed

To enhance mass transfer rate between gas and liquid, a rotating doughnut shaped device in which gas and liquid are contacted in the presence of a high centrifugal field may be applied. In a rotating packed bed (RPB) liquid flow through the packing element subjected to an acceleration rate of at least 300 m/s^2 depending on the rotating speed. Since centrifugal acceleration by far exceeds gravity there are many benefits; the RPB can be operated at high gas

and liquid flow rates over a packing with large surface area and high porosity. Moreover, thinner films and smaller droplets, compared to an absorber running under "normal" gravitation, can increase the gas–liquid mass transfer rate. This in turn may allow smaller equipment size. Gas and liquid contact counter currently in an RPB. In Lin et al.[28] the overall volumetric mass transfer coefficient, for a laboratory scale RPB shown in Figure 2-5, was observed as a function of rotating speed, gas flow rate, liquid flow rate, absorbent concentration, and CO_2 concentration. The RPB used in the experiment had an inner diameter of 7.6 cm and an outer diameter of 16.0 cm, and a height of 2 cm. The total volume of the RPB was 311.4 cm^3. The experiments were run at 300K and 1 atm. The absorbents used were NaOH, MEA, AMP, and a mix of MEA and AMP. Out of the four MEA showed the highest absorption rate. The results show that the overall volumetric mass transfer rate of the RPB was comparable to a tower packed with Sulzer EX (structured packing only available in laboratory scale) packing, making it considerably higher than in a randomly packed column. They further conclude that the main mass transfer resistance lies in the liquid film. The advantages of using an RPB include an increase in gas–liquid contact area and a reduction in the gas–liquid mass transfer resistances. On the negative side RPBs have higher pressure drop compared to conventional packed columns based on pressure drop per theoretical stage[30]. Price and maintenance might be prohibiting the scale-up needed for flue gas cleaning.

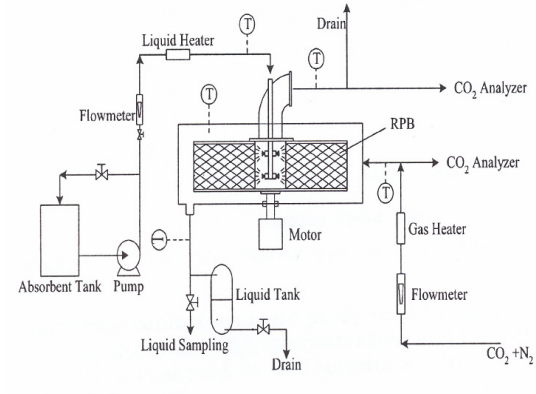

Figure 2-5. Rotating Packed Bed principle from ref. [28]

2.3.3 The CO_2 wheel

Shimomura et al.[31] introduced an application to use for removal of CO_2 from flue gases called "The CO_2 Wheel". It uses a Ljugstrom air preheater with Li_4SiO_4 loaded on the rotor. A principal sketch of the CO_2 wheel is presented in Figure 2-6. According to an analytical model developed by Shimomura et al.[31] it can capture CO_2 from thermal power plants at approximately 30–40 percent of the cost of other existing technologies. When the preheater is placed in the exhaust of a coal fired power plant, it will theoretically capture large volumes of CO_2 on the cold gas side and release it on the hot gas side on a continuous basis. The hot side is heated by an external heater. The technology is assumed to be space saving compared to existing

technologies, a wheel system for a 250 MW coal fired power plant was evaluated. Estimated dimensions of the rotor for the CO_2 wheel are approximately 20 m diameter by 1.5 m depth. Predicted capture of CO_2 gas of the total outlet is 63 percent including the gas from the heating furnace.

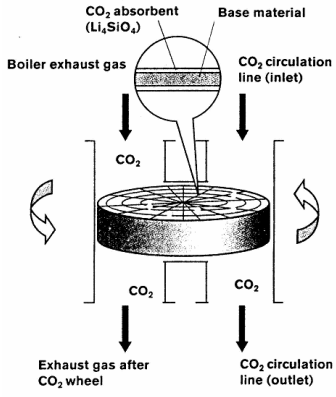

Figure 2-6. Principle of the CO2-wheel from ref.[31]

Further, no consumables are required and no waste is generated from the system. On the negative side this technology needs to incorporate a furnace, possible an LNG furnace, to heat the "wheel" in order to release the CO_2. Moreover, there has been no pilot scale testing, it is currently only possible to perform bench scale tests.

References

[1] Kohl AL, Nielsen RB Gas Purification (5th edition). Huston, Texas: Gulf Publishing Company, 1997.

[2] Svendsen HF, Hoff KA, Poplsteinova J, da Silva EF. Absorption as a Method for CO2 Capture, Second Nordic Minisynopsium on Carbon Dioxide Capture and Storage. Göteborg, October 2001

[3] Desideri U, Paolucci A. Performance modelling of a carbon dioxide removal system for power plants. Energy Conversion and Management. 1999;40:1899-1915.

[4] Gibbins J, Lucquiaud M, Li J, Lord M, Liang X, Reiner D, Sun S. Capture ready fossil fuel plants: definitions, technology options and economics. Proceedings of 8th International Conference on Greenhouse Gas Control Technologies. Trondheim, Norway, June 2006

[5] Hoff KA, Mejdell T, Juliussen O, Børresen E, Lauritsen KG, Semb HT, Svendsen HF. Solvents selection for a post combustion CO_2 capture process. Proceedings of 8th International Conference on Greenhouse Gas Control Technologies. Trondheim, Norway, June 2006

[6] Aroonwilas A, Tontiwachwuthikul P. High-efficiency structured packing for CO_2 separation using 2-amino-2-methyl-1-propanol (AMP). Separation and Purification Technology 1997;12:67–79.

[7] Mimura T, Simayoshi H, Suda T, Iijima T, Mituoka S. Development of Energy Saving Technology for Flue Gas Carbon Dioxide Recovery in Power Plant by Chemical Absorption Method and Steam System., Energy Conversion Management 1997;38:51-62.

[8] Tobiesen FA, Svendsen HF, Hoff KA. Desorber Energy Consumption in Amine Based Absorption Plants. Int. J. Green Energy 2005;2:201-216.

[9] Astarita G, Mass Transfer With Chemical Reaction, Elsevier Publishing Company. 1967

[10] Sartori G, Savage DW. Sterically hindered amines for CO_2 removal from gases. Ind. Eng. Chem. Fundam. 1983;22:239-249.

[7] Veawab A, Tontiwachwuthikul P, Aroonwilas A, Chakma A., Performance and Cost Analysis for CO_2 Capture from Flue Gas Streams: Absorption and Regeneration Aspects. Preprints from Sixth International Conference on Greenhouse Gas Technologies, Kyoto, Japan, October 2002

[12] Bolland O. Report from GHGT-5. http://www.tev.ntnu.no/GlobalWatch/co2/rapport_fra_ghgt5.htm

[13] Astarita G., Savage D.W., Bisio A., Gas Treating With Chemical Solvents, John Wiley & Sons, New York/Chicester/Brisbane/Toronto/Singapore, 1983,

[14] Bishnoi S., Rochelle G.T., Thermodynamics of Piperazine/Methyldiethanolamine/Water/Carbon Dioxide, Ind. Eng. Chem. Res., 2002, 41, 604-612

[15] http://www.basf.de/en/produkte/chemikalien/interm/amine/amdea/?id=V00--22ntsv**bsf300

[16] Kumar PS, Hogendoorn JA, Feron PHM, Versteeg GF. Equilibrium Solubility of CO_2 in Aqueous Potassium Taurate Solutions: Part 1. Crystallization in Carbon Dioxide Loaded Aqueous Salt Solutions of Amino Acids. Ind. Eng. Chem. Res. 2003;42:2832–2840.

[17] Kumar PS, Hogendoorn JA, Feron PHM, Versteeg GF. Equilibrium Solubility of CO_2 in Aqueous Potassium Taurate Solutions: Part 2. Experimental VLE Data and Model. Ind. Eng. Chem. Res. 2003;42:2841–2852.

[18] Erga O, Juliussen O, Lidal H. Carbon dioxide recovery by means of aqueous amines. Energy Convers. Mgmt. 1995;36:387–392.

[19] Kumar PS, Hogendoorn JA, Feron PHM, Versteeg GF. New absorption liquids for the removal of CO_2 from dilute gas streams using membrane contactors. Chemical Engineering Science 2002;57:1639–1651.

[20] Zheng XY, Diao YF, He BS, Chen CH, Xu XC, Feng W. Carbon Dioxide Recovery From Flue Gases by Ammonia Scrubbing, Preprints from Sixth International Conference on Greenhouse Gas Technologies, Kyoto, Japan, October 2002

[21] Hsunling B, An CY. Removal of CO_2 Greenhouse Gas by Ammonia Scrubbing. Ind. Eng. Chem. Res. 1997; 36: 2490-2493.

[22] Bonenfant D, Mimeault M, Hausler R. Determination of the Structural Features of Distinct Amines Important for the Absorption of CO_2 and Regeneration in Aqueous Solution. Ind. Eng. Chem. Res. 2003;42:3179-3184.

[23] Huang H, Chang SG. Method to Regenerate Ammonia for the Capture of Carbon Dioxide. Energy and Fuels, 2002;16:904-910.

[24] Nakagawa K, Ohashi T. A Novel Method of CO_2 Capture from High Temperature Gases. J. Electrochem. Soc. 1998;145:1344-1346.

[25] Kato M, Essaki K, Yoshikawa S, Nakagawa K, Uemoto H. Novel CO_2 absorbents Using Lithium-containing Oxides, Preprints from Sixth International Conference on Greenhouse Gas Technologies, Kyoto, Japan, October 2002

[26] Huang HP, Shi Y, Li W, Chang SG. Dual Alkali Approaches for the Capture and Separation of CO_2. Energy and Fuels 2001;15: 263-268.

[27] Kojima T, Nagamine A, Ueno N, Uemiya S. Absorption and fixation of carbon dioxide by rock weathering. Energy Convers. Mgmt. 1997;38:461-466.

[28] Lin CC, Liu WT, Tan CS. Removal of Carbon Dioxide by Absorption in a Rotating Packed Bed. Ind. Eng. Chem. Res. 2003;42:2381-2386.

[29] Feron HMF. CO_2 separation with polyolefin membrane contactors and dedicated absorption liquids: performances and prospects. Separation and Purification Technology 2002:27;231-242.

[30] Kelleher T, Fair JR. Distillation Studies in a High-Gravity Contactor, Ind. Eng. Chem. Res. 1996; 35:4646-4655.

[31] Shimomura Y. Coal-fired plant technology - The CO2 wheel: A revolutionary approach to carbon dioxide capture. Modern Power Systems 2003:15-18.

3 Absorber Model

When designing absorption with chemical reaction there are several factors that have to be accounted for. The absorption may be affected by diffusion and convection in the gas phase, and diffusion, convection, and reaction in the liquid phase. One of the most important considerations when designing is the temperature variation within the column due to the heat of absorption of CO_2 and the heat of evaporation of water from the solvent. This is because the temperature may vary significantly over the column, which again influences the equilibrium line, as well as the rate of the chemical reactions involved and the physical properties of the liquid and the gas. For all absorption columns with dumped or structured packing the fluid dynamics of counter current, two phase flow have to be considered in order to describe mass transfer, pressure drop, load limits, and liquid hold up. Several correlations are available in order to estimate the values of these properties since it is impossible to calculate from first principles.

Reactive absorption of CO_2 in an aqueous solution of an alkanolamine can be described by a simplified five component system. An insoluble carrier gas, one reactive acid gas, one volatile component of solution, a non-volatile reactive solvent, and a non-volatile product exist. Gas dissolved in the liquid phase reacts reversibly with non volatile reactive component and forms non-volatile product. The reaction only occurs in the liquid phase.

3.1 Mass Transfer with Chemical Reaction

For a thorough review of the subject briefly introduced in this section see Danckwerts et al.[1], Astarita [2], and Astarita et al.[3]. Where nothing else is indicated the material is drawn from the three aforementioned sources. The occurrence of chemical reaction in absorption systems has two different effects on the overall behaviour of the system. First when a component is absorbed in the liquid it reacts and is therefore consumed. This implies that the driving force for additional absorption remains higher than it would if no chemical reaction was involved. The second effect is that the driving force for mass transfer may be significantly increased when chemical reactions are taking place. The rate enhancement of the absorption may be so large in some cases that one may neglect the liquid side mass transfer resistance. The reaction between an alkanolamine and CO_2 can usually be simplified as an irreversible second-order reaction.

$$CO_2 + \nu R_3 N \xrightarrow{Absorption} P \tag{3.1}$$

For an irreversible second-order reaction the governing equations for reactive gas absorption of CO_2, using film theory, are:

$$D_{CO_2} \frac{d^2 C_{CO_2}}{dx^2} - k_2 C_{CO_2} C_{R_3 N} = 0 \tag{3.2}$$

$$D_{R_3N}\frac{d^2C_{R_3N}}{dx^2}-\nu k_2 C_{CO_2}C_{R_3N}=0 \tag{3.3}$$

Where k_2 is the rate constant for the reaction. With the boundary conditions:

$$x=0:\quad C_{CO_2}=C_{CO_2}^{inf},\quad \frac{dC_{R_3N}}{dx}=0 \tag{3.4}$$

$$x=\delta:\quad C_{CO_2}=C_{CO_2}^{0},\quad C_{R_3N}=C_{R_3N}^{0} \tag{3.5}$$

Figure 3-1 shows the general form of the concentration profiles of solvent and solute in the system described above.

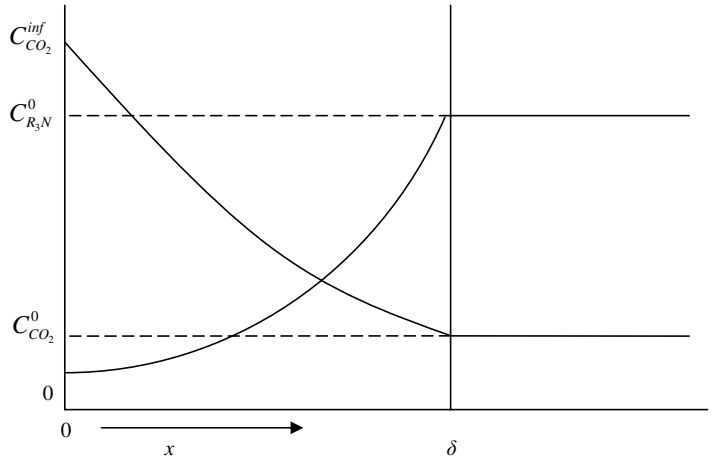

Figure 3-1. Concentration profile for second-order reaction, film model.

Since the system of differential equations, equations (3.2) and (3.3), is coupled and non-linear it is impossible to obtain an exact analytic solution. It is possible to solve the system of equations numerically, but it is computationally expensive when simulating e.g. an absorption tower. Thus it is most common to use approximate analytic relations which generally are expressed in terms of the enhancement factor (*E*). *E* is the ratio of the chemical mass transfer coefficient to the physical mass transfer coefficient:

$$E=\frac{k_{L,CO_2}^{chem}}{k_{L,CO_2}} \tag{3.6}$$

The theory of coupled chemical reactions and mass transfer can be developed on the basis of very crude models of the fluid mechanics such as the two film theory. In general there are three different asymptotic cases when dealing with chemical gas absorption: slow, fast, and instantaneous reaction. In general absorption using aqueous alkanolamines occurs in the fast or the instantaneous regime, or in the transition between the two.

In the slow reaction regime most of the reaction takes place in the bulk of the liquid, thus no rate enhancement takes place. In the fast reaction regime all the reaction takes place in the liquid film leaving the bulk of the liquid in chemical equilibrium. In the transition between fast and instantaneous reaction there is a reaction zone within the liquid film, implying that inside the film close to the gas interface and the bulk liquid interface only diffusion is happening and no reaction. Then in the instantaneous regime the reaction zone has shrunk and forms a reaction plane.

3.1.1 Instantaneous Reaction

If one assumes the reaction to be irreversible the gas and the alkanolamine cannot coexist anywhere in the liquid, see Figure 3-2 for the concentration profiles when the reaction is instantaneous.

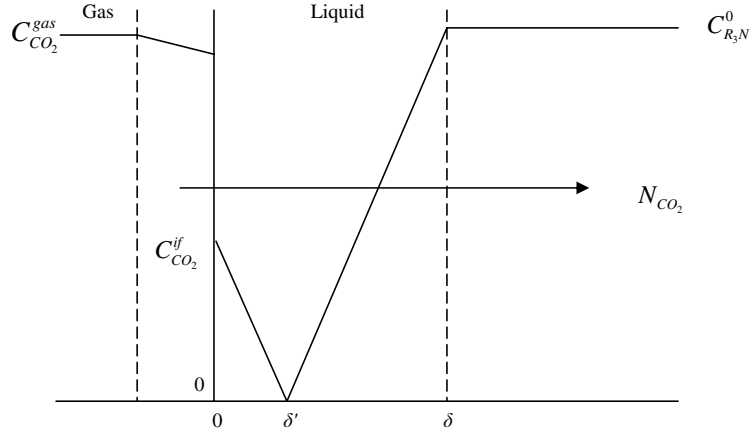

Figure 3-2. Concentration profiles in the liquid film for instantaneous reaction, film model.

The solute gas and reactant must diffuse to the reaction plane at distance δ' from the gas liquid interface. Due to stoichiometry R_3N must reach the reaction plane ν times as fast as CO_2.

$$\nu \frac{D_{CO_2} C_{CO_2}^{if}}{\delta'} = \frac{D_{R_3N} C_{R_3N}^{0}}{\delta - \delta'} \tag{3.7}$$

The value of δ' is obtained from equation (3.7):

$$\delta' = \delta \frac{\nu D_{CO_2} C_{CO_2}^{if}}{\nu D_{CO_2} C_{CO_2}^{if} + D_{R_3N} C_{R_3N}^{0}} \tag{3.8}$$

And given

$$k_{L,CO_2} = \frac{D_{CO_2}}{\delta} \tag{3.9}$$

$$k_{L,CO_2}^{chem} = \frac{D_{CO_2}}{\delta'} \tag{3.10}$$

Using equations (3.6) and (3.8) - (3.10), E_∞ for a bimolecular irreversible instantaneous reaction using film theory can be found:

$$E_\infty = \frac{\delta}{\delta'} = 1 + \frac{D_{R_3N} C_{R_3N}^0}{\nu D_{CO_2} C_{CO_2}^{if}} \tag{3.11}$$

E_∞ for a bimolecular irreversible instantaneous reaction can also be found using the penetration theory and the result is given in equation (3.12) without derivation, the derivation can be found in e.g. Astaria[2]:

$$E_\infty^{pen} = \frac{1 + \frac{D_{R_3N} C_{R_3N}^0}{\nu D_{CO_2} C_{CO_2}^{if}}}{\sqrt{D_{R_3N} / D_{CO_2}}} \tag{3.12}$$

Comparing equations (3.11) and (3.12) makes it clear that when the diffusivities of CO_2 and R_3N are equal equation (3.11) and (3.12) give identical results for E.

3.1.2 Fast Reaction

A common simplification used when describing the fast reaction regime for a second order reaction is to assume a pseudo first order reaction. Figure 3-3 shows the concentration profiles for a situation where the pseudo first order approximation can be applied.

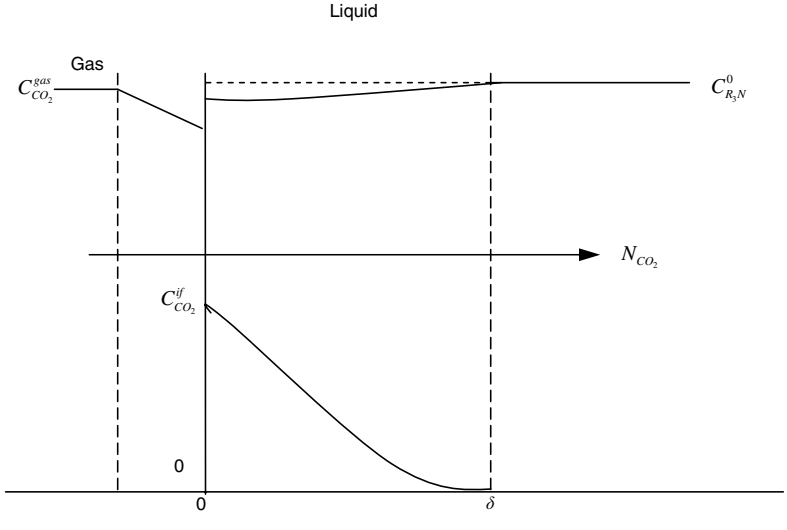

Figure 3-3. Concentrations in the gas and liquid film for a pseudo first order reaction using film theory.

For a pseudo first order reaction it is assumed that the concentration of R_3N is the same throughout the liquid both in the bulk and in the liquid film. This assumption is valid when the concentration of amine is much higher than the interfacial concentration of CO_2. A dimensionless parameter commonly encountered when dealing with mass transfer with chemical reaction M is given in equation (3.14). M defines the ratio of maximum conversion in the film with reaction over maximum transport through film without reaction as shown in equation (3.13).

$$M = \frac{k_2 C_{CO_2}^{if} C_b \delta}{k_{L,CO_2} C_{CO_2}^{if}} \tag{3.13}$$

Then inserting equation (3.9) into (3.13)

$$M = \frac{k_2 D_{CO_2} C_b}{k_{L,CO_2}^2} \tag{3.14}$$

M given by equation (3.14) is also the dimensionless parameter found when writing equation (3.2) on dimensionless form. The parameters M and E_∞ can be used to find whether the absorption is taking place in the slow, fast or instantaneous regimes. When $\sqrt{M} \ll 1$ the reaction is slow and physical absorption dominates the absorption rate. When $\sqrt{M} > 10E_\infty$ the absorption is in the instantaneous regime and E may be approximated with equation (3.11) or (3.12). On the other hand if $\sqrt{M} < 1/2\,E_\infty$ and $\sqrt{M} > 3$ the reaction can be considered to be in the fast regime and the absorption can be approximated to follow pseudo first order behavior. E for a pseudo-first order reaction using film can be approximated by equation (3.15):

$$E = \sqrt{M} \tag{3.15}$$

Equation (3.15) can be found by solving equation (3.2) for a first order reaction where the molecular CO_2 concentration in the bulk is approximately zero. By inspection of equations (3.15) and (3.41) it is clear that the absorption rate of CO_2 into a solution in the fast pseudo-first order regime is independent of k_{L,CO_2}.

3.1.3 Transition from Fast to Instantaneous Reaction

An analytical solution of equations (3.2) and (3.3) can be obtained if certain simplifications are implemented and the reaction, equation (3.1), follows simple second order kinetics. The solution was given by van Krevelen and Hoftijzer[4], and they showed that the simplified analytical solution and numerical solutions were in good agreement. Following is the derivation of the simplified analytical solution found in ref.[4].

Elimination of the term $k_2 C_{CO_2} C_{R_3N}$ from equations (3.2) and (3.3) gives the following equation:

$$D_{CO_2} \frac{d^2 C_{CO_2}}{dx^2} = \frac{D_{R_3N}}{\nu} \frac{d^2 C_{R_3N}}{dx^2} \tag{3.16}$$

Then assuming that no molecular CO_2 exists in the bulk of the solution resulting in the following boundary conditions:

$$x = 0: \quad C_{CO_2} = C_{CO_2}^{if}, \quad \frac{dC_{R_3N}}{dx} = 0 \tag{3.17}$$

$$x = \delta: \quad C_{CO_2} = 0, \quad C_{R_3N} = C_{R_3N}^0 \tag{3.18}$$

Integrating (3.16) twice and substituting boundary conditions (3.17) and (3.18).

$$C_{R_3N}^{if} = C_{R_3N}^0 \left\{ 1 - \frac{D_{CO_2}}{D_{R_3N}} \frac{\nu C_{CO_2}^{if}}{C_{R_3N}^0} \left[\frac{-\left(dC_{CO_2}/dx\right)_{x=0}}{C_{CO_2}^{if}/\delta} - 1 \right] \right\} \tag{3.19}$$

The first term in the square bracket in equation (3.19) is the ratio of the interface concentration gradient to the gradient of the absorbing component in physical absorption, thus the value of E is given:

$$\frac{-\left(dC_{CO_2}/dx\right)_{x=0}}{C_{CO_2}^{if}/\delta} = E \tag{3.20}$$

Then substituting equations (3.11) and (3.20) into equation (3.19) an expression for $C_{R_3N}^{if}$ is found.

$$C_{R_3N}^{if} = C_{R_3N}^0 \frac{E_\infty - E}{E_\infty - 1} \tag{3.21}$$

Equation (3.21) degenerates into the correct asymptotes: $C_{R_3N}^{if}$ when $E = E_\infty$ (instantaneous reaction) and $C_{R_3N}^{if} = C_{R_3N}^0$ when $E_\infty \gg E \gg 1$ (fast pseudo-first order reaction). Knowledge of the value of $C_{R_3N}^{if}$ does not in itself allow for a solution of the problem. What is required is knowledge of the concentration gradient of molecular CO_2 at the interface, thus the concentration distributions only need to be evaluated rigorously in the neighbourhood of the interface. In this neighborhood we may assume that C_{R_3N} is constant since the gradient of C_{R_3N} is zero at the interface. Hence, equation (3.2) may be written approximately as:

$$D_{CO_2} \frac{d^2 C_{CO_2}}{dx^2} - k_2 C_{CO_2} C_{R_3N}^{if} = 0 \tag{3.22}$$

subject to the boundary conditions (3.17) and (3.18). The problem can now be solved analytically and the concentration gradient of CO_2 at the interface is given by:

$$\left(\frac{dC_{CO_2}}{dx}\right)_{x=0} = C_{CO_2}^{if}\frac{\sqrt{k_2 C_{R_3N}^{if}/D_{CO_2}}}{\tanh\sqrt{k_2\delta^2 C_{R_3N}^{if}/D_{CO_2}}} \tag{3.23}$$

Obtaining the value of *E* by combining equation (3.20) and (3.23):

$$E = \frac{\sqrt{k_2\delta^2 C_{R_3N}^{if}/D_{CO_2}}}{\tanh\sqrt{k_2\delta^2 C_{R_3N}^{if}/D_{CO_2}}} \tag{3.24}$$

Substituting equation (3.21) into the square root at the right hand side of equation (3.24):

$$\sqrt{\frac{k_2\delta^2 C_{R_3N}^{if}}{D_{CO_2}}} = \sqrt{\frac{k_2\delta^2 C_{R_3N}^{0}}{D_{CO_2}}\frac{E_\infty - E}{E_\infty - E}} \tag{3.25}$$

Where the quantity $k_2\delta^2 C_{R_3N}^{0}/D_{CO_2}$ is the equivalent to the dimensionless number *M* discussed earlier. Thus, by inserting *M* into equation (3.25) and then equation (3.25) into equation (3.24) the following expression for *E* is obtained:

$$E = \frac{\sqrt{M\dfrac{E_\infty - E}{E_\infty - 1}}}{\tanh\left(\sqrt{M\dfrac{E_\infty - E}{E_\infty - 1}}\right)} \tag{3.26}$$

Equation (3.26) gives *E* as an implicit function and is based on film theory, and is capable of giving values of *E* in the fast and the instantaneous regime and the transition between the the two regimes. Some concern about the applicability the very simplified film theory to real engineering cases has been expressed. E.g. Brian et al.[5] used E_∞ calculated with equation (3.12) based on penetration theory in equation (3.26) for *E* based on film theory, and validated the use by comparing the results to solutions of equations (3.2) and (3.3) with mass transfer coefficients based on E_∞ penetration theory. They found that the results of the simplified analytical solution based on film theory using based on penetration theory agreed within 16 percent with the results of the numerical solution of the differential equations based on penetration theory. Due to the fact that equation (3.26) is an implicit expression for *E* and requires and iterative solution several authors have presented explicit approximations of equation (3.26). Astarita et al.[3] presented the following expression:

$$E = \left[\left(1 + \frac{n^{n/(n-1)}\left(E_i - 1\right)^{1/(n-1)}E_i}{\left(1+M\right)^{n/(2n-2)}}\right)^{1/n} - 1\right] \times \frac{\left(1+M\right)^{n/(2n-2)}}{n^{1/(n-1)}\left(E_i - 1\right)^{1/(n-1)}} \tag{3.27}$$

Where *n* is a constant that decides the smoothness of the fast-instantaneous transition a higher value of *n* gives a smoother transition. *n = 2* is a good approximation for a simple bimolecular

reaction scheme according to the authors. For a review of other explicit expression of E for irreversible second order reactions see Wellek et al.[6].

3.2 Packed Column Model

3.2.1 Models Published in the Literature

In the literature several publications concerning modeling of adiabatic rate based CO_2 absorption in packed columns exist. Following is a brief summary of the main different approaches used for rate based modeling of CO_2 absorption in alkanolamine solutions. The first work concerning static modeling of adiabatic rate based chemical absorption CO_2 was done by Pandya[7]. He set up differential mass and enthalpy balances, and used ideal gas and ideal solution to describe the gas- and liquid-phase and an explicit expression for the enhancement factor resulting in a boundary value problem which was solved by using a shooting method. Pandya[7] showed one calculation example with aqueous MEA as solvent, but no validation against experimental data was presented. Tontiwachwuthikul et al.[8] used principally the same model for systems with aqueous NaOH and MEA as solvents and compared to experimental pilot plant data carried out in their work. The enhancement factor was calculated by an explicit model presented by Welleck et al.[6]. Their calculations show good agreement with experimental data for NaOH-CO_2 and MEA-CO_2 systems. They furthermore presented experimental data for CO_2 absorption with aqueous AMP solutions, a sterically hindered alkanolamine, but no modeling of the AMP-CO_2 system was presented. Pacheco and Rochelle[9] used RATEFRAC, the rate-based distillation module of Aspen Plus combined with electrolyte-NRTL to account for the non-idealities in the liquid phase and using Maxwell-Stefan and enhancement factor theory for absorption of CO_2 and H_2S into aqueous solutions of MDEA. In the most elaborate modeling effort presented so far Kucka et al.[10] set up a rigorous rate-based model for sour gas absorption and applied it to CO_2 absorption in aqueous MEA. The model involves solving a system of partial differential and algebraic equations discretizing in both axial- and film direction. They used Aspen Custom Modeler to solve the systems of equations. The use of enhancement factors was not implemented in their work. To verify the model published pilot plant data found in ref.[8] were simulated with good accuracy for the partial pressure of CO_2, but the temperature of the liquid phase was not captured with the same accuracy. In their work the electrolyte-NRTL model was used to account for the non-idealities liquid phase, while in the gas phase SRK was used. In addition to the models presented in the literature several different commercial software packages custom made for modeling acid gas capture with alkanolamines are available.

3.2.2 Model Development

Due to the nature of the process a rate based model is chosen and since it is a packed column differential mass and energy balances are set up. The model in this work is based on the model developed by Pandya[7] where the process is described by the two film theory and utilization of the assumptions 1-7:

1. The reaction is fast enough to take place in the liquid film and the bulk of the liquid is in equilibrium.
2. Liquid side heat transfer resistance is small compared to the gas phase, thus the liquid interface temperature is the same as the liquid bulk temperature.
3. The liquid side mass transfer resistance for the volatile solvent is negligible.
4. The interfacial surface area is the same for heat and mass transfer.
5. Axial dispersion is not accounted for.
6. The absorption tower is considered to be adiabatic.
7. Both the liquid phase and the gas phase are formally treated as ideal mixtures.

The last assumption concerning liquid phase ideality may seem unrealistic since the system described contains weak electrolytes. Several different thermodynamic models that account for the chemical equilibrium reactions as well as liquid phase non-idealities exist and will be described in chapter 4, Thermodynamic Model. These models can be used for calculating CO_2 partial pressure and liquid speciation over a large loading area. But common features shared by the models that take non-idealities into account is complexity and a large number of adjustable parameters that have to be fitted to experimental solubility data. The models require solving a set of non-linear equations making all of the models computationally time-consuming. Furthermore, it seems uncertain that the quality of experimental data for the solubility of CO_2 in aqueous alkanolamines is good enough to justify the use of elaborate models with many adjustable parameters Gabrielsen et al.[11]. Thus a simple model based on liquid phase ideality and one chemical equilibrium reaction with the non-idealities accounted for in the combined Henry's Law and equilibrium constant is found adequate for the conditions encountered in flue gas cleaning.

As can be seen in equation (2.7) there are only two products in the equilibriated solution due to the reaction between CO_2 and an aqueous tertiary or sterically hindered alkanolamine. The changes in concentration of reactants and products can be related to the rate of absorption of CO_2 by stoichiometry through:

$$\frac{N_{CO_2} a A_c}{1} = \frac{L}{1}\frac{dx_{R_3N}}{dz} = \frac{L}{1}\frac{dx_{H_2O}}{dz} = \frac{L}{-1}\frac{dX_{CO_2}}{dz} = \frac{L}{-1}\frac{dx_{R_3NH^+}}{dz} \tag{3.28}$$

where the mole fraction of chemically bound CO_2 in the bulk of the liquid phase is equal to the mole fraction of bicarbonate ions in the bulk of the liquid phase ($X_{CO_2} = x_{HCO_3^-}$). If the absorbent is a primary or secondary alkanolamine equation (2.6) shows that there are only two species in significant amounts in the loading are that is interesting for flue gas cleaning. The stoichiometry gives the following relations for the rates of absorption:

$$\frac{N_{CO_2} a A_c}{1} = \frac{L}{2}\frac{dx_{R_2NH}}{dz} = \frac{L}{-1}\frac{dX_{CO_2}}{dz} = \frac{L}{-1}\frac{dx_{R_2H_2^+}}{dz} \tag{3.29}$$

where the mole fraction of chemically bound CO_2 in the bulk of the liquid phase is equal to the mole fraction of carbamate ions in the bulk of the liquid phase ($X_{CO_2} = x_{R_2NCOO^-}$).

The total material and energy balance equations and the component material balances for each phase are set up using a differential segment of the packed absorber as shown in Figure 3-4.

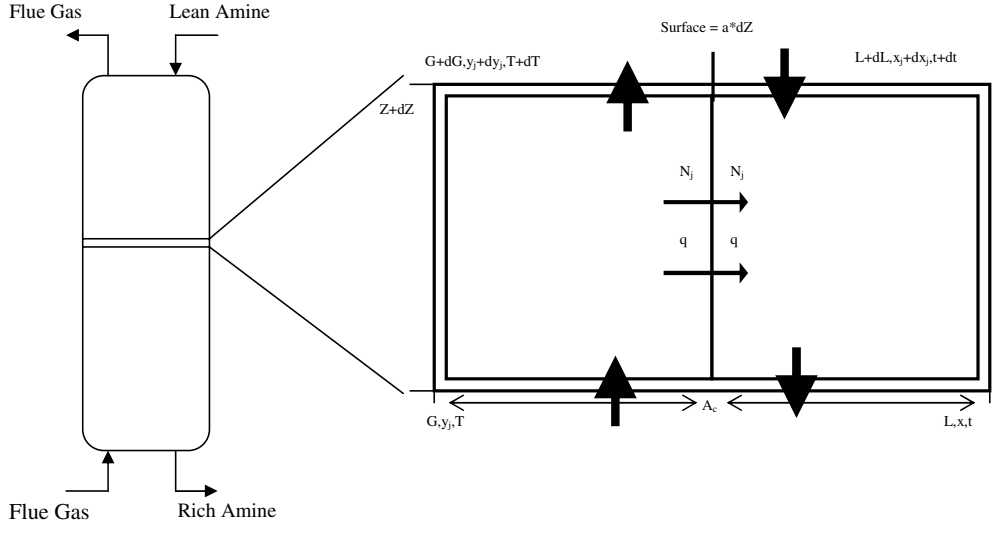

Figure 3-4. Differential element of a packed column.

Then including the stoichiometric relations for the chemical reaction the following system of eight differential equations can be set up for a bicarbonate forming reaction (for derivation of the model see Appendix B):

$$\frac{dG}{dz} = -\left(N_{CO_2} + N_{H_2O}\right) a A_c \tag{3.30}$$

$$\frac{dy_{CO_2}}{dz} = \frac{N_{CO_2} a A_C \left(y_{CO_2} - 1\right) + N_{H_2O} y_{CO_2} a A_c}{G} \tag{3.31}$$

$$\frac{dy_{H_2O}}{dz} = \frac{N_{H_2O} a A_C \left(y_{H_2O} - 1\right) + N_{CO_2} y_{H_2O} a A_c}{G} \tag{3.32}$$

$$\frac{dL}{dz} = -N_{H_2O} a A_c \tag{3.33}$$

$$\frac{dX_{CO_2}}{dz} = \frac{\left(N_{H_2O} X_{CO_2} - N_{CO_2}\right) a A_C}{L} \tag{3.34}$$

$$\frac{dx_{H_2O}}{dz} = \frac{\left(N_{H_2O}\left(x_{H_2O} - 1\right) + N_{CO_2}\right) a A_C}{L} \tag{3.35}$$

$$\frac{dT_G}{dz} = -\frac{q a A_c}{G c_{p,G}} \tag{3.36}$$

$$\frac{dT_L}{dz} = \frac{\left(N_{CO_2} c_{p,CO_2} + N_{H_2O} c_{p,H_2O}\right) a A_c \left(T_L - T_G\right)}{L c_{p,L}} - \frac{q a A_c}{L c_{p,L}} + \frac{\left(N_{CO_2} \Delta H_{CO_2} + N_{H_2O} \Delta H_{H_2O}\right)}{L c_{p,L}} \tag{3.37}$$

For a carbamate forming reaction equation (3.35) must be exchanged with equation (3.38).

$$\frac{dx_{H_2O}}{dz} = \frac{N_{H_2O}\left(x_{H_2O} - 1\right) a A_C}{L} \tag{3.38}$$

This is because water is not a reactant in the carbamate forming reaction.

A pressure drop correlation is straight forward to include in the model as a ninth differential equation to be solved with the system of differential equations. Such pressure drop correlations are found in e.g. Billet and Schultes[12] or Rocha et al.[13,14].

3.2.3 Mass and Heat Transfer

The flux of the volatile components over the phase boundary can be expressed by:

$$N_i = K_{Gi}\left(p_i - p_i^*\right) \tag{3.39}$$

Where p_i^* is the partial pressure of component *i*, that would have been in equilibrium with the liquid phase and p_i is the partial pressure of component *i* in the gas bulk. In order to find $p_{CO_2}^*$ the thermodynamic developed in chapter 4 of this work is used. The equilibrium partial pressure of water $p_{H_2O}^*$ is expressed by an Antoine equation[15]. Mass-transfer coefficients and the specific gas-liquid interfacial can be calculated using correlations from e.g. Billet and Schultes[12] or Rocha et al. [13,14]. Using the two film model and assuming no liquid side resistance for the mass transfer of water, since the liquid phase mainly is water, the overall mass transfer coefficient for water is:

$$K_{G,H_2O} = k_{G,H_2O} \tag{3.40}$$

Using the two film model for the gas- and liquid-side mass-transfer coefficients K_{G,CO_2} is expressed as:

$$\frac{1}{K_{G,CO_2}} = \frac{1}{k_{G,CO_2}} + \frac{H_{CO_2}}{Ek_{L,CO_2}} \tag{3.41}$$

In this work E is calculated using equation (3.26). A Henry's Law relationship is used to find $C_{CO_2}^{inf}$ needed in the expression for E.

The heat transfer coefficient in the gas phase was found by using the Chilton-Colburn analogy. And the expressions for the Chilton-Colburn coefficients were found in Bird et al.[16]. The Chilton-Colburn j-factors are:

$$j_H = \frac{h}{\rho \hat{C}_p v_0}\left(\frac{\hat{C}_p \mu}{\lambda}\right)^{\frac{2}{3}} \tag{3.42}$$

$$j_D = \frac{k_y}{v_0}\left(\frac{\mu}{\rho D_a}\right)^{\frac{2}{3}} \tag{3.43}$$

Using the empirical analogy $j_H = j_D$ isolating h on the left hand side and simplifying the expression on the right hand side the final expression is for the heat transfer coefficient in the gas phase is:

$$h = k_y\left(\frac{\rho \hat{C}_p \lambda^2}{D_a^2}\right)^{\frac{1}{3}} \tag{3.44}$$

The expression for the heat flux between the gas and the liquid phase is given by:

$$q = h\left(T_G - T_L\right) \tag{3.45}$$

Using the model described combined with an accurate thermodynamic model and correlations for physicochemical properties, a packed CO_2 absorber can be modelled and designed.

3.2.4 Packed Column Model Computational Implementation

The system of ordinary differential equations presented in chapter 3.2.2 results in a boundary value problem that is highly nonlinear, thus analytical methods can not be used to solve the system. The liquid is fully described at the top of the absorber column and the gas is fully described at the bottom of the column. Thus, the boundary values for the system are given by the inlet compositions, temperatures and flow rates of the gas and the liquid. In other works e.g. refs.[7,8] a shooting method has been applied to solve the system of differential equations. When the shooting method is applied in the formerly mentioned references, the outlet concentration of

the CO_2 must be specified in order to solve the equations. Furthermore, it is assumed that the both the temperature and the moisture content of the outlet gas are in equilibrium with the inlet liquid which in turn are used to determine the outlet liquid conditions which are used to start a solution procedure using the shooting method.

In this work a collocation was used through a built-in routine in MATLAB® version 7.0 called *bvp4c*, Kierzenka and Shampine[17]. When using this routine to solve the problem only the boundary values i.e. the conditions of the gas and the liquid need to be specified. Furthermore, an initial guess for the profile of the values of the variables for which the system is solved for must be provided as well as an initial guess for the number and position of mesh points needed to solve the system. Luckily the routine *bvp4c* has very low sensitivity towards the initial estimates of variable profiles and number of mesh points, so under the conditions encountered in this work convergence was not a problem. An advantage when using this method is that it does not require the user to provide analytical partial derivatives. A clear advantage of this method compared to the shooting method, as it has been implemented in other works, is that the outlet concentration of CO_2 in the gas does not have to be specified and no assumptions have to be made regarding the temperature or humidity of the outlet gas.

References

[1] Danckwerts PV. Gas-Liquid Reactions. McGraw-Hill. 1970

[2] Astarita G, Mass Transfer With Chemical Reaction, Elsevier Publiching Company. 1967

[3] Astarita G, Savage DW, Bisio A. Gas Treating with Chemical Solvents. Wiley: New York. 1983.

[4] van Krevelen DW, Hoftijzer PJ. Kinetics of Gas-Liquid Reactions Part I. General Theory. Rec. Trav. Chim. 1948;67:563-586.

[5] Brian PLT, Hurley JF, Hasseltine EH. Penetration Theory for Gas Absorption Accompanied by a Second Order Chemical Reaction, AIChE J. 1961;7:226-231.

[6] Wellek RM, Brunson RJ, Law FH. Enhancement Factors for Gas-Absorption with Second-Order Irreversible Chemical Reaction. Can. J. Chem. Engng. 1978;56:181-186.

[7] Pandya, JD. Adiabatic Gas Absorption and Stripping with Chemical Reaction in Packed Towers. Chem. Eng. Comm. 1983; 19: 343-361.

[8] Tontiwachwuthikul P, Meisen A, Lim CJ. CO_2 Absorption by NaOH, Monoethanolamine and 2-Amino-2-Methyl-1-Propanol Solutions in a Packed Column. Chem Eng Sci. 1992;47:381-390.

[9] Pacheco MA, Rochelle GT. Rate-Based Modeling of Reactive Absorption of CO_2 and H_2S into Aqueous Methyldiethanolamine. Ind. Eng. Chem. Res. 1998;37:4107- 4117.

[10] Kucka L, Müller I, Kenig EY, Górak A. On the Modeling and Simulation of Sour Gas Absorption by Aqueous Amine Solutions. Chem. Eng. Sci. 2003;58: 3571-3578.

[11] Gabrielsen J, Michelsen ML, Stenby EH, Kontogeorgis GM. A Model for Estimating CO_2 Solibility in Aqueos Alkanolamines. Ind. Eng. Chem. Res. 2005;44:3348-3354

[12] Billet R, Schultes M. Prediction of Mass Transfer Columns With Dumped and Arranged Packings Updated Summary of the Calulation method of Billet and Schultes. Trans IChemE. 1999;77:498 -504.

[13] Rocha JA, Bravo JL, Fair JR. Distillation columns containing structured packings: A comprehensive model for their performance. 1. Hydraulic models. Ind. Eng. Chem. Res. 1993;32:641-651

[14] Rocha JA, Bravo JL, Fair JR. Distillation columns containing structured packings: a comprehensive model for their performance. 2. Mass-transfer model. Ind. Eng. Chem. Res. 1996;35:1660-1667.

[15] Smith JM, Van Ness HC, Abbot MM. Introduction to Chemical Engineering Thermodynamics (6h Edition). McGraw-Hill International edition

[16] Bird RB, Stewart WE, Lightfoot EN. Transport Phenomena, Second Edition. John Wiley & Sons, Inc. 2002

[17] Kierzenka J, Shampine L. A BVP solver based on residual control and the MATLAB PSE. ACM Trans. Math. Softw. 2001;21:299-316.

4 Thermodynamic Model

To develop efficient processes for separation of CO_2 from flue gases, thermodynamic modeling of the vapor liquid phase equilibrium is the first step. A thermodynamic model is necessary to describe the partial pressure of CO_2 over an aqueous solution of alkanolamines and it can quantify the energy required for regeneration of the alkanolamine. Danckwerts et al.[1] were among the first to develop a thermodynamic model for aqueous CO_2-alkanolamine systems. They used a pseudo-equilibrium constant for the absorption reaction with all activity coefficients equal to one, but corrected approximately for the effects of ionic strength. One of the first widely used models was published by Kent and Eisenberg[2]. They represented the CO_2 and H_2S partial pressures over aqueous solutions of MEA and DEA assuming all activity and vapour phase fugacity coefficients equal to one and fitting two of the chemical equilibrium constants representing the amine equilibria to experimental data. Jou et al.[3] modified this model to include tertiary alkanolamines. Deshmukh and Mather[4] developed a model with activity and fugacity coefficients calculated based on the Debye–Hückel theory and the Guggenheim equation. Austgen et al.[5,6] and Posey and Rochelle[7] developed a thermodynamic framework based on the electrolyte –NRTL model by Chen et al.[8] and Chen and Evans[9]. A common feature for the previously mentioned models is that they all describe the vapor– liquid phase equilibrium (VLE) by utilizing Henry's law constants and different models to describe the liquid and the vapor phase. More recently equations of state (EoS), including the chemical equilibrium reactions in the liquid phase, have been used to describe both phases. Vallée et al.[10] and Chunxi and Fürst[11] developed models based on the electrolyte equation of state by Fürst and Renon[12]. Kuranov et al.[13] developed a model based on the quasichemical hole model by Smirnova and Victorov[14]. The most recent approach, called e-LCVM, is developed by Vrachnos et al.[15]. Finally, Gubbins et al.[16] use the statistical association fluid theory (SAFT) EoS[17,18] to model the VLE of a ternary mixture of water, CO_2 and either MEA or DEA. In this approach no specific chemical reactions of absorption are included in the model. It seems like the chemical reactions are accounted for by assigning association sites to the molecules.

Common features shared by most of the models mentioned above is complexity and a large number of adjustable parameters which have to be fitted to experimental data. The complexity is due to the fact that both chemical and phase equilibrium are described simultaneously, and further the liquid phase is a solution containing weak electrolytes, but probably with a substantial ionic strength. All of the models require solving a set of nonlinear equations, which is computationally time-consuming. A common feature of the models mentioned is the aim to describe the partial pressure of CO_2 over a wide range of conditions e.g. beyond the saturation

point for chemical absorption, further it seems uncertain that the quality of experimental data for the solubility of CO_2 in aqueous alkanolamines is good enough to justify the use of elaborate models which are dependent on a high number of adjustable parameters that has to be fitted.

The objective in this work is to propose a model that describes the partial pressure of CO_2 in the relatively narrow range of conditions encountered in the capture of CO_2 from flue gases in coal fired power plants, low pressure and a relatively narrow temperature range, making it feasible to use a much simpler approach to describe the VLE of CO_2 in single aqueous alkanolamines. This approach simplifies the VLE calculations substantially; only one explicit equation has to be solved for the CO_2 partial pressure over the aqueous alkanolamine solution.

4.1 Model Development

4.1.1 Partial Pressure of CO_2

Part of this work has already been published in Gabrielsen et al. [19,20] for aqueous solutions of MEA, DEA, MDEA and AMP, but improved correlations and new systems are presented here. Using equation (2.6) an equilibrium constant for the reaction of CO_2 with R_2NH can be written:

$$K'_{CO_2} = \frac{\left[CO_2(aq.)\right]\left[R_2NH\right]^2}{\left[R_2NH_2^+\right]\left[R_2NCOO^-\right]} \tag{4.1}$$

or

$$\left[CO_2(aq.)\right] = K'_{CO_2}\frac{\left[R_2NH_2^+\right]\left[R_2NCOO^-\right]}{\left[R_2NH\right]^2} \tag{4.2}$$

Equation (4.2) gives an expression for the concentration of CO_2 in the liquid phase. The concentration of the different species in equation (4.2) can be expressed as a function of the loading and the initial concentration of alkanolamine:

$$\left[R_2NH\right] = (1-2\theta)a_0 \tag{4.3}$$

$$\left[R_2NH_2^+\right] = \left[R_2NCOO^-\right] = a_0\theta = X_{CO_2} \tag{4.4}$$

Inserting the concentrations defined in (4.3) and (4.4) into equation (4.2) gives equation (4.5) which describes the concentration of dissolved CO_2 in the solution:

$$\left[CO_2(aq.)\right] = K'_{CO_2}\frac{(a_0\theta)^2}{(a_0(1-2\theta))^2} = K'_{CO_2}\frac{{X_{CO_2}}^2}{(a_0(1-2\theta))^2} \tag{4.5}$$

Then using Henry's law:

$$p_{CO_2} = K'_{CO_2}H\frac{{X_{CO_2}}^2}{(a_0(1-2\theta))^2} \tag{4.6}$$

Assuming that the carbamate mole fraction accounts for all forms of dissolved CO_2, and combining the chemical equilibrium constant and the Henry's law constant, the final expression for the partial pressure of CO_2 over and aqueous MEA and DEA solution is

$$p_{CO_2} = K_{CO_2} \frac{X_{CO_2}^{\ 2}}{\left(a_0 (1-2\theta)\right)^2} \tag{4.7}$$

where K_{CO_2} is the combined Henry's law and chemical equilibrium constant given in equation (4.10).

For bicarbonate forming solutions such as tertiary and sterically hindered alkanolamines the following expression, based on equation (2.7), for the partial pressure of CO_2 is used[19]:

$$p_{CO_2} = K_{CO_2} X_{CO_2} \frac{\theta}{(1-\theta)} \tag{4.8}$$

where

$$\left[R_3NH^+\right] = \left[HCO_3^-\right] = \theta a_0 = X_{CO_2} \tag{4.9}$$

The expression used for the combined Henry's Law and chemical equilibrium constant is for the different alkanolamine solutions:

$$\ln K_{CO_2} = A + \frac{B}{T} + C\frac{\theta}{T^2} + DX_{CO_2} + E\sqrt{X_{CO_2}} \tag{4.10}$$

The two first adjustable parameters, A and B, represent the standard temperature dependence of the chemical equilibrium constant and are used for all of the alkanolamine systems. The three last adjustable parameters, C, D and E involving the total loading approximate an ionic strength dependence as suggested by Astarita[1921] to account for non-idealities in the system. The different systems correlated have different functionalities of the parameters. In general no more than three parameters are needed to correlate the partial pressure of CO_2 over the solution. The system containing MDEA is the only system that requires four fitted parameters.

4.1.2 Heat of Absorption of CO_2

The parameters B and C in the equation (4.10) are directly related to the heat of desorption of CO_2. Starting from the Gibbs-Helmholtz equation (4.11):

$$\left[\frac{\partial}{\partial T}\left(\frac{\Delta G}{T}\right)\right]_P = -\frac{\Delta H}{T^2} \tag{4.11}$$

and assuming that K_{CO_2} is affected very little by pressure expression (4.12) can be derived for the temperature dependence of K_{CO_2}.

$$\frac{d\ln K_{CO_2}}{dT} = \frac{\Delta H}{RT^2} \tag{4.12}$$

Inserting the derivative, with respect to temperature, of equation (4.10) into equation (4.12) and changing sign gives the heat of absorption of CO_2

$$\Delta H_{CO_2} = R\left(B + 2C\frac{\theta}{T} \right) \tag{4.13}$$

where R is the universal gas constant. Thus the heat of absorption can easily be calculated and compared to experimental data.

4.1.3 Parameter Regression

All experimental data, from the sources cited, within the loading range for which the model was assumed to be valid were included in the parameter regression. Experimental values of the equilibrium constant K_{CO_2} were calculated for each experimental point using the following expressions for MEA and DEA

$$\ln\left(K_{CO_2 exp} \right) = \ln\left(\frac{p_{CO_2 exp}\left(a_0\left(1-2\theta\right)\right)^2}{\left(X_{CO_2} \right)^2} \right) \tag{4.14}$$

and for MDEA, AMP, PZ and PZ-MDEA

$$\ln\left(K_{CO_2 exp} \right) = \ln\left(\frac{p_{CO_2 exp}\left(1-\theta\right)}{X_{CO_2}\theta} \right) \tag{4.15}$$

A modified Marquardt routine was used for the parameter estimation, with the objective function

$$OBJ = \sum_{i=1}^{NP}\left(\ln\left(\frac{K_{CO_2 calc,i}}{K_{CO_2 exp,i}} \right) \right)^2 \tag{4.16}$$

4.2 Model Results and Discussion

The values of the parameters A-E used in equation (4.10) with confidence intervals for six different alkanolamine solutions are given in Table 1. Parameters are regressed for MEA, DEA, AMP, Piperazine, and mixed Piperazine/MDEA solutions. A different number and combination of parameters gave the optimal fit using the lowest number of parameters for the different systems. This might not only be attributed to the non-idealities of the system, but also to the number of experimental data point used for each system and the quality of the data used. The AMP system is adequately described with only two parameters, A and B. Whereas the MDEA system required four parameters, A, B, D and E to achieve a reasonable accuracy of the partial pressure of CO_2 over the solution. Comparison to calorimetric values for the heat of absorption was also important, when available, to decide which parameters and data to use.

Table 4-1. Regressed parameters for the equilibrium constant used in equation (4.10).

System	A	B	C	D	E
MEA–CO_2	26.97±1.37	-8639±546	-695540 ±112000	0	0
DEA–CO_2	30.15±2.20	-8839±663	0	-126.2±22.2	0
MDEA–CO_2	28.44±1.59	-5864±500	0	51.11±19.6	-25.41±6.46
AMP-CO_2	29.99±1.29	-7985±425	0	0	0
PZ-CO_2	28.78±3.03	-8323±1030	0	212.0±59.1	0
PZ-MDEA-CO_2	24.13±1.19	-5462±397	0	0	0

4.2.1 CO_2 Partial Pressure MEA

In the parameter regression for the MEA–CO_2 system 90 experimental points from three different sources, Jou et al.[22], Lee et al.[23], and Mason et al.[24], were used. The three sources of experimental data were chosen for different reasons. Jou et al.[21] was chosen because it is the newest available source and it is from a research group that has published several results for this system earlier, but they found it necessary to publish new data. They point out differences from earlier published data and point out in a clear way why the new data are better compared to the old. Further a wide range of temperatures are covered. One disadvantage concerning this publication is that it only reports results for one concentration of MEA, 30%wt. Lee et al.[22] was included to have data for a 15 %wt solution of MEA. Mason et al.[23] is an earlier source but it has results at very low and very high concentrations of MEA, which is why it was included in the regression. This amount of experimental data assures that both the temperature and concentration dependence of the model is well accounted for. Figure 4-1 shows a comparison between the model correlation and the experimental data for CO_2 partial pressures over a 30 %wt. aqueous solution of MEA (a) and a comparison of model correlation with all experimental data for the partial pressure of CO_2 used in the parameter regression (b).

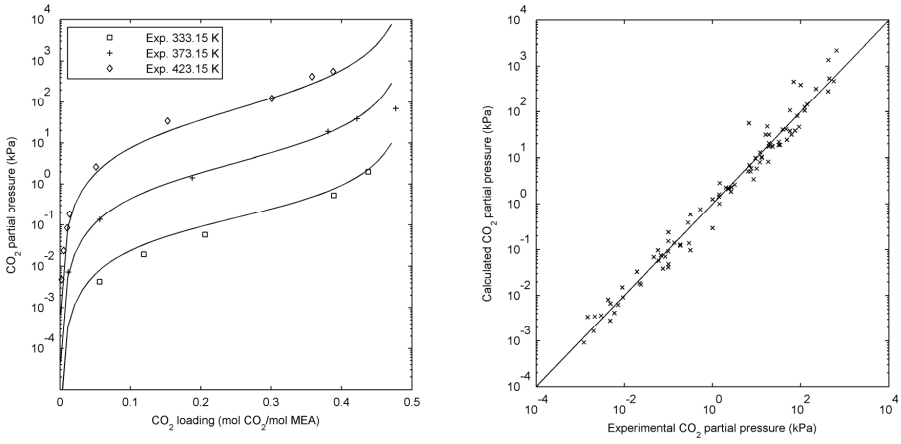

a b

Figure 4-1. (a) Comparison of model correlation results (solid lines) with experimental data for CO2 equilibrium partial pressures over an aqueous 30 wt % MEA solution. (b) Comparison of model correlation with all experimental data for the partial pressure of CO2 used in the parameter regression for aqueous MEA solutions.

4.2.2 CO_2 Partial Pressure DEA

In the parameter regression for the DEA–CO_2 system, 24 experimental points from two different sources, Lawson et al.[25] and Lal et al.[26] were used. Most experimental data on DEA systems containing CO_2 are measured at high pressures or with mixed acid gases, thus not useful in the parameter regression in this work. But to show the capabilities of the model a secondary alkanolamine was included. Figure 4-2 (a) presents a comparison between the model correlation and experimental results for CO_2 partial pressures over a 25 %wt. aqueous solution of DEA. As shown the model gives excellent results for all but one of the experimental points correlated, which at a high loading is most likely due to the carbamate reversion. Figure 4-2 (b) shows a comparison of the experimental and calculated CO_2 partial pressure for all the experimental values used in the regression of parameters in the model.

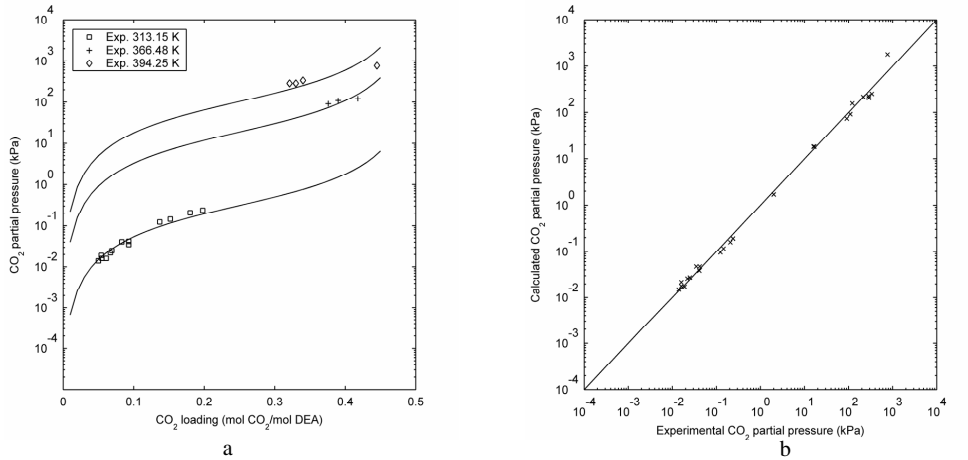

a b

Figure 4-2. (a) Comparison of model correlation results (solid lines) with experimental data for CO2 equilibrium partial pressures over an aqueous 25 wt % DEA solution. (b) Comparison of model correlation with all experimental data for the partial pressure of CO2 used in the parameter regression for aqueous DEA solutions.

4.2.3 CO_2 Partial Pressure MDEA

In the parameter regression for the MDEA–CO_2 system 52 experimental points from one source, Sidi-Boumedine et al.[27], was used. This source was chosen because it is the most recent and the data seem to be more consistent than data published earlier. They used a computer based experimental setup, and two other manual set ups were used to verify the results under one of the conditions measured. Figure 4-3 (a) and (b) present a comparison between the model correlation and the experimental results for CO_2 partial pressures over 25.73 %wt. and 46.88 %wt. aqueous solutions of MDEA respectively.

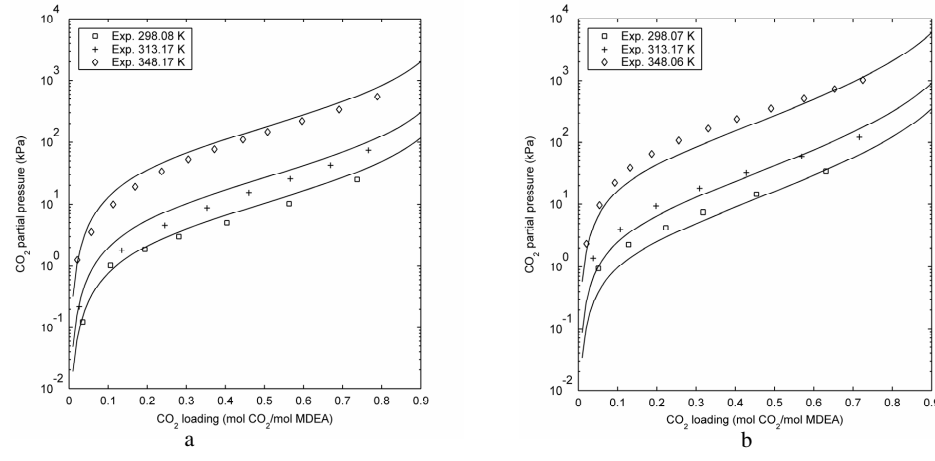

a b

Figure 4-3. (a) Comparison of model correlation results (solid lines) with experimental data for CO2 equilibrium partial pressures over an aqueous 25.73 wt % MDEA solution. (b) Comparison of model correlation results (solid lines) with experimental data for CO2 equilibrium partial pressures over an aqueous 46.88 wt % MDEA solution.

In Figure 4-4 (a) a comparison for all experimental data used in the regression of parameters for the model describing MDEA is shown as a function of the calculated data. From the plots it is easy to see that at low concentration of MDEA the model generally overestimates the partial pressure and at high concentration the model slightly underestimates the partial pressure at low loadings. Figure 4-4 (b) shows that the model successfully represents experimental data from a source not used in the parameter regression (Jou et al.[3]) and was included to show the extrapolation capabilities of the model to temperatures higher than the ones included in the experimental data used for the parameter regression for the MDEA system.

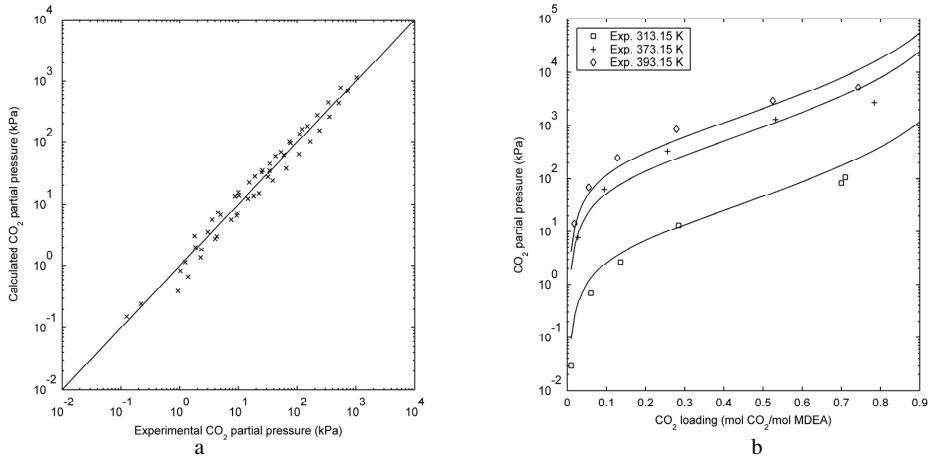

Figure 4-4. (a) Comparison of model correlation with all experimental data for the partial pressure of CO2 used in the parameter regression for aqueous MDEA solutions. (b) Comparison of model extrapolation results (solid lines) with experimental data for CO2 equilibrium partial pressures over an aqueous 50 wt % MDEA solution.

4.2.4 CO_2 Partial Pressure AMP

VLE data from Park et al[28] and Roberts and Mather[29] were used when fitting the parameters for K_{CO_2} for aqueous AMP solutions, 51 experimental points were included in the parameter regression. These experimental data were chosen because they cover a concentration and temperature range and they are quite consistent even though they come from different sources. Figure 4-5 (a) shows a comparison between the model correlation and the experimental data[28] for CO_2 partial pressures over a 30 %wt. aqueous solution of AMP. It can be seen that the correlation gives satisfactory results over the loading range and temperatures considered. Figure 4-5 (b) shows a comparison of model correlation with all experimental data for the partial pressure of CO_2 used in the parameter regression.

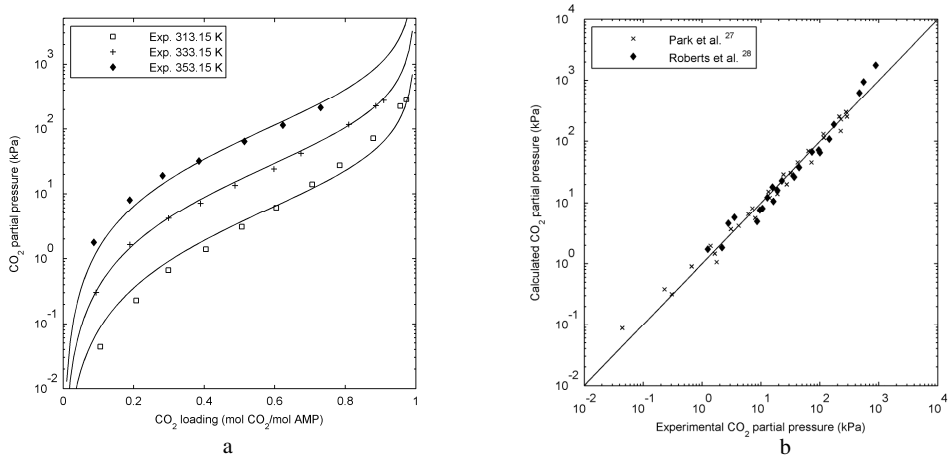

Figure 4-5. (a) Comparison of model correlation results (solid lines) with experimental data for CO2 equilibrium partial pressures over an aqueous 30 wt % AMP solution. (b) Comparison of model correlation with all experimental data for the partial pressure of CO2 used in the parameter regression for aqueous AMP solutions.

Figure 4-6 shows a comparison between CO_2 partial pressures calculated using the proposed model and experimental data from Teng et al.[30] and Tontiwachwuthikul et al.[31], that were not included in the parameter regression, for CO_2 partial pressures over an 18 %wt. aqueous solution of AMP. The experimental data for 313.15 K are from refs.[30,31], 343.15 K is from ref.[30] and for 333.15 and 353.15 K the data are from ref.[31]. It can be seen that the model reproduces the data fairly well, but furthermore there is an inconsistency between the two different data sets that is clearly seen at the lowest temperature.

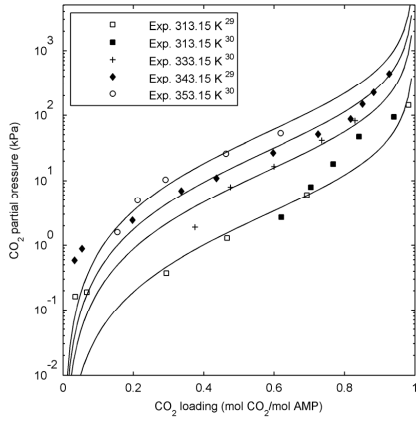

Figure 4-6. Comparison of model results (solid lines) with experimental data refs.[30],[31]not included in parameter regression for CO2 equilibrium partial pressures over an aqueous 18 wt % AMP solution.

Furthermore four data points from ref.[30] at low loading are completely misrepresented; this is most likely due to erroneous measurements. Figure 4-6 may serve as an illustration of the problems in finding reliable and consistent experimental VLE data for CO_2-AMP-H_2O.

4.2.5 CO_2 Partial Pressure Piperazine

Piperazine (PZ) is a ring structured amine with two amine groups. The main use of PZ in CO_2 absorption is as an activator to enhance the overall reaction rate of aqueous MDEA solutions. The chemical equilibrium taking place in the liquid phase when CO_2 is absorbed in an aqueous solution of PZ can be written using the following eight equilibrium equations (Ermatchkov et al.[32]):

$$2H_2O \rightleftharpoons H_3O^+ + OH^- \tag{4.18}$$

$$CO_2 + 2H_2O \rightleftharpoons H_3O^+ + HCO_3^- \tag{4.19}$$

$$HCO_3^- + H_2O \rightleftharpoons H_3O^+ + CO_3^{2-} \tag{4.20}$$

$$PZH^+ + H_2O \rightleftharpoons PZ + H_3O^+ \tag{4.21}$$

$$H_2O + H^+PZCOO^- \rightleftharpoons PZCOO^- + H_3O^+ \tag{4.22}$$

$$PZCOO^- + H_2O \rightleftharpoons PZ + HCO_3 \tag{4.23}$$

$$^-OOCPZCOO^- + H_2O \rightleftharpoons PZCOO^- + HCO_3 \tag{4.24}$$

$$^+HPZH^+ + H_2O \rightleftharpoons PZH^+ + H_3O^+ \tag{4.25}$$

If both the carbamate and dicarbamate of PZ were unstable a theoretical loading maximum of 2 moles of CO_2 per mole of PZ for chemical absorption would be expected according to the following overall reaction:

$$PZ + 2CO_2 + H_2O \rightleftharpoons {}^+HPZH^+ + 2HCO_3^- \tag{4.26}$$

But according to Aroua et al.[33] the overall reaction setting the theoretical loading limit to 1.5 is:

$$3PZ + 2CO_2 \rightleftharpoons {}^-OOCPZCOO^- + 2PZH^+ \tag{4.27}$$

According to Cullinane et al.[34] PZ can mainly be expected to exist in a protonated form when CO_2 is absorbed in the loading range from 0 to 1. The stable dicarbamate species mainly forms when the loading exceeds 1. Thus in this work the reaction between CO_2 and PZ in aqueous solution is simplified to follow the same reaction scheme as a tertiary or sterically hindered alkanolamine, equation (2.7) since the experimental data used for parameter regression are in the loading area between 0 and 1. This is of course a very crude simplification since two different protonated species of PZ exists, PZH^+ and H^+PZCOO^-.

In this work 17 experimental points from Bishnoi et al.[35] were used to fit the adjustable parameters in the equation (4.10) for the combined Henry's Law/chemical equilibrium constant. The experimental data covered only one concentration of PZ and two different temperatures. The capability of extrapolation to other concentrations of PZ was not investigated due to lack of experimental data.

In Figure 4-7 (a) a set of experimental points for the partial pressure of CO_2 over an aqueous solution of PZ is presented together with the correlation carried out in this work.

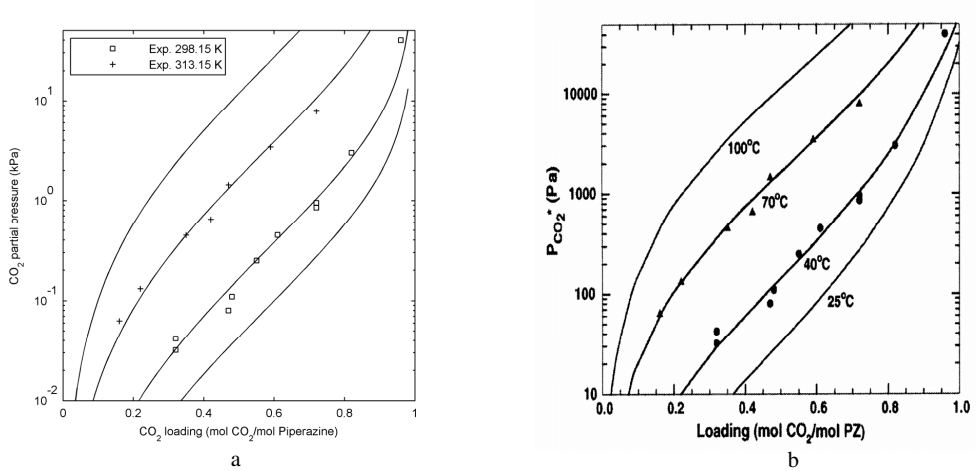

a b

Figure 4-7. (a) Correlated values for the partial pressure of CO2 over an aqueous solution of 0.6 M Piperazine at four different temperatures compared with experimental data from Bishnoi et al.[35]. (b) Figure copied from Cullinane et al.[34] where the lines are based on the e-NRTL model.

The correlation is very good, and further two isotherms outside the temperature range of the experimental data are included to evaluate the models capability of extrapolation. As a basis for comparison Figure 4-7 (b) was included. This is a copy of a figure in Cullinane et al.[34] for the exact same system. The only difference is that the model includes all eight chemical equilibrium presented for PZ equations (4.18-4.25), electrolyte-NRTL to account for the non-idealities in the liquid phase, a Henry's Law relationship for the volatile components, and SRK to account for the non-idealities in the vapor phase. As one can see the two different models behaviour is similar when it comes to estimating the partial pressure of CO_2 over the solution. One weak point of the model in this work is the incapability to calculate the speciation of the solution, but other than that it is hard to see any advantages one can gain by using the complex model presented Cullinane and co-workers.

An immediate question that arises after seeing these results is; why does the simple model work. It does not capture the detailed chemical reactions in the solution in the selected loading range as it has done in the systems presented earlier. By inspecting the detailed speciation presented in the work of Cullinane et al.[34] found by using the e-NRTL model one plausible

explanation is that, in general, the concentration of the carbamate species is low in the loading range examined, especially the dicarbamate. So one may assume that the equilibrium actually described in the model in this work is:

$$\left[PZH^+ + H^+PZCOO^-\right] + HCO_3^- \rightleftharpoons \left[PZ + PZCOO^-\right] + CO_2(aq.) + H_2O \quad (4.28)$$

4.2.6 CO_2 Partial Pressure Blended Piperazine/MDEA

The PZ/MDEA blend is utilized in sour gas sweetening with intent to use PZ as a kinetic promoter for the slowly reacting MDEA following a shuttle mechanism described in Astarita[36]. Studies carried out by Bishnoi et al.[37] suggests that the effect of PZ on the partial pressure of CO_2 over a PZ/MDEA/H_2O solution with a relatively small amount of PZ compared to MDEA on a mol basis (1:10) is only significant for loadings less than 0.2. At higher loading the solution behaves as a "pure" aqueous MDEA solution with respect to CO_2 partial pressure. In the modeling of the VLE of CO_2 in a PZ/MDEA blend, PZ is accounted for by being included in the total amount of alkanolamine so it is assumed that it behaves as MDEA. This assumption should be valid when there is a relatively large difference in the concentration of PZ and MDEA in the blend. This is the reason why an attempt with a simple model is carried out. In the parameter regression 42 experimental points from Liu et al.[38] were used. Points with total loading above 0.8 were not included and only series with a much smaller amount of PZ than MDEA. Figure 4-8 (a) shows a comparison between the model correlation and the experimental data for CO_2 partial pressures over a mixed alkanolamine solution consisting of 0.35 M PZ and 3.15 M MDEA. Figure 4-8 (b) shows a comparison of model correlation with all experimental data for the partial pressure of CO_2 used in the parameter regression. Three different blend ratios were included 0.17 M PZ and 1.53 M MDEA, 0.35 M PZ and 3.15 M MDEA and 0.53 M PZ and 4.77 M MDEA.

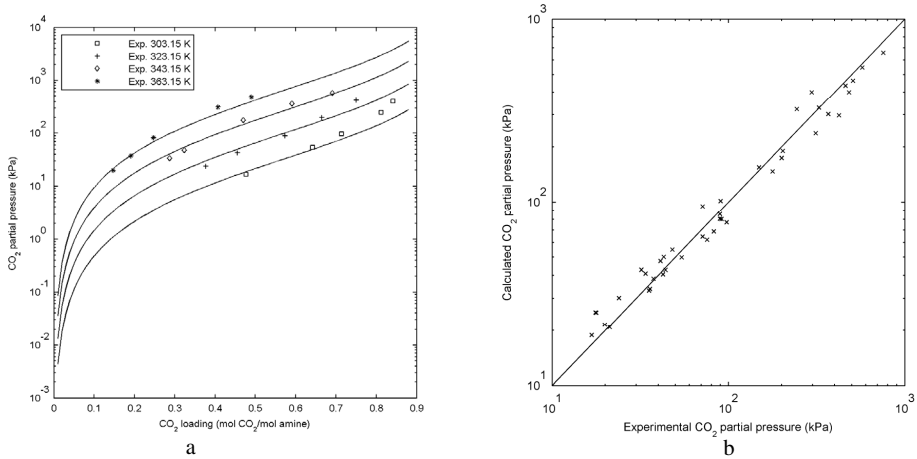

a b

Figure 4-8. (a) Comparison of model correlation results (solid lines) with experimental data for CO2 equilibrium partial pressures over a blended aqueous solution of 0.35 M PZ and 3.15 M MDEA, experimental data from ref.[38]. (b) Comparison of model correlation with all experimental data for the partial pressure of CO2 used in the parameter regression for blended aqueous PZ/MDEA solutions.

In Figure 4-9 (a) the model is used to describe a solution with a higher ratio of PZ to MDEA than the ones used when the adjustable parameters were obtained. The model in general does a better job when values of the partial pressure of CO_2 are estimated for solutions with relatively high loadings. At lower loadings the model overestimates the partial pressure of CO_2; this is due to the reaction of PZ to form carbamate, which is significant due to relatively high contents of PZ in the solution. Figure 4-9 (b) shows how well the model extrapolates to loadings below the area where the data used for parameter fitting lies.

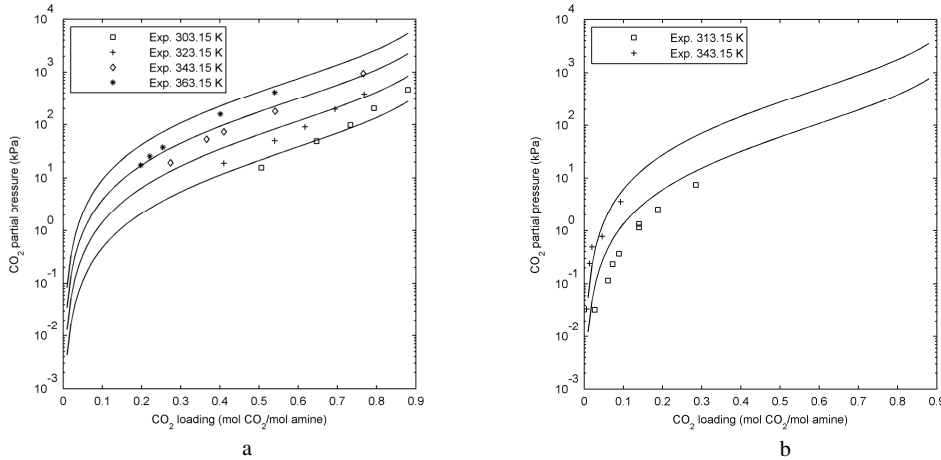

a b

Figure 4-9. (a) Extrapolated values for the partial pressure of CO2 over a blended aqueous solution of 0.7 M Piperazine and 2.8 M MDEA at two different temperatures. Experimental data from Liu et al.[38]. (b) Extrapolated values for the partial pressure of CO2 over a blended aqueous solution of 0.6 M Piperazine and 4.0 M MDEA at two different temperatures. Experimental data from Bishnoi et al.[37].

The model extrapolates quite well, especially at 70°C the higher of the two temperatures, the experimental data are from ref.[37]. The trend of the model is very similar to the trend of the experimental data at the low temperature as well. The main error is that the temperature dependence is not presented correctly, this is expected since at low loadings the main reaction is formation of PZ mono-carbamate, which has a much larger heat of reaction than the formation of bicarbonate the dominating reaction at higher loadings where the data used for parameter regression lies.

4.2.7 Heat of Absorption of CO_2

In Table 4-2 the heat of absorption calculated using the model in this work is compared to experimental data from Carson et al.[39] which were obtained using isothermal displacement calorimetry.

Table 4-2. Heat of Absorption, experimental values are from Carson et al.[39].

System	Model [kJ/mol CO_2]	Experimental [kJ/mol CO_2]
MEA–CO_2	-81.1	-82
DEA–CO_2	-73.5	-69
MDEA–CO_2	-48.8	-49
AMP-CO_2	-66.4	Not Available
Piperazine-CO_2	-69.2	Not Available
Piperazine-MDEA-CO_2	-45.4	Not Available

Carson et al.[39] argue that neither loading nor concentration of the alkanolamine has any significant influence on the heat of absorption under the saturation point so the experimental data are values extrapolated to infinite dilution and at 298.15 K. As it is seen the values obtained in this work show good agreement with values obtained using calorimetry. Other authors have reported data for the heat of absorption of CO_2 with alkanolamines using gas solubility data and applying the integrated form of the Clausius-Clapeyron equation which is used to relate the latent heat of vaporization of a material with its vapor and liquid properties during vaporization or condensation[3,40,41]. The method for calculating heats of absorption from gas solubility data is described in Crynes et al[42]. The values found in other works using gas solubility data for MDEA are of an absolute value 10 kJ/mol higher than the values obtained in this work and through calorimetry. For MEA and DEA the values acquired by modeling gas solubility data agree well with values from this work and from calorimetry. The value for MEA is calculated at 298.15 K and a loading of 0.24 since that is approximately in the middle of the loading area where the

expression is valid. Unfortunately no experimental calorimetric data for the systems containing AMP and PZ were found. The value for the system with the blended alkanolamine systems seems very low. Normally one would expect the value for the heat of absorption of a blended alkanolamine would be between the values of the systems containing the two single amines. In this work the blended system has a lower value than the single with the lowest value, MDEA. This might be due to the fact that the experimental data used are from different sources, and as shown for the AMP system experimental data form different sources can be inconsistent. Furthermore the blended systems used in the parameter regression predominantly consisted of MDEA and behaved as and MDEA system.

4.3 Summary Thermodynamic Modeling

Partial pressures of CO_2 over aqueous solutions of MEA, DEA, MDEA, AMP, PZ and PZ/MDEA have been correlated using a simple approach where only one chemical equilibrium reaction is taken into account, and assuming ideal gas and ideal liquid properties. The approach combines the Henry's law constant and the chemical reaction equilibrium constant for the formation of carbamate for primary and secondary alkanolamines (MEA, DEA) or bicarbonate for sterically hindered and tertiary alkanolamines (AMP, MDEA), resulting in an explicit expression for calculating the partial pressure of CO_2 over an aqueous alkanolamine solution. The diamine PZ has been treated in a similar way as the sterically hindered and tertiary alkanolamines. Heat of absorption values derived from the model agree with experimental data from the literature where available. In Table 4-3 a summary of the different systems treated is presented including the number of parameters fitted, number of experimental points used in the parameter fitting, the percent absolute average deviation (%AAD) and the percent average deviation (%AD). As it can bee seen the %AAD is quite high, but compared to other models applied to the same systems and the simplicity of the model used as well as the uncertainty in the experimental data the results are satisfactory. When looking at the values of %AD it is also clear that for all of the systems treated the partial pressure calculated using the proposed model is in average slightly higher than the experimental values. This is especially pronounced in the MEA system. The same trend can be seen in the parity plots presented earlier.

Table 4-3. Summary of the six different systems treated in the thermodynamics chapter including number of parameters fitted, number of experimental points used in the parameter fitting, the percent absolute average deviation (%AAD) and the percent average deviation (%AD) of the correlated compared to the experimental partial pressure of CO2 over the solution.

	# of parameters	# of points	%AAD	%AD
MEA–CO_2	3	90	57.5	23.1
DEA–CO_2	3	24	22.7	3.9
MDEA–CO_2	4	52	31.4	5.6
AMP-CO_2	2	51	26.1	4.6
PZ-CO_2	3	17	19.7	3.6
PZ-MDEA-CO_2	2	42	15.3	1.4

References

[1] Danckwerts PV, McNeil KM. The Absorption of Carbon Dioxide into Aqueous Amine Solutions and the Effects of Catalysis. Trans. Inst. Chem. Eng. 1967;45:32-37.

[2] Kent RL, Eisenberg B. Better Data for Amine Treating. Hydrocarbon Process. 1976;55:87-90.

[3] Jou FY, Mather A, Otto F. Solubility of H2S and CO2 in Aqueous Methyldiethanolamine Solutions. Ind. Eng. Chem. Process Des. Dev. 1982;21:539-544.

[4] Deshmukh RD, Mather AE. A Mathematical Model For Equilibrium Solubility of Hydrogen Sulfide and Carbon Dioxide in Aqueous Alkanolamine Solutions. Chem. Eng. Sci. 1981;36:355-362.

[5] Austgen DM, Rochelle GT, Peng X, Chen CC. Model of Vapour–Liquid Equilibria for Aqueous Gas–Alkanolamine Systems Using the Electrolyte–NRTL Equation. Ind. Eng. Chem. Res. 1989;28:1060-1073.

[6] Austgen DM, Rochelle GT, Chen CC. Model of Vapour–Liquid Equilibria for Aqueous Gas–Alkanolamine Systems. 2. Representation of H_2S and CO_2 Solubility in Aqueous MDEA and CO_2 Solubility in Aqueous Mixtures of MDEA with MEA or DEA. Ind. Eng. Chem. Res. 1991;30:543-555.

[7] Posey ML, Rochelle GT. A Thermodynamic Model of Methyldiethanolamine–CO_2–H_2S–Water. Ind. Eng. Chem. Res. 1997;36:3944-3953.

[8] Chen CC, Britt HI, Boston JF, Evans LB. Local Composition Model for Excess Gibbs Energy of Electrolyte Systems. Part I: Single Solvent, Single Completely Dissociated Electrolyte Systems. AIChE J. 1982;28:588-596.

[9] Chen CC, Evans LB. A Local Composition Model for the Excess Gibbs Energy of Aqueous Electrolyte Systems. AIChE J. 1986;32:444-454.

[10] Vallée G, Mougin P, Jullian S, Fürst W. Representation of CO2 and H2S Absorption by Aqueous Solutions of Diethanolamine Using an Electrolyte Equation of State. Ind. Eng. Chem. Res. 1999;38:3473-3480.

[11] Chunxi L, Fürst W. Representation of CO_2 and H_2S in aqueous MDEA solutions using an electrolyte equation of state. Chemical Engineering Science 2000;55:2975-2988.

[12] Fürst W, Renon H. Representation of Excess Properties of Electrolyte Solutions Using a New Equation of State. AIChE J. 1993;39:335-343.

[13] Kuranov G, Rumpf B, Maurer G, Smirnova N. VLE modelling for aqueous systems containing methyldiethanolamine, carbon dioxide and hydrogen sulphide. Fluid Phase Equilib. 1997;136:147-162.

[14] Smirnova NA, Victorov AI Thermodynamic Properties of Pure Fluids and Solutions from the Hole Group-contribution Model. Fluid Phase Equilib. 1987;34:235-263.

[15] Vrachnos A, Voutsas E, Magoulas K, Lygeros A. Thermodynamics of Acid Gas–MDEA–Water Systems. Ind. Eng. Chem. Res. 2004;43:2798-2804.

[16] Button JK, Gubbins KE. SAFT Prediction of Vapour–Viquid Equilibria of Mixtures Containing Carbon Cioxide and Aqueous Monoethanolamine or Diethanolamine. Fluid Phase Equilib. 1999;175:158-160.

[17] Chapman WG, Gubbins KE, Jackson G, Radosz M. SAFT: Equation of State Solution Model for Associating Fluids. Fluid Phase Equilib. 1989;52:31-38.

[18] Chapman WG, Gubbins KE, Jackson G, Radosz M. New Reference Equation of State for Associating Liquids. Ind. Eng. Chem. Res. 1990;29:1709-1721.

[19] Gabrielsen J, Michelsen ML, Stenby EH, Kontogeorgis GM. A Model for Estimating CO_2 Solibility in Aqueos Alkanolamines. Ind. Eng. Chem. Res. 2005;44:3348-3354

[20] Gabrielsen J, Michelsen ML, Stenby EH, Kontogeorgis GM. Modeling of CO_2 Absorber Using an AMP Solution, AIChE J. 2006;52:3443-3451.

[21] Astarita G, Mass Transfer With Chemical Reaction, Elsevier Publishing Company. 1967

[22] Jou F-Y, Mather AE, Otto F D. The Solubility of CO_2 in a 30 Mass Percent Monoethanolamine Solution. Can. J. Chem. Eng. 1995;73:140-147.

[23] Lee J I, Otto FD, Mather AE. The Measurement and Prediction of The Solubility of Mixtures of Carbon Dioxide and Hydrogen Sulphide in a 2.5 N Monoethanolamine Solution. Can. J. Chem. Eng. 1976;54:214-219.

[24] Mason JW, Dodge BF. Equilibrium Absorption of Carbon Dioxide by Solutions of the Ethanolamines. Trans. Amer. Inst. Chem. Eng. 1936;32:27-48.

[25] Lawson JD, Garst AW. Gas Sweetening Data: Equilibrium Solubility of Hydrogen Sulfide and Carbon Dioxide in Aqueous Monoethanolamine and Aqueous Diethanolamine Solutions. J. Chem. Eng. Data. 1976;21:20-30.

[26] Lal D, Otto FD, Mather AE. The Solubility of H_2S and CO_2 in a Diethanolamine Solution at Low Partial Pressures. Can. J. Chem. Eng. 1985;63:681-685.

[27] Sidi-Boumedine R, Horstmann S, Fischer K, Provost E, Fürst W, Gmehling J. Experimental determination of carbon dioxide solubility data in aqueous alkanolamine solutions. Fluid Phase Equilib. 2004;218:85-94.

[28] Park SH, Lee KB, Hyun JC, Kim SH. Corellation and prediction of the solubility of Carbon Dioxide in Aqueous Alkanolamine and Mixed Alkanolamine Solutions. Ind. Eng. Chem. Res. 2002;41:1658-1665.

[29] Roberts BE, Mather AE. Solubility of CO_2 and H_2S in a Hindered Amine Solution. Chem. Eng. Comm. 1988;64:105-111.

[30] Teng TT, Mather AE. Solubility of CO_2 in an AMP Solution. J. Chem. Eng. Data. 1990;35:410-411.

[31] Tontiwachwuthikul P, Meisen A, Choon JL. Solubility of CO_2 in 2-Amino-2-methyl-1-propanol Solutions. J. Chem. Eng. Data. 1991;36:130-133.

[32] Ermatchkov V, Perez-Salado Kamps A, Maurer G. Chemical equilibrium constants for the formation of carbamates in (carbon dioxide + piperazine + water) from ^{1}H-NMR-spectroscopy, J. Chem. Thermodynamics. 2003;35:1277-1289.

[33] Aroua MK, Salleh RM. Solubility of CO_2 in Aqueous Piperazine and its Modeling Using the Kent-Eisenberg Approach, Chem. Eng. Technol. 2004;27:65-70.

[34] Cullinane JT, Rochelle GT. Thermodynamics of aqueous potassium carbonate, piperazine, and carbon dioxide, Fluid Phase Equilib. 2005;227:197-213.

[35] Bishnoi S, Rochelle GT. Absorption of carbon dioxide into aqueous piperazine: reaction kinetics, mass transfer and solubility, Chem. Eng. Sci. 2000;55:5531-5543.

[36] Astarita G, Savage DW, Bisio A. Gas Treating with Chemical Solvents. Wiley: New York. 1983.

[37] Bishnoi S, Rochelle GT, Thermodynamics of Piperazine/Methyldiethanolamine/Water/Carbon Dioxide, Ind. Eng. Chem. Res., 2002, 41, 604-612.

[38] Liu HB, Zhang CF, Xu GW. A Study on Equilibrium Solubility for Carbon Dioxide in Metyldiethanolamine-Piperazine-Water Solution, Ind. Eng. Chem. Res. 1999;38:4032-4036.

[39] Carson JK, Marsh KN, Mather AE. Enthalpy of Solution of Carbon Dioxide in (water + monoethanolamine, or diethanolamine, or N-methyldiethanolamine) at T = 298.15 K[a]. J. Chem. Thermodynamics. 2000; 32:1285-1296.

[40] Jou FY, Otto FD, Mather AE. Vapor-Liquid Equilibrium of Carbon Dioxide in Aqueous Mixtures of Monoethanolamine and Methyldiethanolamine. Ind. Eng. Chem. Res. 1994;33;2002-2005.

[41] Lee JI, Otto FD, Mather AE. Solubility of Carbon Dioxide in Aqueous Diethanolamine Solutions at High Pressures. J. Chem. Eng. Data, 1972;17:465-468.

[42] Crynes BL, Maddox RN. How to Determine Reaction Heats from Partial-Pressure data. Oil and Gas Journal. 1969;67:65-67.

5 Chemical Reaction Kinetics for CO_2 in an AMP Solution

Despite the fact that the chemical kinetics of CO_2 absorption in AMP solutions have been the subject of numerous studies, there is no universal agreement on the chemical kinetic expressions[1,2]. A second order reaction rate constant (k_2) for the reaction between CO_2 and AMP is given by Saha et al.[1]. Saha et al.[1] show that the most probable reaction scheme for CO_2 absorption in aqueous AMP is the formation of carbamate, through a zwitterion mechanism acting as a transition intermediate, followed by carbamate reversion to bicarbonate. Thus the chemical equilibrium reaction followed is equation (2.7). Recently Camacho et al.[3] presented an expression for k_2 where possible temperature profiles in the reaction zone were taken into account. This expression gives values for k_2 that are approximately two orders of magnitude lower than the values presented by other authors. Due to the fact that there seems to be disagreement between different authors and that the kinetics have been determined only in a limited concentration and temperature range, a new experimental study of the kinetics of CO_2 absorption into AMP solutions is of interest. In the work of Saha et al.[1] the highest AMP concentration considered is 2 M and the highest temperature considered is 45°C. In a commercial absorber, concentrations up to 3 M could be possible and temperatures up to 60°C might be encountered. Thus, for industrial applications both higher concentrations and temperatures are of interest. There is uncertainty as to whether an Arrhenius equation for the rate constant obtained at lower temperatures can be extrapolated to higher temperatures. Thus, experimental studies covering a range from 1.0 M to 3.0 M AMP and a temperature range from 30°C to 50°C using a string of discs absorber have been carried out in order to verify the chemical rate constant and to extend the concentration and temperature range where it is known.

5.1 Experimental

5.1.1 Background

In order to design absorption equipment for chemical absorption the kinetic constants of the involved chemical reactions must be known. Physicochemical properties like diffusion and solubility are closely linked with the reaction kinetics making it difficult to design an experimental apparatus measuring the chemical kinetics specifically. Several different gas/liquid contactors designed for measurement of chemical kinetic constants exist and can in general be divided into two groups, Astarita[4]:

1. Absorbers for which the liquid dynamics are well understood and amenable to rigorous calculation.

2. Absorbers which reproduce, on a laboratory scale, the characteristics of industrial absorbers.

The wetted wall, laminar jet, rotating drum and the single sphere absorber are found in the first category; in the second category are the string of spheres and string of discs. In this work a string of discs contactor has been used. The string of discs disturbs the liquid film at regular intervals to imitate the situation in a packed tower and thus normally used to imitate packed column absorption. In order to calculate the mass transfer coefficient from the rate of absorption the mass transfer area should be well defined.

Since k_2 cannot be directly measured for reactive chemical absorption a theory must be utilized in order to calculate it from data that are possible to measure. In this work the two film theory utilizing an expression for the enhancement factor is used. The reactions that are investigated are furthermore assumed to be in the fast regime where the conditions for pseudo first order are followed. E in the pseudo first order regime can be estimated using equation (3.15) when the two film theory is used. Furthermore assuming that all the mass transfer resistance is in the liquid phase the following expression describing the flux of CO_2 from the gas to the liquid is valid.

$$J_{CO_2} = Ek_L\left(C_{CO_2}^{\inf} - C_{CO_2}^{0}\right) \tag{5.1}$$

where

$$J_{CO_2} = \frac{N_{CO_2}}{a} \tag{5.2}$$

Assuming pseudo first order reaction and that all CO_2 reacts with the chemical absorbent leading to no molecular CO_2 in the bulk of the liquid. If equations (3.15) and (5.2) are combined it is clear that the absorption rate of CO_2 into the solution is independent of k_L if it can be approximated to be in the pseudo-first order regime as seen in equation (5.3).

$$J_{CO_2} = \sqrt{k_2 C_B D_{CO_2}}\, C_{CO_2}^{\inf} \tag{5.3}$$

Solving equation (5.3) for k_2

$$k_2 = \frac{J_{CO_2}{}^2}{C_B D_{CO_2} C_{CO_2}^{\inf\ 2}} \tag{5.4}$$

Since the partial pressure of CO_2 throughout the column is not uniform and thus not the concentration of free CO_2 at the liquid interface, an expression taking the average must be utilized. $\Delta C_{CO_2,LM}$ can be seen as the logarithmic driving force expressed in concentration of CO_2 between the liquid interface and the liquid bulk.

$$\Delta C_{CO_2,LM} = \frac{\left(C^{\inf}_{CO_2,in} - C^{0}_{CO_2,out}\right) - \left(C^{\inf}_{CO_2,out} - C^{0}_{CO_2,in}\right)}{\ln\left(\frac{C^{\inf}_{CO_2,in} - C^{0}_{CO_2,out}}{C^{\inf}_{CO_2,out} - C^{0}_{CO_2,in}}\right)} \tag{5.5}$$

But since $C^{0}_{CO_2,out}$ is assumed to be equal to zero the expression used is

$$\Delta C_{CO_2,LM} = \frac{C^{\inf}_{CO_2,in} - C^{\inf}_{CO_2,out}}{\ln\left(\frac{C^{\inf}_{CO_2,in}}{C^{\inf}_{CO_2,out}}\right)} \tag{5.6}$$

then the interfacial concentration of molecular CO_2 is given by:

$$C^{\inf}_{CO_2} = \Delta C_{CO_2,LM} \tag{5.7}$$

Inserting (5.7) into (5.4) and utilizing Henry's law:

$$k_2 = \frac{{J_{CO_2}}^2 H^2_{CO_2}}{C_{AM} D_{CO_2} {p_{CO_2}}^2} \tag{5.8}$$

Equation (5.8) is used to calculate k_2 from the experimental data. In the calculations using equation (5.8) it is assumed that the concentration of AMP (C_{AM}) is uniform throughout the string of discs. This assumption is valid since the amount of CO_2 absorbed is much smaller than the total amount of AMP.

In order to develop an expression to calculate the interfacial mass transfer area a base (NaOH) with known kinetics is used. When the kinetics of the reaction is known, one may combine equations (5.2) and (5.8). Assuming no gas phase mass transfer resistance the expression for the mass transfer area is:

$$a = \frac{N_{CO_2} H_{CO_2}}{\sqrt{k_2 C_{NaOH} D_{CO_2}}\, p_{CO_2}} \tag{5.9}$$

If the experiments used to find k_2 are carried out under conditions where the mass transfer resistance in the gas phase should be accounted for and a correlation for k_g is needed. Then using the two film theory $K_{g,ov}$ can be expressed.

$$K_{G,ov} = \frac{k_g E k_L}{E k_L + H_{CO_2} k_G} \tag{5.10}$$

Then, assuming that that there is no free CO_2 in the bulk of the liquid:

$$J_{CO_2} = K_{G,ov} p_{CO_2} \tag{5.11}$$

Inserting for $K_{g,ov}$ and rearranging the expression:

$$\frac{p_{CO_2}}{J_{CO_2}} = \frac{1}{k_G} + \frac{H_{CO_2}}{\sqrt{k_2 C_{NaOH} D_{CO_2}}} \tag{5.12}$$

Solving for k_2:

$$k_2 = \frac{\left(H_{CO_2} k_G J_{CO_2}\right)^2}{C_{NaOH} D_{CO_2} \left(J_{CO_2} - p_{CO_2} k_G\right)^2} \tag{5.13}$$

To find expression for the mass transfer area when including mass transfer resistance in the gas film, equations (5.2) and (5.12) are combined:

$$a = \left(\frac{1}{k_G} + \frac{H_{CO_2}}{\sqrt{k_2 C_{NaOH} D_{CO_2}}} \right) \frac{N_{CO_2}}{p_{CO_2}} \tag{5.14}$$

5.1.2 Experimental Setup and Method

The string of discs apparatus contains a string of discs made of unglazed ceramic material. In this specific apparatus there are 43 discs with a diameter of 0.015 m and a thickness of 0.004 m resulting in a geometric surface area of 0.0219 m^2. The discs are arranged on a string in a vertical row at alternating straight angles as can be seen in Figure 5-1. A flow sheet for the experimental setup is also given. The string of discs contactor is operated in a counter-current mode. The liquid is fed from the top through a tube that ends in a jet and is removed in a small tube from a funnel as shown. The gas is fed from the bottom and the distance from the feed point to the first disc should be long enough to calm the gas flow. The liquid and gas flows can be independently adjusted using a peristatic liquid pump and gas blower respectively. The flow of the blower is controlled by a Siemens Micromaster Frequency Transmitter. The concentration of CO_2 in the feed gas is controlled by using Bronkhorst Hi-Tec mass flow controllers and the concentration of the CO_2 bleed is monitored using an IR Rosemount Binos 100 online CO_2 analyzer. The inner diameter of the glass column is 0.026 m.

To be able to use the expressions developed earlier to calculate the mass transfer area and the chemical rate constant, the absorption flux and the concentration of molecular CO_2 in the liquid must be known form the experiments. The total absorption flux of the solute is calculated by taking the solute balance over the entire system. It is given by the flow of the solute into the system minus the amount going out of the system through the bleed gas to the gas analyzer. This method of flux calculation gives higher accuracy compared to a method based on the balance just over the disc contactor. In the later case numerical uncertainty arises due the subtraction of two nearly equal numbers. The overall absorption rate in the disc contactor is given by:

$$N_{CO_2} = Q_{CO_2}^{in} - Q_{CO_2}^{out} \tag{5.15}$$

where N_{CO_2} is the molar absorption rate (mol/s), $Q_{CO_2}^{in}$ and $Q_{CO_2}^{out}$ are the molar flows of CO_2 in and out of the system respectively.

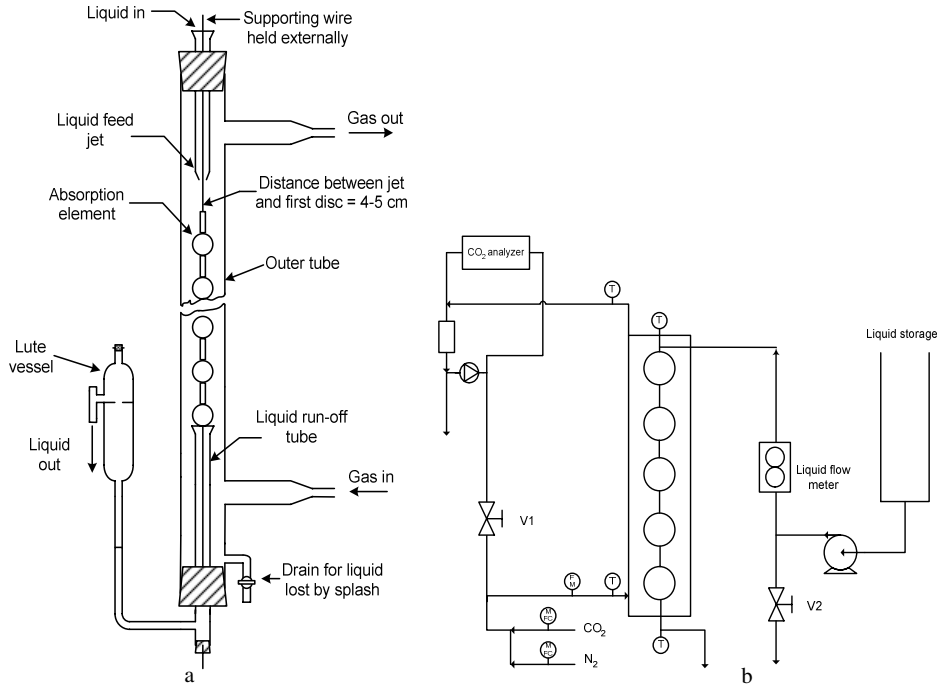

Figure 5-1. (a) Arrangement of string of discs absorber column (b) Experimental set-up of the string of discs absorption column.

The amount of the solute entering into the system can be obtained from the mass flow controller reading. The amount of the solute going out of the system is obtained starting from a mass balance of the inert gas flow:

$$Q_{N_2}^{out} = Q_{N_2}^{in} \tag{5.16}$$

Next dividing equation (5.16) with $y_{N_2}^{out}$ on both sides:

$$Q_{tot}^{out} = \frac{Q_{N_2}^{in}}{y_{N_2}^{out}} \tag{5.17}$$

Multiplying both sides with $y_{CO_2}^{out}$ and assuming that the gas is saturated with water:

$$Q_{CO_2}^{out} = Q_{N_2}^{in} \frac{y_{CO_2}^{out}}{y_{N_2}^{out}} = Q_{N_2}^{in} \frac{y_{CO_2}^{out,wet}}{1 - \left(\frac{p_{H_2O}^{vap}}{P_{tot}} \right) - y_{CO_2}^{out,wet}} \tag{5.18}$$

But since the gas leaving is the same as the gas analyzed for CO_2, and since it is dry, the expression used to find the amount of CO_2 leaving the system is:

$$Q_{CO_2}^{out} = Q_{N_2}^{in} \frac{y_{CO_2}^{out,dry}}{1 - y_{CO_2}^{out,dry}} \tag{5.19}$$

In the apparatus it is assumed that the concentration of chemically bound CO_2 in the solution at any point of the string of discs is zero, and thus the concentration of AMP is constant over the string of discs.

5.2 Mass Transfer Area

The mass transfer area is found by CO_2 absorption into 0.2 M NaOH assuming pseudo-first order reaction and assuming gas film mass transfer resistance and can thus be calculated using equation (5.14). The expression for the gas film mass transfer coefficient was found in Ma´mun et al.[5] and for all liquid rates the percentage gas side mass transfer resistance was approximately 4.7. The experiments were carried out at 30°C and since the only parameter that was varied was the liquid rate, which was varied between 15 and 80 ml/min the gas flow was kept constant at 2.8 m^3/hr. The kinetic constant and all physicochemical properties needed to calculate the mass transfer area from the experiments were obtained from Pohorecki et al.[6] except the viscosity of the solution which was found in Vazquez et al.[7]. The viscosity of the NaOH solution is used when calculating the diffusivity of CO_2. Thus, the diffusivity represents an uncertainty in the calculation of the mass transfer area since it is crucial that all physicochemical data used in the calculation of the mass transfer area are the same as the one used when finding the kinetic expression for the solvent, in this case NaOH, used to find the mass transfer area. As a test two different expressions for the diffusivity of CO_2 in water were used, the other source for the diffusivity of the CO_2 in water was Ko et al.[8]. The deviation between the two different expressions for the diffusivity is approximately 4% thus yielding in a 2% deviation in the calculated mass transfer area. This is as expected when examining equation (5.9) used to calculate the mass transfer area. It is also clear that the experimentally found area is more sensitive towards the Henry's law constant and the measured flux of CO_2 than the diffusivity of CO_2 in the liquid phase. But clearly the largest sensitivity is towards the CO_2 concentration in the bleed gas where a 5% change in the bleed CO_2 concentration gives approximately 8% change in the experimental area. Thus it is very important to do exact calibrations of the IR analyzer and to wait long enough in order for the system to reach steady state before recording the experimental data. The reason for the strong dependency is that the value of the CO_2 concentration in the bleed gas is used both when calculating the flux of CO_2 and for the concentration of free CO_2 in the liquid. As it is seen in Figure 5-2 the mass transfer area is clearly a function of liquid rate. At low liquid rate the surface is probably not completely wetted and at very high liquid rates ripples that cause a high surface area might appear. Under the conditions presented in this work this was not visually observed, but it would probably be

difficult to detect. The geometrical mass transfer area is equal to the experimental effective mass transfer area at flow rates of approximately 40 ml/min.

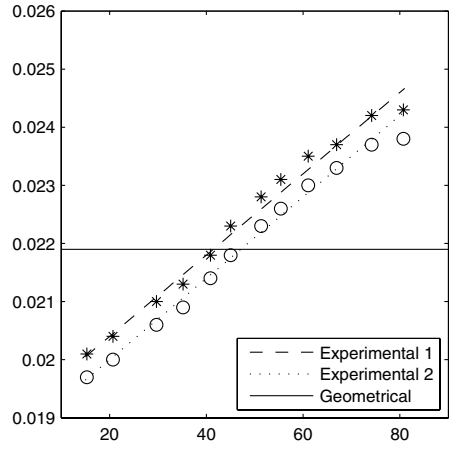

Figure 5-2. Comparison of geometric and experimental mass transfer area for the string of discs apparatus

5.3 Validation Using MEA

An attempt to validate the string of discs absorber as an apparatus to measure k_2 for the reaction between CO_2 and aqueous alkanolamine solutions was carried out. The experiments presented using a 30%-wt solution of MEA were conducted by SINTEF[9]. MEA was chosen as a reference system due to the relatively well defined kinetic constant. The experimental data for the temperatures 25, 30, 40 and 50°C and with a liquid rate of approximately 53 ml/min and a gas rate of approximately 3 m^3/h were reported. As seen in Figure 5-2 a liquid rate of approximately 55 ml/min results in a mass transfer area slightly higher than the geometric surface area of the contactor. When calculating J_{CO2} using equation (5.2) for these experiments the mass transfer area used was the experimentally mass transfer area. In Figure 5-3 an Arrhenius plot of experimental data are compared with a correlation presented by Versteeg et al.[10]. The chemical rate constant in Figure 5-3 was calculated using equation (5.13) and an expression for H_{CO_2} presented by Tsai et al.[11]. The percentage of mass transfer resistance in the gas phase for these experiments varied between approximately 13 and 23% and is important to include in the calculations. The expression for the mass transfer coefficient was found in Ma´mun et al.[5]. Two different correlations for D_{CO_2} in the solution were used. One from Ko et al.[8] and another using the diffusivity of CO_2 in water and a Stokes-Einstein viscosity relationship as described in Versteeg et al.[10]. Calculations of k_2 using H_{CO_2} from Hoff et al.[12] were carried out as well. In Table 5-1 %AAD are presented for the four different cases where

the two different physicochemical properties H_{CO_2} and D_{CO_2} are varied. It is clear that there is a large variation in the calculated value of k_2 depending on the physicochemical properties used.

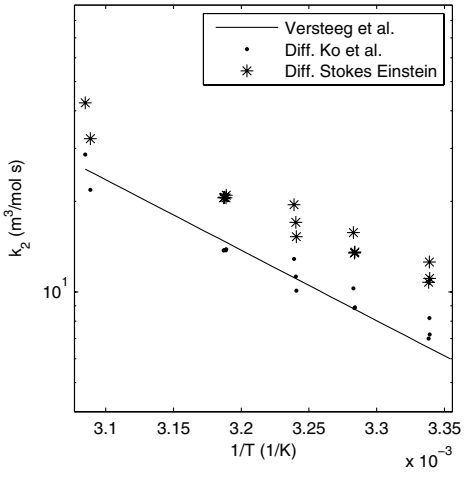

Figure 5-3. 30% wt MEA experimental vs correlation from Versteeg et al.[10] using one expression for the Henry's Law constant, ref.[11], but two different expression for the diffusivity of CO2 in the solution one based on a the diffusivity of CO2 in water and the Stokes Einstein relationship, the other From Ko et al.[8].

The deviations between experimental data and values found using a correlation from the literature clearly show that one has to be extremely careful when choosing expressions for the various physicochemical properties when trying to validate an experimental method for finding kinetic constants in reactive gas absorption. In order to get a fair comparison the same expressions for the physicochemical properties should be used.

Table 5-1 %AAD between k_2 found experimentally and a correlation from literature Versteeg et al.[10].

Henry's Law Constant	Diffusivity	%AAD
H_{CO_2} ref.[11]	D_{CO_2} Ko et al.[8]	10.6
	D_{CO_2} Stokes-Einstein	61.09
H_{CO_2} ref.[12]	D_{CO_2} Ko et al. [8]	41.3
	D_{CO_2} Stokes-Einstein	113.9

5.4 Experimental Procedure

AMP was obtained from Acros Organics with a stated purity of 99%. AMP is a white solid at room temperature. The melting point for AMP is 31°C at atmospheric pressure; therefore the AMP had to be melted before it was mixed with water in order to obtain a solution with the preferred concentration. Solutions with concentrations 1, 1.5, 2 and 3 M were prepared by weighing in. AMP analysis by titration, as described in section 6.1.3 Liquid Analysis, of the

prepared solutions was carried out in order to verify the concentration of the solutions. The solutions were found to 0.99, 1.53, 2.02 and 2.99 M at room temperature. The string of discs absorber as presented in Figure 5-1 and described in the section 5.1.2 was used for the experiments. The liquid flow rate was kept at approximately 40 ml/min for all of the experiments. Three different temperatures were used during the experiments: 30, 40 and 50°C. The IR Rosemount Binos 100 CO_2 analyzer was calibrated at least once a day in order to get reliable results. The apparatus was cleaned by running de-ionized water through the system after every time it was used.

5.5 Results and Discussion

Table 5-2 through Table 5-4 report the experimental partial pressures and absorption fluxes of CO_2 as well as the physicochemical properties that are needed to calculate k_2 via equation (5.13). The percentage of mass transfer resistance in the gas phase for these experiments varied between approximately 2.0 and 6.4 % and is included in the calculations. The expression for the mass transfer coefficient was found in Ma´mun et al.[5]. Inspection of the experimentally obtained values of k_2 shows that in many cases it changes with the partial pressure of CO_2 at a given temperature and concentration of AMP. This is not expected. In the experimental data obtained in this work, k_2 generally decreases as p_{CO_2} increases. This behavior may be attributed to many reasons, most likely due the uncertainty when obtaining $p_{CO_2}^{out}$ and maybe the system had not reached steady state yet when the data were obtained. This is further supported by looking at the data reported for the 1.5 M solution of AMP. These were the last experiments carried out, thus the operator had gained more experience in using the equipment. When looking at the k_2 values reported at 313 and 323 K for 1.5 M AMP, they show no consistent sinking trend with increasing partial pressure of CO_2. But for the k_2 values reported at 303 K and 1.5 M AMP there is a consistent sinking trend. One possible explanation for this can be provided by analyzing the raw data from the experiment. Is seems as if the operator did not wait long enough for steady state to occur at 303 K.

Table 5-2 k_2 values for the reaction of CO_2 with AMP in an aqueous solution at 303 K

[AMP] mol/dm^3	$D_{CO_2}\times10^9$ m^2/s*10^9	H_{CO_2} kPa m^3/mol	p_{CO_2} kPa	J_{CO_2}*10^4 mol/m^{2}s	k_2 m^3/mol s
1.0	1.99	3.54	0.281	1.15	1.10
			0.505	1.98	1.02
			0.842	3.17	0.93
			0.960	3.23	0.75
1.5	1.94	3.74	0.257	1.28	1.28
			0.468	2.19	1.12
			0.777	3.42	0.99
			0.994	4.27	0.94
2.0	1.90	3.93	0.258	1.31	1.14
			0.454	2.20	1.04
			0.757	3.61	1.00
			0.957	4.35	0.91
3.0	1.86	4.29	0.416	2.25	1.09
			0.696	3.62	1.00
			0.886	4.58	0.99

Table 5-3 k_2 values for the reaction of CO_2 with AMP in an aqueous solution at 313 K

[AMP] mol/dm^3	$D_{CO_2}\times10^9$ m^2/s*10^9	H_{CO_2} kPa m^3/mol	p_{CO_2} kPa	J_{CO_2}*10^4 mol/m^{2}s	k_2 m^3/mol s
1.0	2.49	4.34	0.267	1.23	1.72
			0.465	2.05	1.55
			0.783	3.26	1.40
			0.884	3.67	1.38
1.5	2.44	4.60	0.250	1.28	1.64
			0.425	2.24	1.76
			0.700	3.62	1.68
			0.894	4.53	1.60
2.0	2.38	4.82	0.225	1.35	1.96
			0.403	2.32	1.80
			0.675	3.78	1.69
			0.850	4.67	1.62
3.0	2.33	5.26	0.357	2.44	2.15
			0.604	3.97	1.98
			0.768	4.96	1.91

Table 5-4 k_2 values for the reaction of CO_2 with AMP in an aqueous solution at 323 K

[AMP] mol/dm^3	$D_{CO_2}\times10^9$ m^2/s*10^9	H_{CO_2} kPa m^3/mol	p_{CO_2} kPa	J_{CO_2}*10^4 mol/m^{2}s	k_2 m^3/mol s
1.0	3.10	5.29	0.445	2.01	1.94
			0.740	3.29	2.00
			0.826	3.74	1.98
1.5	2.98	5.52	0.231	1.32	2.45
			0.385	2.36	2.85
			0.637	3.75	2.64
			0.811	4.66	2.51
2.0	2.96	5.85	0.224	1.40	2.56
			0.378	2.45	2.78
			0.605	3.99	2.86
			0.777	4.79	2.50
3.0	2.88	6.36	0.318	2.61	3.78
			0.529	4.19	3.51
			0.682	5.22	3.27
			0.696	5.17	3.05

In the literature the reaction between CO_2 and AMP in an aqueous solution has been reported to be an overall second-order reaction that is first order with respect to both CO_2 and AMP. In Figure 5-4 and Figure 5-5 logarithmic plots of J_{CO_2} as a function of p_{CO_2} are shown for the concentrations 1, 1.5, 2 and 3M of AMP respectively. Inspection of equation (5.3) shows that the plots should be linear with a slope of unity for each temperature if the reaction is first order with respect to CO_2 concentration in this case presented by the partial pressure.

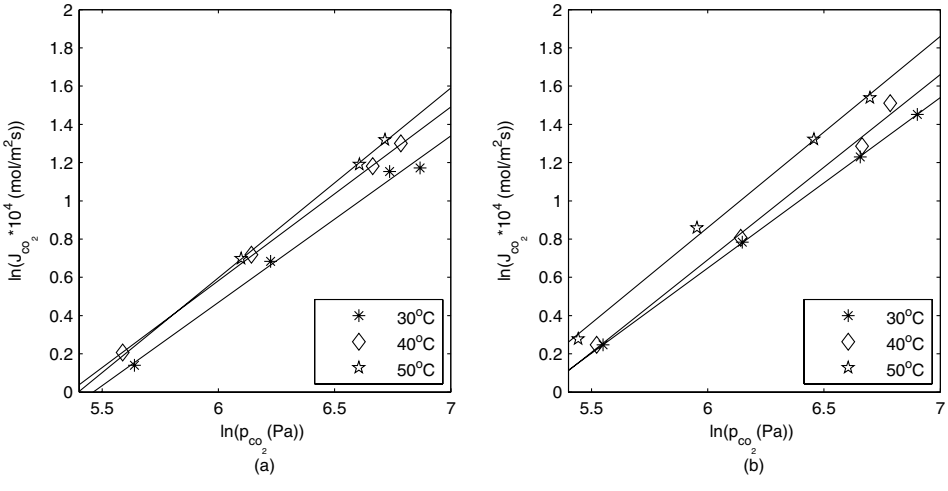

Figure 5-4. Specific rate of absorption as a function of p_{CO_2} for (a) a 1 M solution of AMP and (b) a 1.5 M solution of AMP at three different temperatures.

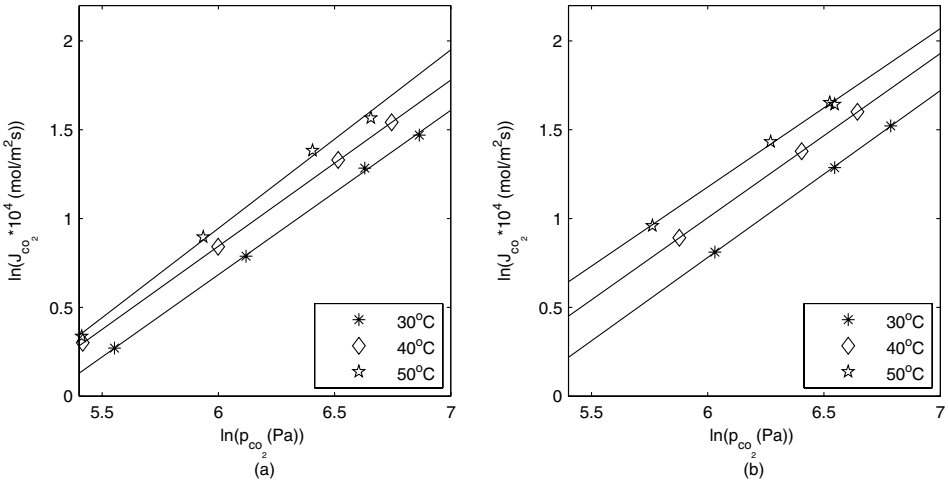

Figure 5-5. Specific rate of absorption as a function of p_{CO_2} for (a) a 2 M solution of AMP and (b) a 3 M solution of AMP at three different temperatures.

The fact that the slope in most of the plots is not unity and not even all of them have the same value as the temperature is varied, but different values varying between 0.87 and 1.00 suggests that the data produced are not completely reliable. Because of the inconsistencies in the experimental data it was decided that they were not reliable enough to develop an Arrhenius equation for the reaction between CO_2 and AMP. But the values of the rate constants calculated are in the same order of magnitude as the values calculated using the Arrhenius expression developed by Saha et al.[1]. Therefore, the Arrhenius expression presented by Camacho et al.[3] is assumed to be erroneous. On average the values for k_2 found in this work deviate 36% compared to values found using the expression in Saha et al.[1] and for almost all cases the value of k_2 found in this work is higher, but for the 1 M solution some of the values found for k_2 in this work are lower. In Figure 5-6 an Arrhenius plot of all experimental values of k_2 found in this work compared to the values of k_2 found using the correlation presented by Saha et al. [1] can be found.

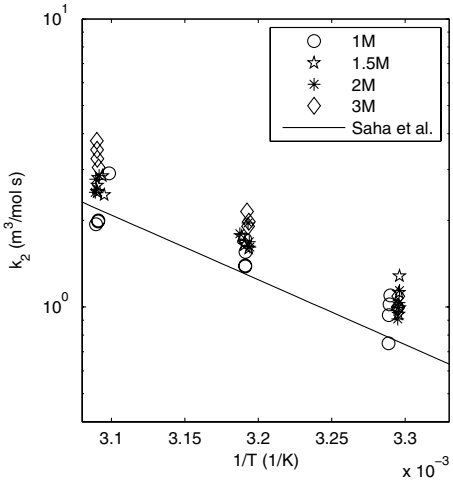

Figure 5-6. All experimental values of k_2 found in this work compared to the values of k_2 found using the correlation presented by Saha et al. [1]

5.5.1 Sensitivity analysis

Due to the rather poor quality of the experimental data found in this work and the large dependency on physicochemical properties a parameter sensitivity test was carried out. The sensitivities are reported in Table 5-5 and Table 5-6. The sensitivity test was carried out for two different experimental conditions. Both were carried out for a 3 M solution of AMP, but at different temperatures and partial pressures. It can be seen that the calculated value of k_2 is extremely sensitive to the tested parameters; H_{CO_2}, D_{CO_2}, a and measured dry CO_2 concentration in the bleed gas. The calculation is not very sensitive to a change in the activity coefficient of water due to non-idealities. A 5% change in value of the measured dry CO_2 concentration in the gas bleed gives approximately 16% change in the experimentally determined kinetic constant for the AMP-CO_2 reaction. One might say that this is extremely sensitive, and calls for very accurate calibration of the IR spectrometer as well as a patient operator.

Table 5-5. Parameter sensitivity for 3M AMP kinetics experiments at 30°C and partial pressure 0.416 kPa.

Parameter	+5%	-5%
Vol% dry CO_2 bleed	-15.69 %	18.90%
H_{CO_2}	10.25 %	-9.75 %
D_{CO_2}	-4.76 %	5.26 %
Mass transfer area	-9.30%	10.80
Activity coeff. H_2O	0.41 %	-0.41 %

Table 5-6. Parameter sensitivity for 3M AMP kinetics experiments at 50°C and partial pressure 0.696 kPa.

Parameter	+5%	-5%
Vol% dry CO_2 bleed	-13.99 %	16.62%
H_{CO_2}	10.25 %	-9.75 %
D_{CO_2}	-4.76 %	5.26 %
Mass transfer area	-9.30%	10.80%
Activity coeff. H_2O	1.24 %	-1.21 %

The reason why the calculation of k_2 is so sensitive to the concentration of CO_2 in the bleed gas is because it is included in both the expression for the flux of CO_2 as well as in the expression for the kinetic constant through the concentration of free CO_2 that can react with AMP in the liquid solution.

5.6 Summary Chemical Reaction Kinetics

Efforts have been made in order to verify an experimental set-up and method for determining chemical rate constants in reactive gas liquid systems using a string of discs absorber. Experimental work has been carried out in order to determine the effective mass transfer area for the string of discs absorber using an aqueous solution of NaOH. It has been shown that the value found for the mass transfer area is strongly dependent on the liquid rate as well as the the physicochemical properties used in the calculation. Validation of the experimental set-up and method was done using a system with a well defined chemical rate constant, the results show promise but are not conclusive. Efforts have been made to find the chemical rate constants for the reaction of CO_2 with AMP in an aqueous solution, but the experimental data are inconclusive. A parameter sensitivity test was carried out and showed possible problems with using the experimental set-up and the method for determination of chemical rate constants in reactive gas-liquid systems. Especially the concentration of CO_2 in the bleed gas and the Henry's Law constant for CO_2 in the solution were of high significance.

References

[1] Saha AK, Bandyopadhyay SS, Biswas AK. Kinetics of Absorption of CO_2 into Aqueous Solutions of 2-amino-2-methyl-1-propanol. Chem. Eng. Sci. 1995;50: 3587-3598.

[2] Bosch H, Versteeg GF, van Swaaij WPM. Kinetics of the Reaction of CO_2 with the Sterically Hindered Amine 2-Amino-2- Methylpropanol at 298 K. Chem. Eng. Sci. 1990;45:1167-1173.

[3] Camacho F, Sánchez S, Pacheco R, Sánchez A, La Rubida MD. Thermal Effects of CO_2 Absorption in Aqueous Solutions of 2-Amino-2-Methyl-1-Propanol. AIChE Journal. 2005;51:2769-2777.

[4] Astarita, G. *Mass transfer with chemical reactions*, Elsevier Publishing Company, Amsterdam/London/New York 1967

[5] Ma´mun S, Dindore VY, Svendsen HF. Kinetics of the Reaction of Carbon Dioxide with Aqueous Solutions of 2-((2-Aminoethyl)amino)ethanol. Ind. Eng. Chem. Res. 2007;46:385-394.

[6] Pohorecki R, Moniuk W, Kineticks of Reaction Between Carbon Dioxide and Hydroxyl ions in Aqueous Electrolyte Solutions, Chem. Eng. Sci. 1988;7:1677-1684.

[7] Vázquez G, Alvarez E, Varela R, Cancela A, Navaza JM, Density and Viscosity of Aqueous Solutions of Sodium Dithionite, Sodium Hydroxide, Sodium Dithionite + Sucrose, and Sodium Dithionite + Sodium Hydroxide + Sucrose from 25 °C to 40 °C, J. Chem. Eng. Data 1996, 41, 244-248.

[8] Ko J-J, Tsai T-C, Lin C-Y, Wang H-M, Li M-H. Diffusivity of Nitrous Oxide in Aqueous Alkanolamine Solutions. J. Chem. Eng. Data. 2001;46:160-165.

[9] SINTEF Oct. 2005, Vassbotn T. Unpublished data.

[10] Versteeg, G.F., Van Dijck, L.A.J., Van Swaaij, W.P.M. On the kinetics between CO_2 and alkanolamines both in aqueous and non-aqueous solutions. An overview, Chem. Eng Comm., 1996, 144, 113-158

[11] Tsai T-C., Ko J-J., Wang H-M., Lin C-Y., Li M-H. Solubility of nitrous oxide in alkanolamine aqueous solutions, J. Chem. Eng. Data. 2000; 45; 341-347.

[12] Hoff KA, Juliussen O, Falk-Pedersen O, Svendsen HF. Modeling and experimental study of carbon dioxide absorption in aqueous alkanolamine solutions using a membrane contactor, Ind. Eng. Chem. Res., 2004;43:4908-4921.

6 Pilot Plant Data

Studies of CO_2 absorption into a 2.9 M solution of AMP in a pilot plant using structured packing in both absorber and desorber have been carried out at the Norwegian University of Science and Technology and SINTEF through the ENGAS research infrastructure in January and February of 2006. Experimental data for eleven runs were collected, including temperature profiles for both the absorber and the desorber and CO_2 concentrations in both the gas-and the liquid phase at the inlet and outlet of the absorber and desorber. The Absorber was run at atmospheric pressure and the desorber was run at approximately 2 bar. The CO_2 concentration in the absorber inlet gas varied between 2.38 and 12.96 %vol. covering the range from natural gas fired to coal-fired power plants. Liquid loadings of CO_2 ranging from 0.072 to 0.479 was covered. The largest loading range covered in one run was 0.170 to 0.459 in run R7. The largest gas phase concentration range covered in one run was 9.83 to 12.93 %-vol. in run R7. The amount of CO_2 absorbed/desorbed in a single run ranges form 2.08 kg/h to 6.65 kg/h. Both of the aforementioned numbers for CO_2 produced are based on the liquid side analysis since they are assumed to be the most accurate. The reboiler heat duty ranges from 4.1 to 10.8 MJ/kg CO_2 depending on the liquid loading. These values are quite high compared to literature data, but in the range of other experiments using the same pilot plant, Tobiesen et al.[1]. Problems were experienced with the formation of a white solid (wax-like) compound in the inlet to a mass flow meter. The solid is most likely a highly concentrated AMP solution saturated with CO_2. The heat loss to the surroundings from the desorber was calculated using pure water as the circulating fluid.

6.1 Experimental

6.1.1 Experimental Set-Up

The set-up where the experiments were run is a complete absorption/desorption pilot scale apparatus. The pilot plant is fully automated to run 24 hours/day on a continuous basis. The gas treating capacity is approximately 140 m^3/h depending on the solvent rate and the gas rate. Most of the experiments in this work were run at approximately 120 m^3/h due to flooding problems at higher gas rates for the solvent used in this work. A simplified flow sheet of the pilot plant is shown in Figure 6-1 and characteristics for the plant are reported in Table 6-1. The plant is a closed system, thus all CO_2 that is desorbed is transferred back to the absorber where it is absorbed.

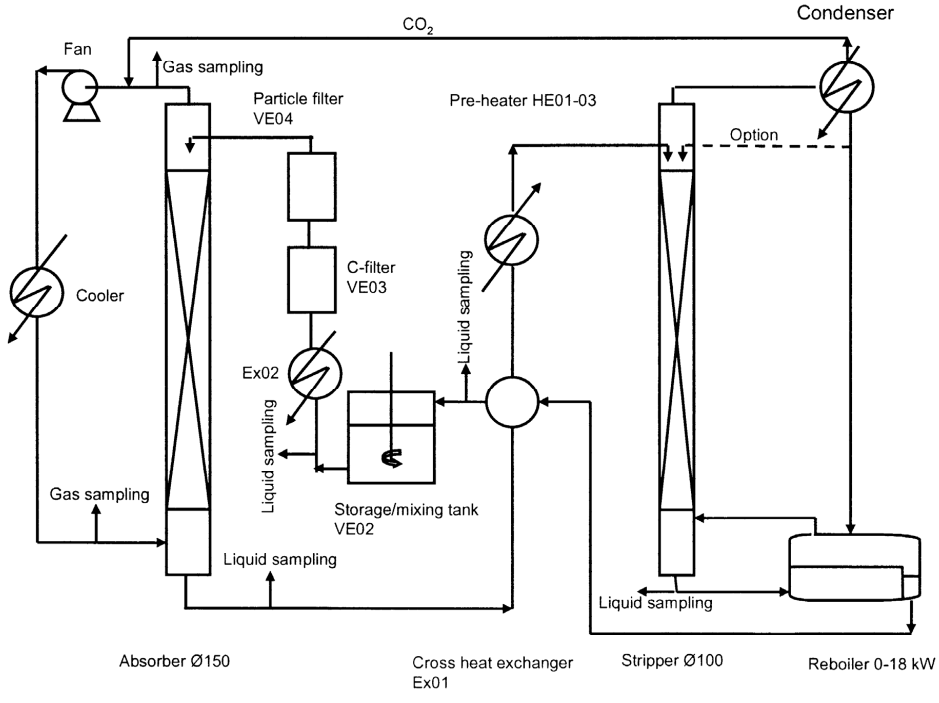

Figure 6-1. Flow sheet for the pilot plant taken from Tobeisen et al[1] .

Table 6-1. Characteristics of the pilot plant absorber and desorber

Absorber Characteristics	
Column internal diameter (m)	0.15
Main packing height (m)	4.36
Packing type	Sulzer Mellapak 250Y
Desorber Characteristics	
Column internal diameter (m)	0.10
Main packing height (m)	3.89
Packing type	Sulzer Mellapak 250Y
Reboiler (m)	Ø0.40*0.80 (D*L)

In both the absorber and desorber PT-100 thermo elements are installed in order to register the temperature profile over the columns. Figure 6-2 shows where the PT-100 thermo elements are placed in the two packed columns, furthermore thermo elements are placed in the incoming and outgoing streams of the packed columns. Table 6-2 gives the position of the PT-100 thermo elements relative to the bottom of the column and a correction to the measured temperatures.

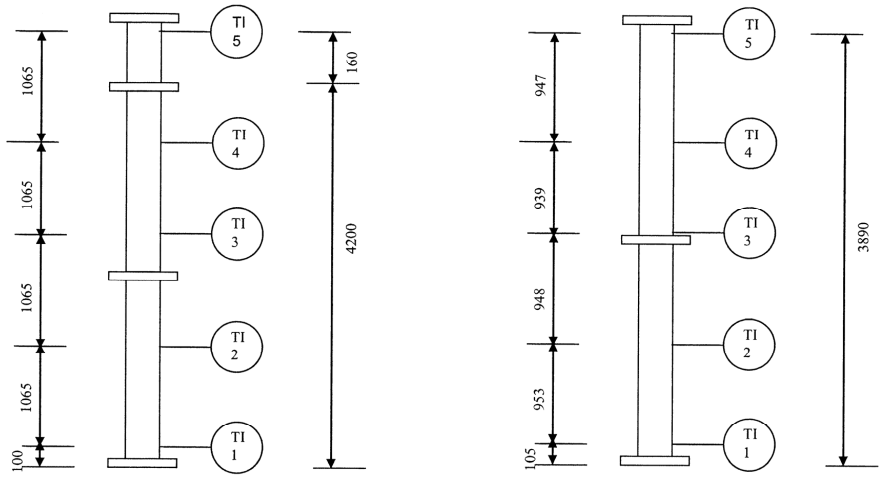

Figure 6-2. (a) Thermo element probe position in the absorber. (b) Thermo element probe position in the desorber.

Table 6-2. Placement and correction of the temperature probes in the absorber and the desorber.

	Thermo Element	Placement from bottom [m]	Correction [K]
Absorber	TI 1	0.100	1.073
	TI 2	1.165	1.462
	TI 3	2.230	0.982
	TI 4	3.295	1.436
	TI 5	4.360	0.94
Desorber	TI 1	0.105	0.199
	TI 2	1.058	-0.250
	TI 3	2.006	0.178
	TI 4	2.945	0.070
	TI 5	3.892	0.333

The correct temperature is the temperature from the thermo element minus the correction given in Table 6-2.

Process data are continuously being logged when the pilot plant is running. The logged data are:

1. gas and liquid flow rates
2. liquid flow rate from the reboiler
3. CO_2 flow rate from the desorber to the absorber,
4. CO_2 concentration in the inlet and outlet gas of the absorber
5. pressure and temperature both in the gas and the liquid phase of the reboiler
6. temperature profiles in the packed columns
7. temperature and pressure in the pipes.

In Table 6-3 the analytical instruments used in the pilot plant is given with the brand and when known the range the instrument is valid in.

Table 6-3. Instrumentation of the pilot plant.

Instrument	Brand	Range
Mass flow controllers	Bronkhorst Hi-Tec	0-15 Nl/min
CO_2 analyser absorber in	IR Rosemount Binos 100	0-50%
CO_2 analyser absorber out	IR Rosemount Binos 100	0-20%
Thermo elements	PT-100	
CO_2 flow from stripper to absorber	Emerson Coriolis mass flow meter.	0-16 kg/h
Flow condensate	Endress + Hauser Promass A.	min 2 kg/h

6.1.2 Experimental Procedure

AMP was obtained from Acros Organics with a stated purity of 99%. AMP is a white solid at room temperature with a melting point of 31°C at atmospheric pressure. Therefore the AMP had to be melted before it was mixed with water in order to obtain a solution with the preferred concentration. 142.5 kg of 3.3 M (30 % wt.) aqueous AMP solutions was prepared using deionised water and fed to the pilot plant. Circulation of the solution in the plant was started at 5 l/min and after 1 hour a sample was taken and analyzed for AMP concentration, the solution was found to be 2.81 M (25.5 %wt.) which is sufficiently low in order not to experience problems with precipitation at high CO_2 loadings. The actual concentration of AMP measured in the solvent sample from the plant is lower than the concentration of the solution prior to loading into the plant. (A 30%wt solution should be 3.3 M at 20°C.) This is most likely due to wash water that has completely drained. It is not clear where in the apparatus the wash water was trapped. The research staff using the equipment has experienced the same problem earlier and the AMP solution was prepared with this in mind. Later 13 kg of 30%wt solution was added to make the plant flexible with regard to liquid rate and gas rate, thus the total amount of solution was approximately 156 kg.

Having done all the initial preparation, the reboiler is then turned on and simultaneously the amine solution is loaded with CO_2 by adding CO_2 into the absorber gas stream and the continuous operation can start. After some initial problems, due to precipitation of a white wax like solid in the mass flow meter monitoring the stream of CO_2 from the desorber to the absorber, the plant ran continuously and was loaded with CO_2 three more times. In total the plant ran 12 days out of which 10 were continuous. The problems concerning the solid build-up in the mass flow meter were fixed by adding a valve and a pump to the pipe in order to pump water into the CO_2 stream in order to dissolve the solid. Figure 6-3 shows the mass flow meter where the plug occurred and the inlet where water could be added. Approximately 250 ml of water was added every morning and evening and the problem was avoided completely. In addition the added water kept the concentration of the AMP solution quite stable. The general experience of the research staff was that when running in continuous mode the alkanolamine

concentration increases with time due to loss of water. The loss of water is small since the pilot plant is designed as a closed system.

Figure 6-3. Coriolis mass flow meter used to measure the CO2 flow from the absorber to the desorber.

In Figure 6-1 it can be seen that there are possibilities for liquid sampling at the inlet and outlet of the absorber/desorber as well as the outlet of the reboiler. The liquid samples were analyzed for both CO_2 concentration and AMP concentration following the procedure described in section 6.1.3, liquid analysis. Furthermore the densities of the loaded solutions were measured using an automatic pipette and a scale. Gas sampling is possible at the inlet and outlet of the absorber and the CO_2 concentration was monitored with online IR analyzers. One uncertainty concerning the experimental data for the gas phase concentration is that the analyses were done on dry gas due to limitations of the analytical equipment, whereas the gas in the pilot plant is wet. Thus a model has to be used in order to calculate the experimental gas phase CO_2 concentration or more specifically the water content of the wet gas. Another uncertainty is the conditions of the gas when it is sampled before it is cooled. In this work Raoult's law with ideal solution was implemented to calculate the gas phase water content and the inlet gas was assumed to be saturated with water at the temperature measured in the inlet gas. The outlet gas was assumed to be saturated with water corresponding to equilibrium with the incoming liquid. Other uncertainties concerning the gas phase analysis is the calibration of the IR analysers which should be done every day, but was not done that often in the beginning. Furthermore, mass flow meters were available for measuring the amount of CO_2 that is transferred from the desorber to the absorber and the amount of condensate returned to the reboiler. Unfortunately the mass flow meter used for the condensate does not measure mass flows under 2 kg/h.

6.1.3 Liquid Analyzes

To analyze for the total liquid CO_2 concentration in the loaded solutions Barium Chloride ($BaCl_2$) and Sodium Hydroxide (NaOH) was added and the solution boiled in order to precipitate barium carbonate ($BaCO_3$) following the reaction:

$$Ba^{2+} + CO_2 + 2OH^- \rightarrow BaCO_3(s) + H_2O \quad (6.1)$$

The precipitation reaction was enhanced by heating the solution to the boiling point and boiling the solution for some minutes, which also helped agglomerate the $BaCO_3$ particles. The $BaCO_3$ particles were then collected by vacuum filtration using a 0.45-μm Millipore filter. Then the precipitate was dissolved in excess Hydrochloric acid (HCl) by the following reaction:

$$BaCO_3 + 2HCl \rightarrow BaCl_2 + CO_2 + H_2O \quad (6.2)$$

The solution is back-titrated with NaOH until a pH of 5.2 is reached using a Metrohm 794 Basic Titrino autotitrator. Blank samples were analyzed in order to correct for possible CO_2 in the NaOH/$BaCl_2$ solutions absorbed from the air during the analysis.

The total amine concentration was determined by direct titration with sulphuric acid using the autotitrator, Metrohm 794 Basic Titrino.

For all the solutions analyzed the liquid density at room temperature was determined and they are presented in appendix C.

6.2 Results and Discussion

6.2.1 Absorber Results

In Table 6-4 the experimental results for the absorber are reported. All the logged experimental values are averages over a time period of approximately 10 minutes under which the liquid samples were taken. The plant was allowed to run for approximately 1.5 hours at stable conditions before samples were taken, thus at a circulation rate of 6 l/min and approximately 180 l of solution in the system the solution has circulated three times under stable conditions.

The parameters that are varied for the different experimental runs are total amount of CO_2 in the system (average loading), gas and liquid flow rate and reboiler heat duty. There are also small unintended variations in the inlet gas temperature due to the fact that manually adjusted cooling water is used to control the gas inlet temperature. The reason why the gas flow was decreased after the two first runs was that flooding was experienced when the reboiler duty was increased to 9.4 kW at low loadings. The experimental runs can be divided into four different loading ranges. Runs R1-R3 are at the lowest average loading, runs R4-R6 are at medium low loading range, R7-R8 medium high, and runs R9-R11 are at the highest average loading. Ideally,

experimental data for even higher loadings should have been collected, but time did not permit further experiments. Furthermore it was more difficult to obtain stable conditions in the higher loading ranges when increasing the reboiler duty, only quite low duties were possible (up to 7.7 kW at 6 l/min). When the reboiler duty was increased to the next step, approximately 9.4kW, the temperatures in the stripper exhibited a sinusoidal variation with amplitude of several degrees. The instabilities would decrease slowly with time until a sudden quick temperature change would occur. The formerly described behavior was periodic. The instabilities in the stripper influenced the conditions in the absorber, where periodic changes in temperatures and CO_2 concentration were detected. In retrospect one might say that the discrete increments available when setting the reboiler duty are too coarse. The pre-heater has finer steps, but using the pre-heater in combination with the reboiler did not improve the results. Most likely the solution flashed in the pipe before entering the stripper.

Both the reboiler duty and the liquid flow are process variables that significantly affect the CO_2 concentrations in the gas and liquid phase in the absorber as well as the stripper. A low liquid flow allows for a wide loading range to be covered in the plant, and thus higher gas inlet CO_2 concentrations. Low gas flow also accommodates high CO_2 gas concentrations. The highest gas inlet concentration in the experimental data is approx. 13 %vol. and the lowest approx. 2.4 %vol. The highest CO_2 flux is obtained in R7 and is approximately 0.15 kmol/h and, as expected, this is the run with the highest inlet CO_2 concentration and the largest difference between lean and rich loading. In Table 6-4 the experimental absorber data for runs R1-R11 are reported.

Three different CO_2 mass balances for the system were obtained; one for the gas phase of the absorber, one for the liquid phase of the absorber and a direct measurement of the CO_2 leaving the condenser. In Table 6-5 the absolute average deviation, as well as the largest positive and the largest negative deviations, for the three different mass balances are given. In Table 6-4 the deviations for all runs are tabulated. It is quite clear that the CO_2 fluxes obtained form the gas and liquid balances over the absorber resemble each other the most of the three. Furthermore, Figure 6-4 shows flux of CO_2 into the liquid as a function of flux of CO_2 from the gas and from the plot one can see that the mass balance deviations follow no specific trend in the eleven runs in this work. Whereas the measured CO_2 fluxes form the reboiler is higher than the flux calculated using the gas and liquid phase mass balances. The good agreement between the gas and liquid phase mass balances and that fact that no specific trend in the deviation occurs is a good indication to conclude that the measured CO_2 flow form the reboiler is inaccurate. At flows above approximately 6 kg/h instabilities in the CO_2 mass flow was observed thus making the measured CO_2 flow even less reliable.

Table 6-4. Experimental results for the absorber.

RUN	R1	R2	R3	R4	R5	R6	R7	R8	R9	R10	R11
Gas Flow (m^3/h)	146	140	121	119	121	123	118	122	123	119	122
Liquid Flow (l/min)	3.00	6.00	6.00	3.00	3.00	6.00	3.00	6.00	3.00	3.00	6.00
AMP concentration (mol/l)	2.83	2.85	2.85	2.89	2.89	2.89	2.89	2.89	2.89	2.89	2.89
Gas CO_2 conc. bottom (% vol)	2.62	2.38	4.17	9.28	4.81	4.58	12.96	7.39	4.90	11.33	10.27
Gas CO_2 conc. Top (% vol)	1.69	1.26	2.36	6.51	3.29	2.90	9.83	5.34	4.03	9.20	8.01
Liquid CO_2 loading top	0.072	0.095	0.084	0.118	0.142	0.147	0.170	0.219	0.309	0.272	0.284
Liquid CO_2 loading bottom	0.178	0.151	0.169	0.379	0.282	0.226	0.459	0.327	0.398	0.479	0.400
Mass Balance (% Ng-Nl)	-0.4	8.7	0.6	1.7	1.6	-1.4	4.9	-8.1	-5.4	5.1	-0.9
Ng-Em	-11.6	0.95	-8.54	-12.31	-6.02	-5.04	1.46	-15.60	-3.92	-17.70	-13.23
Nl-Em	-11.28	-7.17	-9.05	-13.76	-7.52	-3.70	-3.30	-8.15	1.60	-21.72	-12.40
Temperature [°C]											
gas bottom	40	41	39	41	40	41	41	39	40	39	39
z = 0.100 m	40.69	43.30	45.25	43.47	41.72	45.78	43.66	45.63	41.16	41.04	46.04
z = 1.165 m	42.34	46.64	51.05	47.15	44.52	50.83	47.48	51.67	43.12	44.63	52.29
z = 2.230 m	43.50	47.88	52.88	50.07	46.64	52.22	50.68	53.89	44.45	47.40	54.79
z = 3.295 m	44.68	46.18	49.14	53.01	48.55	48.50	54.07	50.39	45.71	50.28	52.51
z = 4.360 m	43.15	42.11	42.48	49.75	45.32	41.89	51.17	41.79	42.62	46.57	42.68
Gas top	43	42	43	49	45	43	51	42	43	47	43
Liquid top	40	41	41	40	41	41	41	40	40	40	40
Liquid bottom	40	42	43	43	41	43	43	43	41	40	44

Table 6-5. %AAD, maximum positive and maximum negative deviation for the three different mass balances.

	%AAD	Max. Pos. Deviation	Max. Neg. Deviation
n gas vs n liquid	3.5	8.7 (R2)	-8.1 (R8)
n gas vs CO_2 condenser	8.8	1.46 (R7)	-17.7 (R10)
n liq vs CO_2 condenser	9.1	1.61 (R9)	-21.72 (R10)

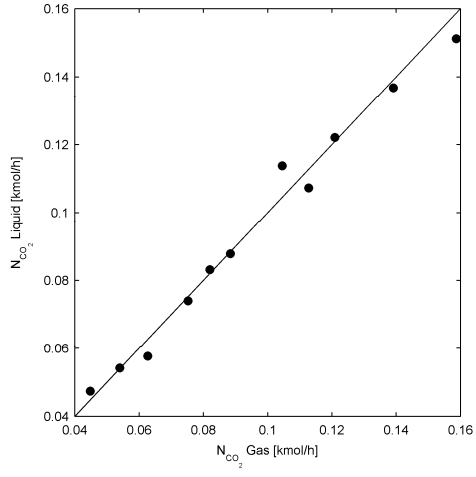

Figure 6-4. Flux of CO_2 into the liquid phase as a function of flux of CO_2 from the gas phase.

6.2.2 Desorber Results

In Table 6-6 the experimental desorber data for runs R1-R11 are reported. To check the amount of AMP that is evaporated in the stripper and carried out with the water and the CO_2, AMP analyses of the liquid leaving the condenser were carried out for two runs, R1 and R4. In both of these runs the desorber operates at high temperature due to the low liquid loading. The results of the AMP analysis for the liquid leaving the condenser in runs R1 and R4 are mole fractions of 0.009 and 0.008 respectively. These results show that if the desorber column is operated on a large scale a water wash section should be used in order to prevent AMP slip to the surroundings. But the results also show that the evaporation of AMP most likely can be neglected when modeling the desorber if energy consumption and CO_2 stripping efficiency are the primary properties to be described by the model.

The stripper was operated at a pressure close to 2 bars, which is a pressure that is feasible to use in industrial plants. The pressure drop over the stripper is approximately 0.01 bars in all of the runs. The heat duty needed varies between 4.1 and 10.8 MJ/kg CO_2. These values seem quite high compared to values reported by Sakwattanapung et al.[2] for a reboiler using 5 M MEA and data reported by Astarita et al.[3] for MEA systems.

Table 6-6. Experimental results for the desorber.

RUN	R1	R2	R3	R4	R5	R6	R7	R8	R9	R10	R11
Reboiler Duty (kW)	5.8	7.60	9.40	7.60	5.80	7.60	7.60	7.70	3.90	5.80	7.70
Liquid Flow (l/min)	3.00	6.00	6.00	3.00	3.00	6.00	3.00	6.00	3.00	3.00	6.00
Condensate Flow (kg/min)	2.39	3.28	4.89	2.83	na	3.07	2.40	2.55	na	na	na
AMP conc. (mol/l) stripper in	2.83	2.85	2.85	2.89	2.89	2.89	2.89	2.89	2.89	2.89	2.89
AMP conc. (mol/l) stripper out	2.76	2.81	2.83	2.80	2.82	2.87	2.82	2.89	2.86	2.85	2.89
Rich CO_2 Loading	0.178	0.151	0.169	0.379	0.282	0.226	0.459	0.327	0.398	0.479	0.400
CO_2 loading stripper out	0.121	0.136	0.133	0.233	0.246	0.210	0.347	0.302	0.407	0.425	0.376
Lean CO_2 Loading	0.072	0.095	0.084	0.118	0.142	0.147	0.170	0.219	0.309	0.272	0.284
Reboiler Heat Duty (kJ/kg CO_2)	8757	10793	8754	4544	6413	7476	4112	5537	6739	4422	5161
Temperature [°C]											
Reboiler	120.67	120.70	121.29	116.56	115.79	115.02	112.44	111.18	104.09	107.15	107.00
z = 0.105 m	121.42	121.02	121.89	116.15	114.14	114.52	109.93	108.66	99.85	101.51	103.18
z = 1.058 m	120.27	120.26	120.97	110.27	111.25	113.96	103.78	109.25	101.91	100.99	104.71
z = 2.006 m	118.26	119.77	119.55	107.68	110.66	113.50	102.78	108.78	101.42	100.49	104.16
z =2.945 m	116.25	118.94	118.44	107.32	110.53	113.41	102.85	108.82	101.54	100.65	104.31
z = 3.892 m	114.50	117.47	117.04	105.18	108.23	111.50	100.95	107.02	98.99	98.62	102.47
Liquid inlet temp. stripper	111	114	114	104	107	110	99	107	97	98	103
Temperature Condensate	12	12	13	16	14	13	19	14	16	15	14
Pressure [bar]											
Stripper Top	2.05	2.11	2.13	1.98	2.07	2.04	1.95	2.07	1.93	1.99	2.02
Reboiler	2.06	2.12	2.14	1.99	2.08	2.05	1.97	2.09	1.94	2.00	2.03

The values in refs.[2,3] vary between 2.06 and 4.75 MJ/kg of CO2. Thus the values reported in refs.[2,3] are comparable or lower than the values reported in this work, although they are expected to be higher since MEA has a higher heat of reaction than AMP. One of the reasons is that ref.[2] includes a system energy loss into the calculation which is subtracted for the reboiler energy before calculating the heat duty per kg CO2. Idem et al.[4] present reboiler duty experimental values for MEA/MDEA mixture that are in the same range as the values presented in refs.[2,3]. So in general the values obtained in this study seem unreasonably high compared to the alkanolamine used, but when comparing to Tobiesen et al.[5] where the same pilot plant is used the values seem reasonable. They present a heat duty of 10.950 MJ/kg CO_2 for a system with rich loading 0.268 and using MEA as a solvent, as expected this is quite a bit higher than R6 in this work with similar rich loading and lean loading. The reasons for the high values are the heat loss to the surroundings and the narrow loading ranges utilized in each run. The high values are, as expected, especially pronounced in the low loading area.

In the experimental runs it is expected that the loading of the solution from the stripper into the reboiler is between the rich and the lean loading. This is the case in all except one of the experimental runs, R9, where the loading from the stripper into the reboiler is higher than the rich loading. This result was unexpected and double checked by doing the liquid analysis twice. The results were the same. This actually means that CO_2 is being absorbed in the stripper and returned with the solution to the reboiler. The reason why this happens is that not enough water is evaporated in the reboiler resulting in a partial pressure of CO_2 which is too high. By comparing the values of the loading into and out of the stripper to the values, into and out of the reboiler for all the experimental runs it is obvious, especially at higher loadings, that almost all of the “stripping” actually is done in the reboiler. This can be seen in the temperature profiles over the stripper as well since the temperature is constant over a large section of the packing height. The constant temperature is a good indication telling that very little mass transfer is occurring.

In Figure 6-5 the heat duty reported in kJ/kg of CO2 is plotted as a function of both lean (a) and rich (b) CO2 loading.

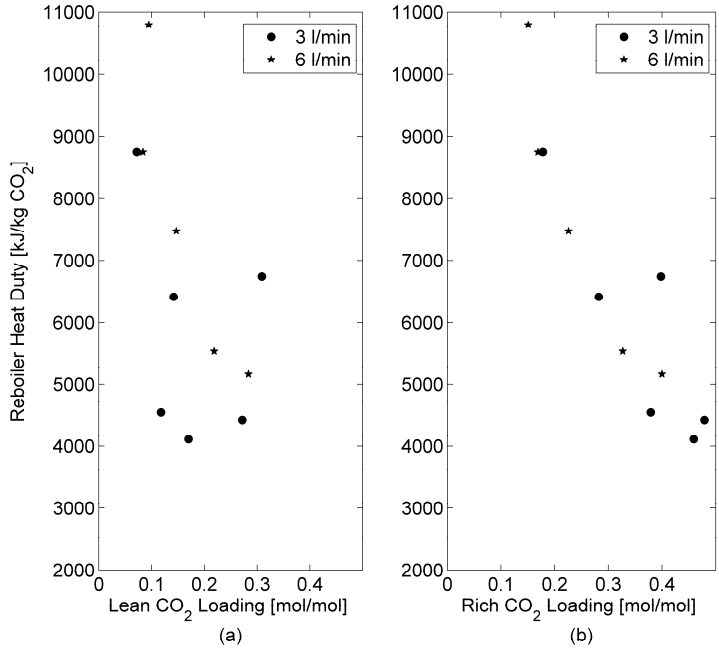

Figure 6-5. Reboiler heat duty as a function of : (a) lean loading, (b) rich loading. Where spheres are experimental data using a solvent flow rate of 3 l/min and stars are experimental data using a flow rate of 6 l/min

In the experimental data the clearest correlation is found between rich loading and heat duty, an increase in rich loading leads to a decrease in heat duty. This seems feasible since the boiling temperature of the solution decreases with increasing loading, thus not as much of the energy is used for heating the solution and furthermore the heat loss to the surroundings is most likely smaller, due to the decrease in temperature difference between the desorber and the surroundings. The lean loading is important, but the correlation would be more pronounced if the rich loading was held constant and lean loading varied. The effect of flow rate is not pronounced in a way that it gives different trend for the heat duty by just looking at the heat duty as a function of rich or lean loading. In Figure 6-6 the reboiler heat duty is plotted as a function of CO_2 produced, and it is clear that the change of flow rate has a pronounced effect. A higher liquid rate requires a higher reboiler heat duty in order to produce the same amount of CO_2 as a lower liquid rate. This follows the intuitive idea that a higher liquid rate would need higher effect.

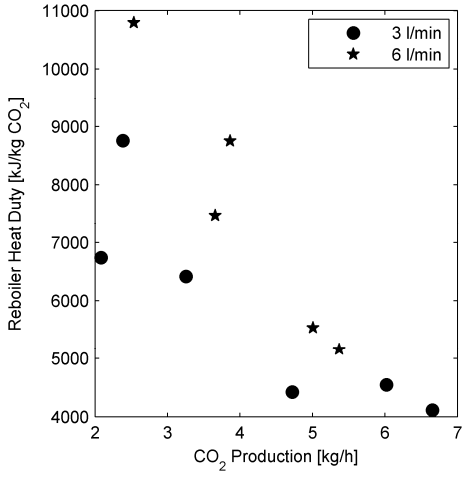

Figure 6-6. Reboiler heat duty as a function of CO2 production

6.2.3 Desorber Heat Loss

The energy distribution for the reboiler heat duty can be split in four main fractions: Sensible heat, heat of vaporization, heat of reaction, and heat loss to the surroundings. Experiments using only water as the circulating fluid had previously been carried out (Tobiesen[6]) in order to calculate the heat loss from the system. When water is used no chemical reaction is occurring and the heat balance for the system is straight forward. The data were collected at two different reboiler heat duties. In Figure 6-7 a flow sheet for the desorber is shown with the system limits for the energy balance used to calculate the heat loss to the surroundings. The ingoing streams of energy are; the water leaving the rich lean heat exchanger with a temperature measured before the Pre-Heater using TI-06, the water leaving the condenser with a temperature measured using TI-08 and reboiler duty ($Q_{reboiler}$). The outgoing streams of energy are: the liquid water leaving the reboiler with a temperature measure in the reboiler liquid by TI-12, the steam leaving the stripper with a temperature measured by TI-11 and the heat given to the surroundings labeled Q_{loss}. It is assumed the all of the steam leaving the stripper is condensed in the condenser and retuned to the reboiler. Thus, the mass flow of the steam leaving the stripper is assumed to be the same as the measured mass flow from the condenser to the reboiler. This also implies that the flow of water into the system from the lean/rich heat exchanger is the same as the flow of water out of the reboiler.

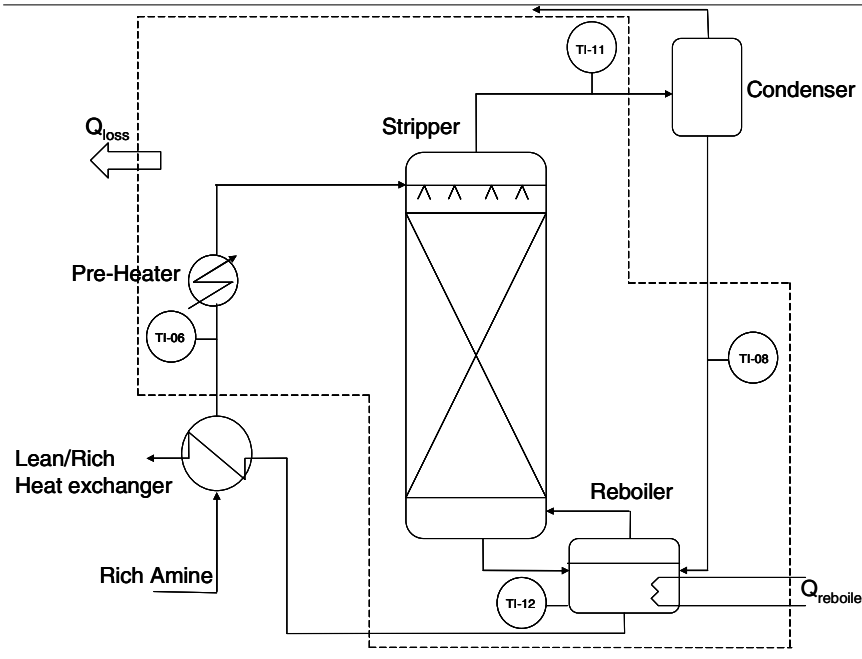

Figure 6-7. Desorber with system limits used in the heat balance to find the heat loss from the desorber.

The thermodynamic properties of the water and the steam were calculated using "The International Association for the Properties of Water and Steam Industrial Formulation 1997 for the Thermodynamic Properties of Water and Steam" (IAPWS-IF97), Wagner et al.[7]. A package written for Matlab by Francoise Brisette[8] from Construction Engineering at Ecole de technologie supérieure, Université du Québec, Montreal, Canada, was used to solve the IAPWS-IF97 equations. For some of the experimental runs the temperature and pressure recorded for the steam did not result in steam when calculating the water properties with IAPWE-IF97, then the temperature was increased slightly in the calculations in order to get the enthalpy of steam at the closest temperature.

Table 6-7. Heat loss to the surroundings from the desorber.

Run	**1**	**2**	**3**	**4**
Flow rate (l/min)	4	4	4	4
$Q_{reboiler}$ (kW)	10.0	10.0	4.0	4.0
Q_{loss} (kW)	1.2	0.8	1.1	1.2
% loss to surroundings	12	8	27	31

In Table 6-7 the heat loss to the surroundings is given. In appendix C all experimental data used to calculate the heat loss are given. It is clear that the heat loss to the surroundings is substantial at both low and high reboiler duties, thus it is clear that the desorber is not adiabatic in the pilot plant used. The temperatures and liquid flow rates used in the heat-loss experiments are similar to the conditions encountered in the absorption/desorption experiments similar heat

losses are expected for both experiments. Based on the results shown in Table 6-7 the average heat-loss to the surroundings for the desorber was 1.1 kW. If the loss of heat to the surroundings is considered when calculating reboiler heat duties for the AMP solution the values obtained are closer to the values expected when comparing to literature data. The range of reboiler heat duties is then from 3.5 to 9.2 MJ/kg of CO_2 stripped from the solution.

References

[1] Tobiesen AF, Svendsen HF, Juliussen O. Experimental Validation of a Rigorous Model for CO_2 Post-Combustion Capture, AIChE J 2006 Submitted for Publication.

[2] Sakwattanapong R, Aroonwilas A, Veawab A. Behavior of reboiler heat duty for CO_2 capture plants using regenerable single and blended alkanolamines. Ind. Eng. Chem. Res. 2005;44 :4465-4473.

[3] Astarita G, Savage DW, Bisio A. Gas Treating with Chemical Solvents; Wiley: New York, 1983.

[4] Idem R, Wilson M, Tontiwachwuthikul P, Chakma A, Veawab A, Aroonwilas A, Gelowitz D. Pilot Plant Studies of the CO_2 Capture Performance of Aqueous MEA and MEA/MDEA Solvents at the University of Regina CO_2 Capture Technology Development Plant and the Boundary Dam CO_2 Capture Demonstration Plant. Ind. Eng. Chem. Res. 2006;45:2414-2420.

[5] Tobiesen FA, Svendsen HF, Juliussen O. Experimental Validation of a Model for CO_2 Post-Combustion Capture Using Monoethanolamine (MEA), Presentation, International Test Network for CO_2 Capture: Report on 8th workshop. http://www.co2captureandstorage.info/docs/capture/2005-13.pdf , accessed August 2006.

[6] Tobiesen FA. Personal communication.

[7] Wagner W, Cooper JR, Dittmann A, Kijima J, Kretzschmar HJ, Kruse A, Mares R, Oguchi K, Sato H, Stocker I, Sifner O, Takaishi Y, Tanishita I, Trubenbach J, Willkommen Th. The IAPWS Industrial Formulation 1997 for the thermodynamic properties of water and steam. Transactions of the ASME. 2000;22:150-182.

[8] http://www.mathworks.com/matlabcentral/fileexchange/loadFile.do?objectId=7523&objectType=file, accessed August 2006.

7 Absorber Model Validation

As discussed in chapter 3.2.1 most published models have only been validated against data from pilot plants using aqueous MEA as the absorbent, and with pilot plant data from Tontiwachwuthikul et al.[1]. Two publications containing results for modeling CO_2 absorption in a packed column using aqueous AMP have been published. Alatiqi et al.[2] use a rate-based approach to model absorption of CO_2 in MEA, DEA, and AMP solutions. The results of the AMP modeling were not validated with experimental data, only compared to absorption of CO_2 in MEA and DEA solutions. Only the MEA results were verified using experimental data. Furthermore the values of the physicochemical properties used in the model and their sources are very unclear e.g. the heat of absorption is claimed to be obtained from Weiland et al.[3], but this reference only has data for MEA solutions. Aboudheir et al.[4] present results, using a rate based model based on the work of Pandya[5], for MEA and AMP validated with pilot plant data[1,6] for absorbers using both random and structured packing. In both sources 2 M AMP solutions are used. The pilot plant data form ref.[6] were obtained using an absorber packed with EX-type laboratory structured packing with a total height of 1.1 m. Concentration profiles of CO_2 were reported, but no information about the temperatures not even inlet or outlet temperatures for the gas and the liquid were reported.

Several problems are encountered when using the experimental data from Tontiwachwuthikul et al.[1] for model e.g. the packing used is only useful in pilot plants. Furthermore, the temperatures under which the experiments are run are much lower than what would be expected in a commercial plant for CO_2 capture form flue gases. Thus, the limiting effects that could be encountered at a larger scale are not tested.

In this work the developed adiabatic absorber model combined with the simple thermodynamic model developed in chapter 4 has been applied to CO_2 absorption using two different aqueous alkanolamine solutions, MEA and AMP, of varying concentrations. For the AMP solution two different columns using both randomly and structured packing have been used for verification, as well as two different temperature ranges. It is clear that the mass-transfer correlation used is of very high importance when modeling absorption towers; one should especially check that the interfacial mass-transfer area is in a range that is feasible. The most important physicochemical input parameters in the model have been identified.

7.1 Validation of the Model Proposed for AMP

The model proposed in this work was validated with pilot plant data from the literature and with pilot plant data presented in chapter 6 of this work. Thus both randomly and structured

packings are used for the model validation. The experimental data from this work and the data from the literature are carried out a different temperatures and using AMP solutions of different concentration. Mass-transfer coefficients and the specific gas-liquid interfacial area for the randomly packed column are calculated using correlations from Billet and Schultes[7]. Although several mass-transfer correlations are available to estimate gas and liquid side mass-transfer coefficients as well as interfacial mass-transfer area, the correlations proposed by Billet and Schultes[7] were selected since this reference contains a large database of parameters for both random and structured packing. For the column containing structured packing the correlations from both Billet and Schultes[7] and Rocha et al.[8,9] were implemented. Two different correlations were tried since the correlations from Rocha et al.[8,9] are specifically developed for columns containing structured packing, but it would be advantageous if the correlations form Billet and Schultes[7] could be used because of the large parameter data base available for both random and structured packing.

The physical properties used in the model with literature sources are given in Table 7-1.

Table 7-1. Physical and Chemical properties used in the absorber model for AMP.

Property	Source	Comment
Liquid Density	Xu et al.[10]	Linear mixing
Specific heat of gas components	Reid et al.[11]	
Specific heat of liquid solution	Chiu et al. [12] and Cheng et al.[13]	Linear mixing
Diffusivity of CO_2 in the liquid solution	Ko et al.[14]	Based on the N_2O analogy
Viscosity of the gas	Reid et al.[11]	Method of Wilke
Thermal conductivity of the gas	Reid et al.[11]	Eucken for pure compounds, Mason and Saxena for mixture
Diffusivity of CO_2 and water in the gas phase	Reid et al.[11]	Fuller equation
Surface tension of the liquid solution	Vazquez et al.[15]	
Viscosity of the liquid solution	Henni et al.[16] and Cheng et al.[13]	The data from ref.[16] was used for correlating pure AMP viscosity and then Grunberg and Nissan with zero interaction parameter was used.
Henry's Law Constant of CO_2 in the liquid solution	Saha et al.[17] and Browning et al.[18]	Based on the N_2O analogy and using an expression to account for the salting out effect with increased CO_2 loading
Diffusivity of AMP in the liquid solution	Chang et al.[19]	

The salting out effect on free CO_2 due to the increased ionic strength is accounted for in the expression for the Henry's Law Constant of CO_2 in the liquid solution using the van Krevelen

correlation. The coefficients for the different ions in the solution were taken from ref.[18]. The van Krevelen coefficient for protonated AMP was not available in ref.[18] so the value for protonated MEA was used. The second order chemical reaction rate constant was calculated using an Arrhenius equation presented in Saha et al.[20] and discussed in chapter 5 of this work.

7.1.1 Validation of the Absorber Model when Using Random Packing

The validation of the model proposed in chapter 3.2 when using a tower with random packing is done by comparison of simulation results with experimental data. The experimental data is taken from Tontiwachwuthikul et al.[1] where results for eight runs of CO_2 absorption into an aqueous AMP solution in a packed column are reported. The absorption is at atmospheric pressure in a column with 0.1 m inner diameter filled with 12.7 mm ceramic Berl saddles, and the total packing height is 6.55 m. The surface area of the Berl sadles is 545 m^2/m^3. The concentration of CO_2 in the gas at inlet conditions is between 15 and 19 % vol and the AMP concentration is 2.0 $kmol/m^3$. The experimental data include concentration and temperature profiles along the column. The proposed model should be able to describe both composition and temperature profiles along the column in order to be a useful tool. Figure 7-1 through Figure 7-3 show comparison between experimental data from runs T26, T25, and T28 and the proposed model. These three runs were chosen since they cover a large area of the liquid CO_2 loading presented in the available data. Run T26 covers the largest loading range of the reported data and run T28 is the run that has the highest liquid loading. In Figure 7-1 experimental data and simulated results for run T26 are presented. The maximum experimental CO_2 liquid loading for run T26 is approximately 0.41.

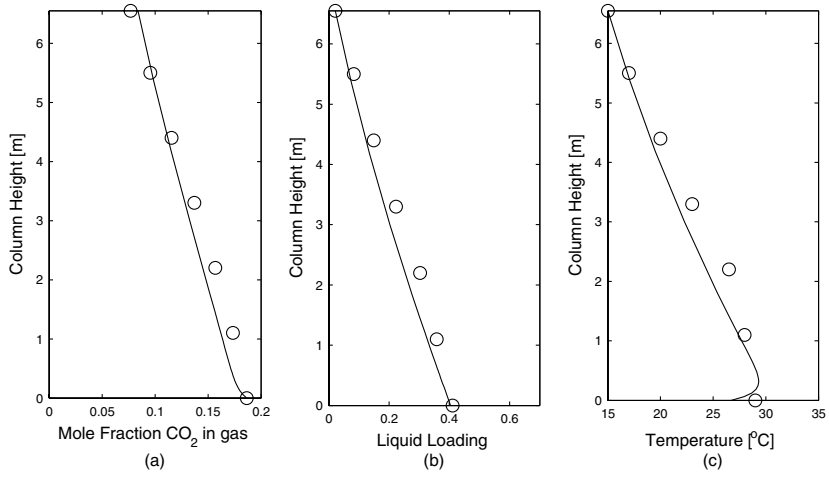

Figure 7-1. Modeled (lines) results and experimental data (circles) for the AMP-CO2 system (run T26): (a) concentration profiles, (b) liquid loading, (c) liquid temperature profiles.

The proposed model gives good results, and the largest discrepancy is the mole fraction of CO_2 in the gas leaving the column. The predicted CO_2 mole fraction is slightly too low. In Figure 7-2 experimental data and simulated results for run T25 are presented. The maximum experimental CO_2 loading in the liquid phase for run T25 is approximately 0.46.

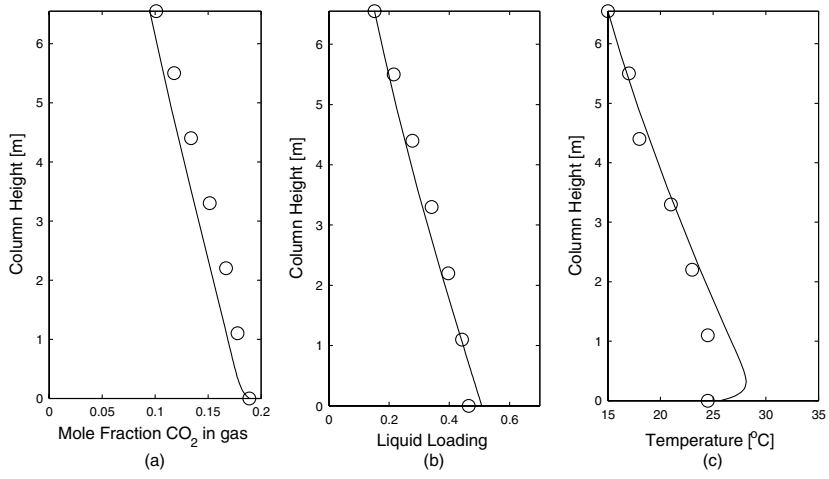

Figure 7-2. Modeled (lines) results and experimental data (circles) for the AMP-CO2 system (run T25): (a) concentration profiles, (b) liquid loading, (c) liquid temperature profiles.

The results using the proposed model are very good for the CO_2 concentration in both the gas and the liquid phase, but the liquid temperature is slightly over predicted at the bottom of the column. Furthermore one can see that the mole fraction of CO_2 in the gas leaving the column is more accurately predicted than the rich liquid loading. This discrepancy is due to material balance issues in the experimental data. The absolute value of the error in the experimental mass balance in this specific run is 7.53 %. In Figure 7-3 experimental data and simulated results for run T28 are presented. The maximum experimental CO_2 loading in the liquid phase for run T28 is approximately 0.58.

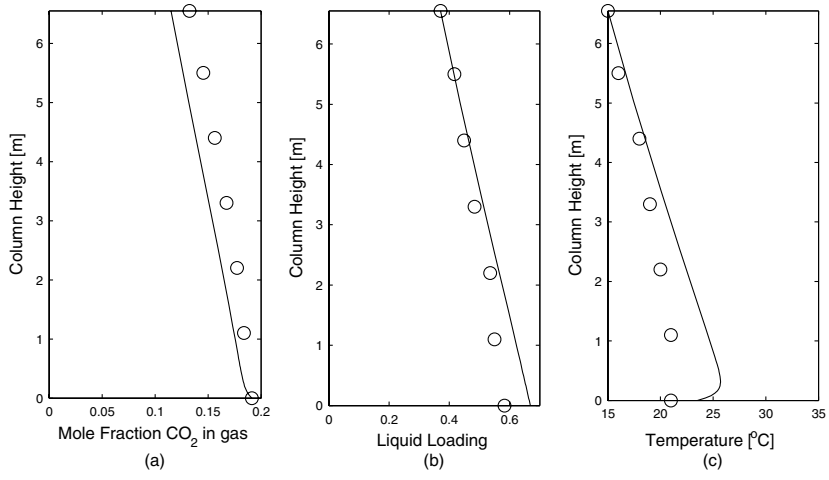

Figure 7-3. Modeled (lines) results and experimental data (circles) for the AMP-CO2 system (run T28): (a) concentration profiles, (b) liquid loading, (c) liquid temperature profiles.

The proposed model gives good results; the largest discrepancy is in the liquid temperature. A tendency that can be seen when looking at all three runs presented is that at increasing loading the liquid temperature is over predicted. This discrepancy is most likely due to the fact that the absorption of CO_2 is over predicted. Furthermore, there is no experimental calorimetric value for the heat of absorption of CO_2 in AMP available in the literature so the value used in this work has not been checked. It would be of interest to find experimental data for the heat of absorption of CO_2 in aqueous AMP solutions and at different CO_2 loadings in order to compare with the expression developed in this work. The heat of absorption of water is not significant at the low temperatures encountered in the data set simulated. According to the mass-transfer correlations used, the column is run at approximately 60 % of flooding and the interfacial mass-transfer area calculated is approximately 90 m^2/m^3. These two numbers do not agree very well since the surface area of the packing is 545 m^2/m^3 and one would assume that when the column is run at approximately 60% of flooding more than 16.5 % of the available surface area should be wetted. Surprisingly the model gives very good results for the absorption of CO_2 even though the mass-transfer correlation gives surprisingly low values for *a*.

7.1.1.1 Sensitivity Analysis of the Absorber Model when Using Random Packing

A sensitivity analysis of the mass transfer based model was carried out. The parameters selected for the analysis were $p^*_{CO_2}$ and the physicochemical properties influencing M, E_∞ and the mass-transfer correlation. The sensitivity of model with respect to the input parameters was checked by increasing a chosen parameter with ten percent and then calculating the change in

the two important variables rich liquid loading and the mole fraction of CO_2 in the clean gas. The results are shown in Table 7-2. Run T25 was chosen as a base case since it represents a wide loading range similar to what one might encounter in flue gas cleaning. At the conditions encountered in this work it is clear that the model is most sensitive to the liquid surface tension, H_{CO_2} and $D_{CO_2,L}$. The surface tension is crucial when calculating the effective mass transfer area.

Table 7-2. Parameter sensitivity tabulating percent deviation in both loading rich solution and mole fraction CO2 in the clean gas when the input parameter is increased with 10 percent using run T25 as a base case.

Input Parameter	Percent Deviation	
	Rich Loading	$y_{CO_2}^{OUT}$
Calculated equilibrium partial pressure of CO_2	-0.04	0.10
Diffusivity of CO_2 in the liquid solution	2.04	-4.39
Diffusivity of AMP in the liquid solution	0.15	-0.20
Surface tension of the liquid solution	-3.28	4.39
Viscosity of the liquid solution	0.87	-1.07
Henry's Law Const. for CO_2 in the liquid solution	-4.15	5.46
Reaction rate constant	2.10	-2.73

H_{CO_2} is used when calculating E_∞, but more importantly it is used in the expression for the overall mass-transfer coefficient. $D_{CO_2,L}$ is used when calculating E and the liquid side mass transfer coefficient. Furthermore it is evident that sensitivity towards the physicochemical properties only used to calculate mass-transfer coefficients and E_∞ is not very high. This could be expected since the absorption is in the fast-reaction regime. The absorption is liquid side controlled for all the runs simulated in this work; the gas side mass-transfer coefficient never exceeds 2 percent of the overall mass-transfer coefficient in any of the simulations carried out. In this work the column is never run under pinch conditions and as expected $p_{CO_2}^*$ has very low influence. In Table 7-3 the approach to equilibrium for the three different experimental runs used for validation of the model is presented where the approach to equilibrium is defined as:

$$App.Eq. = \max\left(\frac{p_{CO_2}^*}{p_{CO_2}}\right) \tag{7.1}$$

Table 7-3. Approach to equilibrium, using equation (7.1), for three different experimental runs from Tontiwachwuthikul et al.[1]

Run	Approach to Equilibrium
T25	0.036
T26	0.021
T28	0.076

It is clearly seen in Table 7-3 that the partial pressure of CO_2 in the gas is much higher than the equilibrium pressure for the solution. In Figure 7-4 plots are shown presenting the partial pressure of CO_2 in the gas and the equilibrium partial pressure of CO_2 with the liquid phase over the column as a function of column position form the bottom of the column for runs T25 and T28. It is evident that the column is run far from pinch conditions.

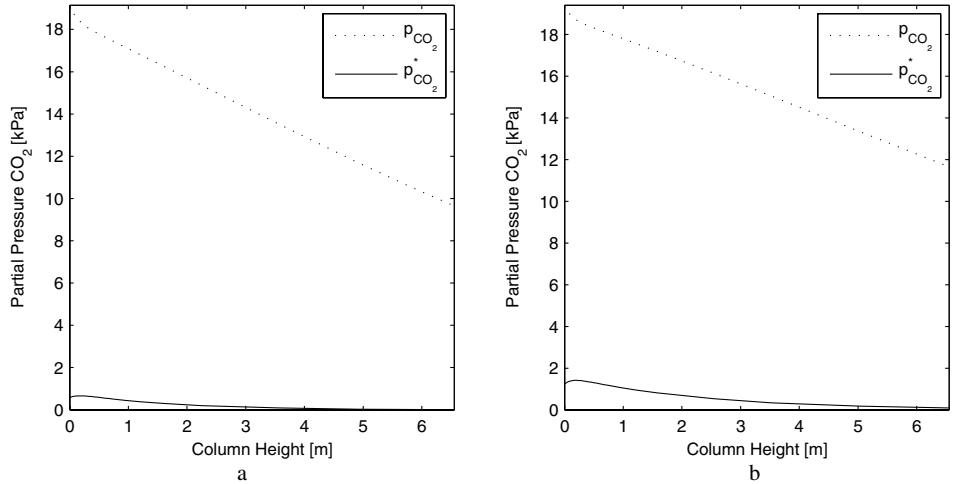

Figure 7-4. Partial pressure of CO2 in the gas (solid line) and the equilibrium partial pressure of CO2 with the liquid phase (dotted line) over the column as a function of column position from the bottom of the column for runs T25 (a) and T28 (b).

However for a larger tower operating at higher temperature, which would be the case in flue gas cleaning, it is likely that the tower would run close to pinch conditions due to the higher temperature and trying to utilize a high cyclic capacity. Thus $p^*_{CO_2}$ would be of higher significance than what is shown for the randomly packed column used for validation in this work.

7.1.2 Validation of the Absorber Model when Using Structured Packing

The validation of the proposed model for a tower using structured packing is done by comparison of simulation results with the experimental data presented in chapter 6 of this work. The experimental data simulated cover four different loading ranges and two different liquid circulation rates. For the lowest liquid rate the column runs at approximately 70% of flooding and at the highest liquid rate the column runs at approximately 80% of flooding. The inlet temperatures of the gas and the liquid are constant and in a range that is plausible for flue gas cleaning. Comparing to the data used in the validation of the randomly packed column this mean

that the evaporation of water plays a more important role in the simulation of the absorber. This is the case because it influences the temperature profile over the column. In Figure 7-5 parity plots comparing experimental flux of CO_2 (a) and rich loading (b) to simulated results using two different mass-transfer correlations are shown. It is clear that when using the correlations presented in Rocha et al.[8,9] the CO_2 absorption is over estimated and when using the correlation presented in Billet and Schultes[7] the CO_2 absorption is underestimated. It is furthermore clear that the flux of CO_2 is a more sensitive variable than the rich liquid loading.

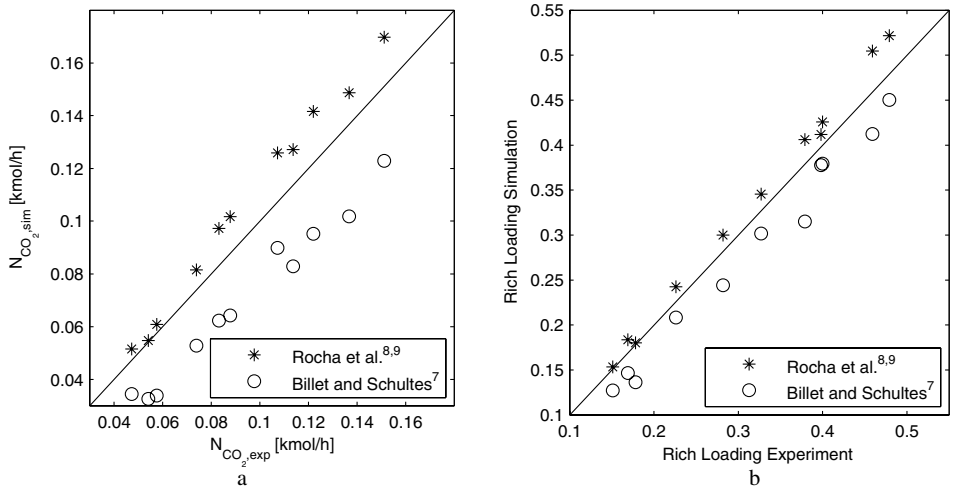

Figure 7-5. Parity plot of (a) experimental vs. simulated flux of CO_2 and (b) experimental vs. simulated rich loading both using two different correlations for the interfacial area and mass transfer.

In Table 7-4 %AAD is presented for the model for both rich loading and flux of CO_2 using both mass-transfer correlations. Furthermore the deviations between the simulated results using the two different models are shown. It is clear from Table 7-4 that the mass-transfer correlations from Rocha et al.[8,9] give the best results when compared to experimental data.

Table 7-4. %ADD between simulated and experimental flux of CO2 and rich liquid loading using two different mass-transfer correlations and deviations between the simulated results using the two different mass-transfer correlations.

	%AAD using Billet and Schultes[7]	%AAD using Rocha et al.[8,9]	%AAD Billet and Schultes[7] vs. Rocha et al.[8,9]
Rich Loading	11.3	6.0	20.0
Flux CO_2	27.2	11.3	53.8

Moreover, when looking at the average deviation between the simulated results using the two different mass-transfer correlations it is evident that special care should be given to the selection of the mass-transfer correlation used. The mass transfer correlation provided by Billet and

Schultes[7] is based on the assumption that the empty space of random or structured packing can, theoretically, be replaced by vertical flow channels. In the theoretical flow channels the liquid is assumed to trickle down evenly distributed while gas flows upwards counter currently. In reality the flow channels deviate from verticality in a way that is determined by the shape of the random or structured packing. The deviation from verticality cannot be defined by surface area and void volume alone, thus the deviation of the behaviour of the flow from vertical flow channels is expressed by six packing specific constants. In the mass-transfer correlation provided by Rocha et al.[8,9] a mechanistically based model has been developed for columns containing structured packing of the corrugated plate type. The model takes into account the flow and physical property characteristics of the falling liquid film as well as the upflowing gas. Furthermore, geometric variables such as corrugation angle and surface enhancement are considered. They put specific attention to the separation of the interfacial area from the mass-transfer coefficient, which is essential when modelling chemical absorption.

In order to investigate the differences between the two different mass-transfer and interfacial area correlations two runs R7 and R11 were chosen as test cases. The runs were chosen to cover the two different liquid flow rates used in the experimental work and because there is a large flux of CO_2 from the gas to the liquid in both runs. When using a mass-transfer correlation for physical absorption processes the product of k_L or k_G and a is used when describing the process, but when treating chemical absorption processes the product is not the most important factor.

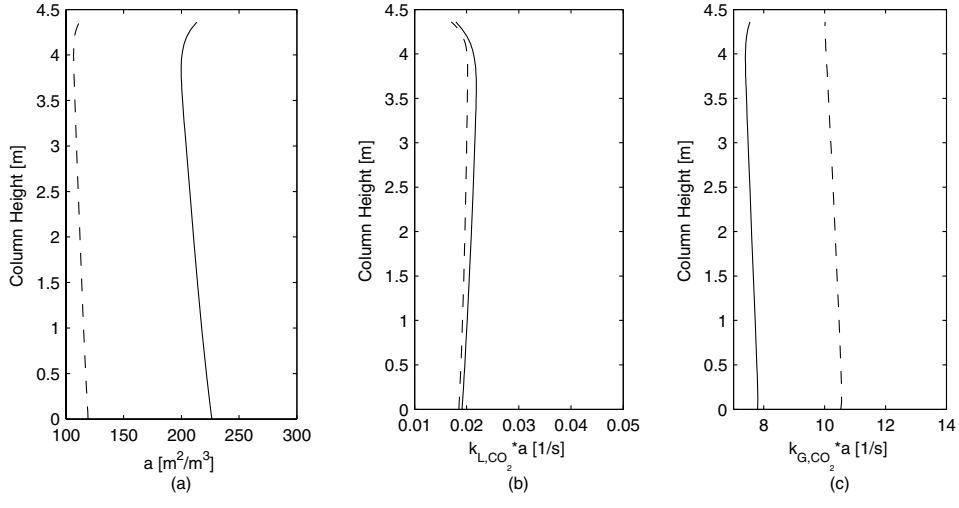

Figure 7-6. Comparison of (a) interfacial mass-transfer area, (b) the product of interfacial mass-transfer area and the liquid side mass-transfer coefficient for CO2 and (c) the product of interfacial mass-transfer area and the gas side mass-transfer coefficient for CO2 for run R7 where the dashed lines are calculated using Billet and Schultes[7] and the lines are calculated using Rocha et al. [8,9].

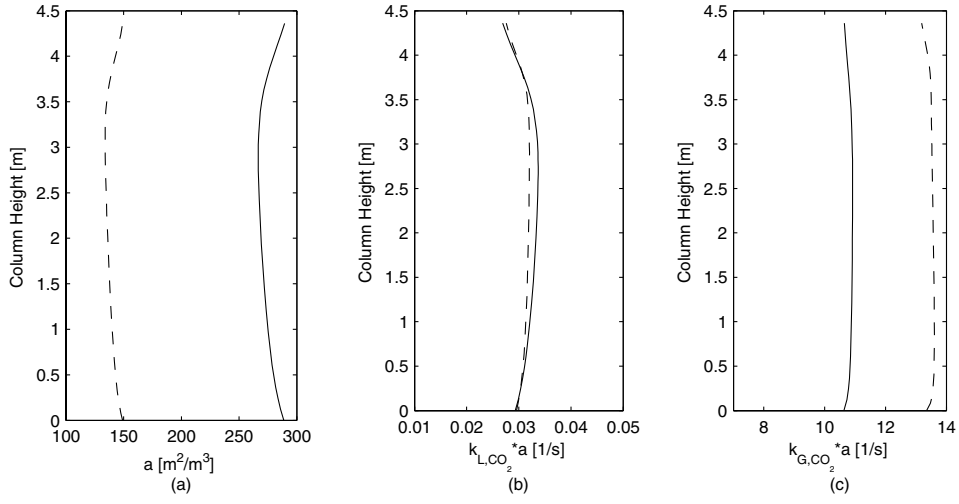

Figure 7-7. Comparison of (a) interfacial mass-transfer area, (b) the product of interfacial mass-transfer area and the liquid side mass-transfer coefficient for CO2 and (c) the product of interfacial mass-transfer area and the gas side mass-transfer coefficient for CO2 for run R11 where the dashed lines are calculated using Billet and Schultes[7] and the lines are calculated using Rocha et al. [8,9].

For chemical absorption processes that can be assumed as pseudo-first order or that are close to pseudo-first order $k_{L,CO2}$ is cancelled out when multiplying with the enhancement factor, as can be seen by inspection of equations (3.15) and (3.41). In Figure 7-6 and Figure 7-7 a and the products $k_{L,CO2}a$ and $k_{G,CO2}a$ are presented. In order to easily compare gas and liquid side mass-transfer resistance the units of $k_{G,CO2}$ have been converted in order to be the same as $k_{L,CO2}$. It is clear in Figure 7-6 and Figure 7-7 that the values of a calculated using the two different correlations is very different. The value of a calculated using Billet and Schultes[7] is approximately half of the value calculated using Rocha et al.[8,9]. Since the packing used in the column, Sulzer Mellapak 250Y, has a surface area of 250 m^2/m^3 the correlations presented by Rocha et al.[8,9] seem to give a value closer to the real value. When the column liquid circulation rate is 3 l/min the calculated value of a is approximately 210 m^2/m^3 and when the column liquid circulation rate is 6 l/min the value is approximately 275 m^2/m^3, the corresponding values using the other correlation[7] is 110 and 140 m^2/m^3. When looking at the products k_La and k_Ga it is clear that for the liquid side the two different correlations give almost identical values, while for the gas side the values using Billet and Schultes[7] are slightly higher. And as expected the mass transfer in the column is controlled by the liquid side. The difference in $k_{L,CO2}$ also changes the value of the enhancement factor since the value of $k_{L,CO2}$ obtained using Billet and Schultes[7] is approximately twice the value obtained using the other correlation thus the value of the enhancement factor is approximately half. In Figure 7-8 pseudo first-order enhancement factors

calculated using equation (3.15) and enhancement factors calculated using equation (3.26) are presented using both mass-transfer correlations for run R11.

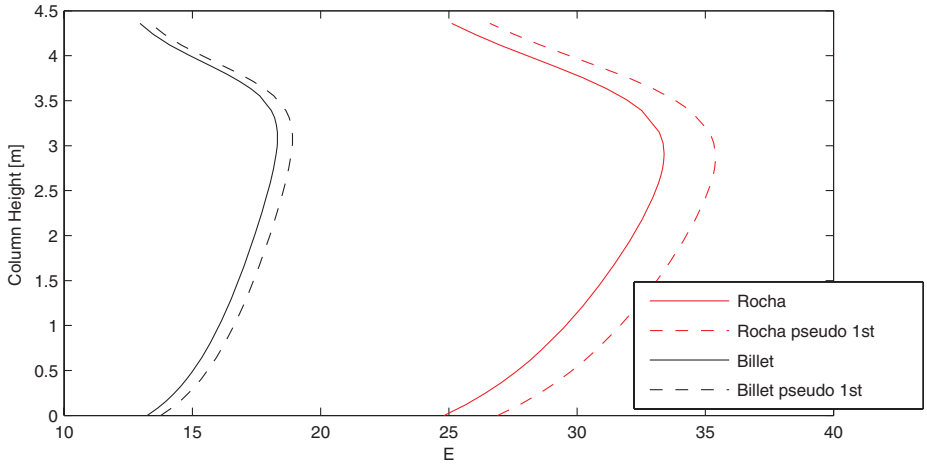

Figure 7-8. Pseudo first-order enhancement factor profiles calculated using equation (3.15) (dashed) and enhancement factor profiles calculated using equation (3.26) (line) for the absorber for the modeling of run R11. The black lines are calculated using Billet and Schultes[7] and the red lines are calculated using Rocha et al. [8,9].

It is clear that using a pseudo-first order enhancement factor would overestimate the value of the enhancement factor. It also shows that the mass-transfer correlation chosen has a great impact on the value of the enhancement factor. Furthermore, this shows that if, instead of using enhancement factors, the differential equations (3.2) and (3.3) are solved the mass-transfer correlations are of great importance since they are needed to estimate the liquid film thickness.

To validate the model all of the experimental runs were simulated. Then three different experimental runs, R4, R7 and R11, were chosen as a basis for the discussion of the results. These three runs were chosen since they represent three different loading ranges and the CO_2 flux is quite large. Furthermore, both liquid circulation rates are represented. In Figure 7-9 through Figure 7-11 the three different runs are represented with simulation results using the mass-transfer and interfacial area correlations from Billet and Schultes[7].

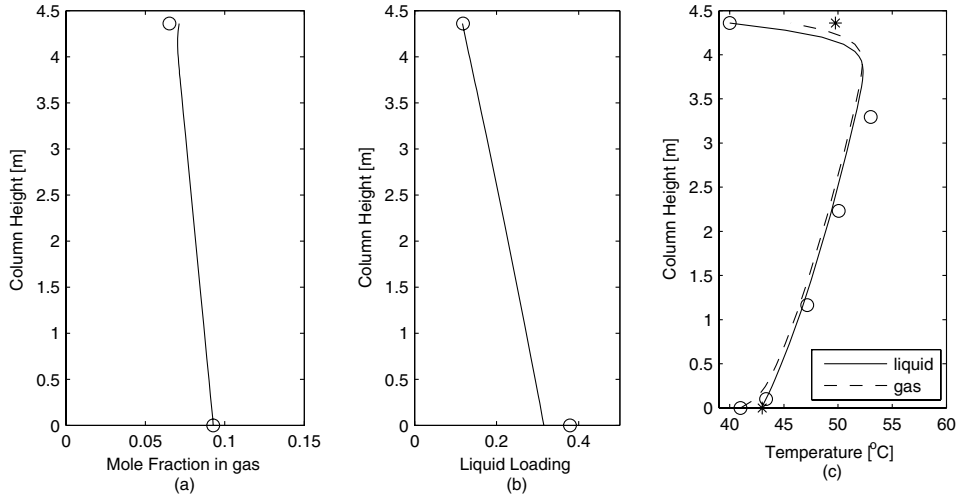

Figure 7-9. Modeled (lines) results and experimental data (circles and stars) for the AMP-CO2 system (run R4): (a) concentration profiles, (b) liquid loading, (c) liquid and gas temperature profiles using Billet and Shultes[7].

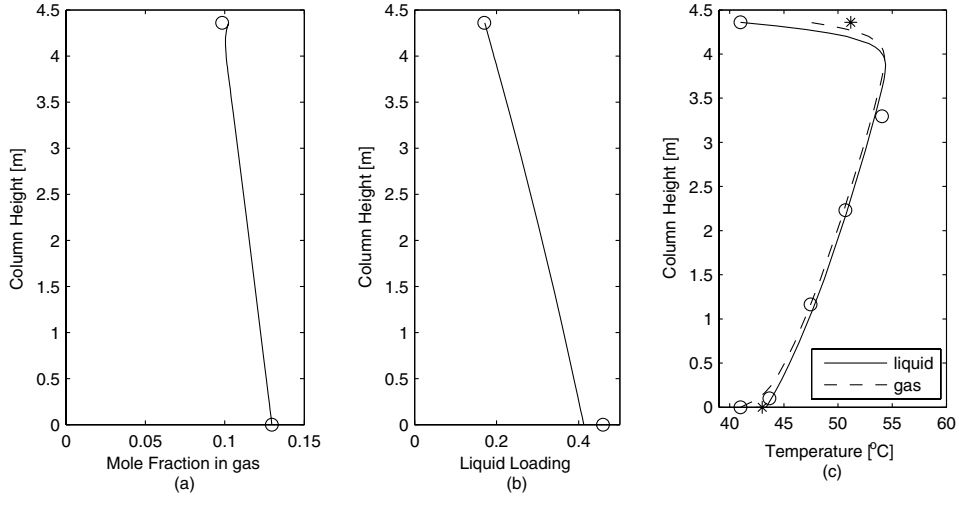

Figure 7-10. Modeled (lines) results and experimental data (circles and stars) for the AMP-CO2 system (run R7): (a) concentration profiles, (b) liquid loading, (c) liquid and gas temperature profiles using Billet and Shultes[7].

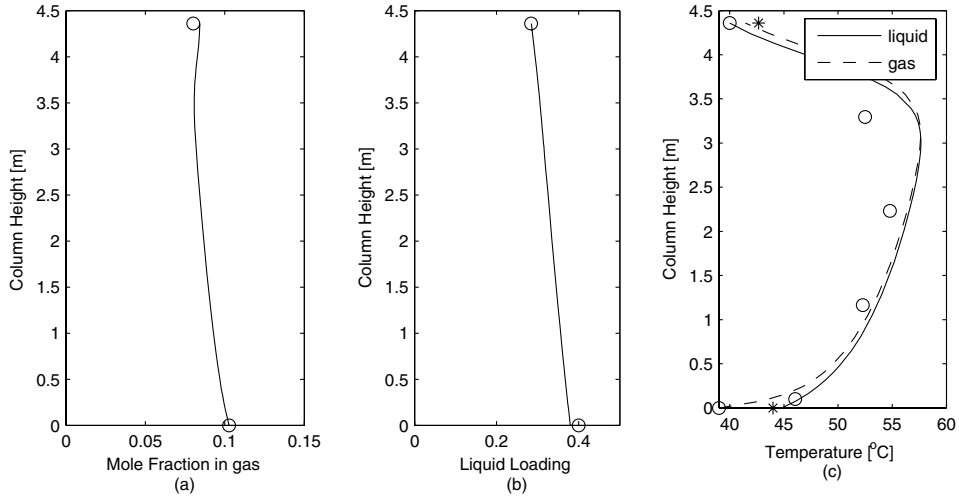

Figure 7-11. Modeled (lines) results and experimental data (circles and stars) for the AMP-CO2 system (run R11): (a) concentration profiles, (b) liquid loading, (c) liquid and gas temperature profiles using Billet and Shultes[7].

As presented earlier the simulated absorption of CO_2 is lower than the experimental for all three runs, probably due to the very low values of *a*. In runs R4 and R7 both the gas and the liquid temperatures are accurate. Both R4 and R7 are run at the same liquid rate of 3 l/min. One can furthermore see that the difference in gas and liquid temperatures are captured quite well, since the stars in the figures represent the experimental outlet temperatures of the gas and the liquid. The fact that the temperatures are captured so well is a bit unexpected since the absorption is underestimated. One would expect that the temperatures would be underestimated since the absorption is underestimated. For run R11 the absorption of CO_2 is captured quite accurately, but the temperature of the column is overestimated. Especially towards the top of the column the temperature is too high. In general this is consistent with the results for the two other runs presented, since the low absorption of CO_2 gave accurate temperature representation. The very pronounced temperature maximum close to the top of the column is due to the evaporation of water as well as the heat of reaction between CO_2 and AMP. Since the mass transfer of water is gas side controlled a higher gas side mass-transfer resistance would give a more evenly distributed temperature profile with a peak at a lower position with a lower max value. Calculations show that a 30 % increase in the gas side mass transfer for water gives a perfect fit to the temperature bulge for run R11. The same change in mass-transfer of water does not have negative impact on the temperature representation for the runs R4 and R7 either. In Figure 7-12 through Figure 7-14 the three different runs are represented with simulation results using the mass-transfer and interfacial area correlations from Rocha et al.[8,9].

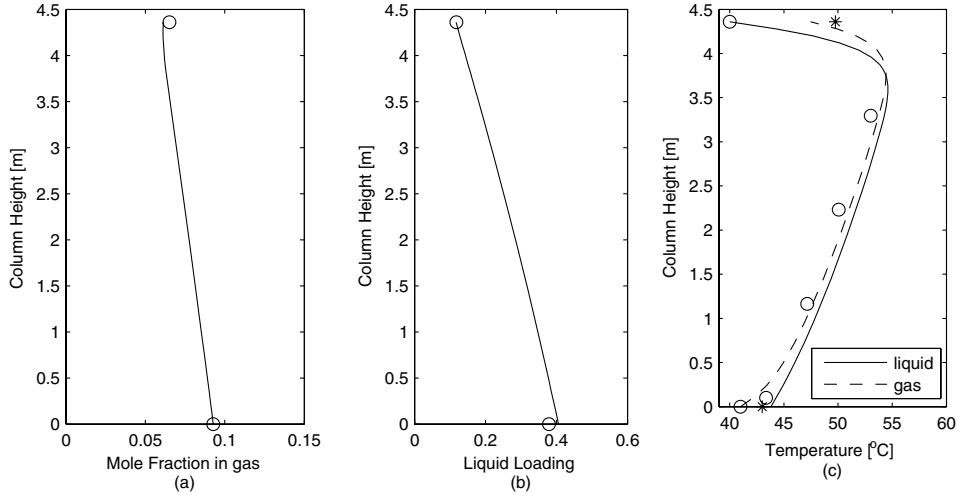

Figure 7-12. Modeled (lines) results and experimental data (circles and stars) for the AMP-CO2 system (run R4): (a) concentration profiles, (b) liquid loading, (c) liquid and gas temperature profiles using Rocha et al.[8,9].

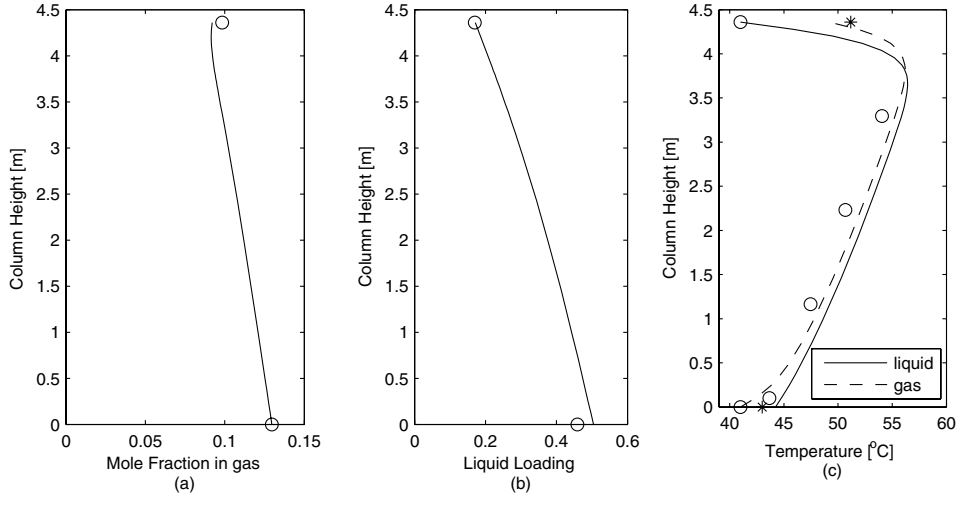

Figure 7-13. Modeled (lines) results and experimental data (circles and stars) for the AMP-CO2 system (run R7): (a) concentration profiles, (b) liquid loading, (c) liquid and gas temperature profiles using Rocha et al.[8,9].

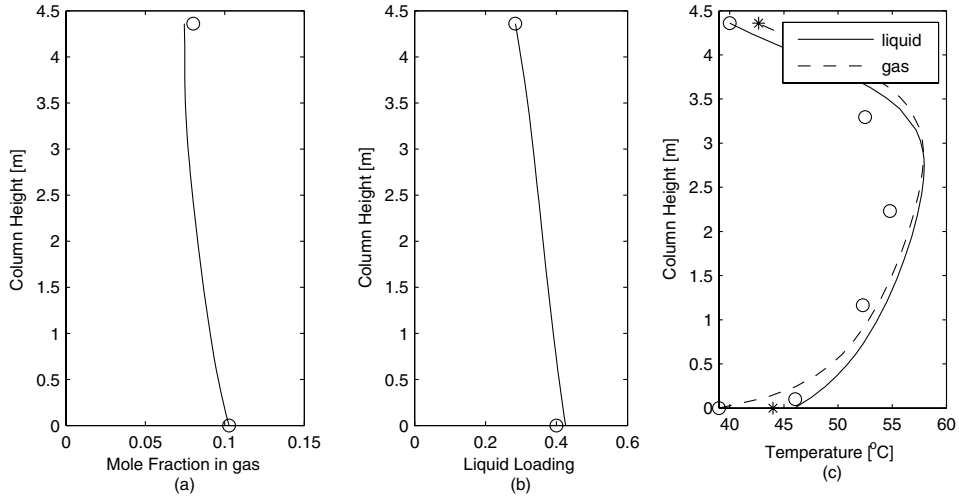

Figure 7-14. Modeled (lines) results and experimental data (circles and stars) for the AMP-CO2 system (run R11): (a) concentration profiles, (b) liquid loading, (c) liquid and gas temperature profiles using Rocha et al.[8,9].

The simulated absorption of CO_2 is higher than the experimental for all three runs, but the over estimation of the absorption is not very high. As expected when the amount of absorbed CO_2 is overestimated the temperatures are overestimated. The overestimation of the temperature is especially pronounced in run R11. This may be surprising since it has the lowest over-estimation of the CO_2 absorption, but the experiment was carried out at the highest liquid rate. Compared to the temperature estimated for run R11 using the Billet and Schultes[7] mass-transfer correlation the peak of the temperature bulge has shifted slightly down in the column, due to the lower value of the gas side mass-transfer coefficient obtained using Rocha et al. [8,9], as can be seen in Figure 7-7.

Table 7-5. Approach to equilibrium, using equation (7.1), in the absorber for all experimental runs using two different correlations for mass and heat transfer.

Run	Approach to equilibrium Rocha et al.[8,9]	Approach to equilibrium Billet and Schultes[7]
R1	0.08	0.05
R2	0.10	0.07
R3	0.10	0.06
R4	0.16	0.08
R5	0.14	0.09
R6	0.20	0.14
R7	0.19	0.11
R8	0.28	0.21
R9	0.29	0.23
R10	0.21	0.14
R11	0.34	0.27

For all the runs R1-R11 the approach to equilibrium was calculated according to equation (7.1). In Table 7-5 the approach to equilibrium for all the runs are presented. As expected runs carried out at higher loading ranges are closer to equilibrium. Moreover, due to the higher temperature in the data using structured packing compared to random packing, the absorber is run closer to equilibrium. It is still far from pinch conditions which could be encountered when trying to design energy efficient processes. But, the thermodynamic equilibrium model is of higher importance than when simulating the randomly packed column. In Figure 7-15 CO_2 partial pressure profiles in the absorber column during R11 are presented. It is clear that the highest equilibrium partial pressure is experienced close to the temperature peak. This shows that for a commercial absorber pinch conditions could be encountered in the middle of the column.

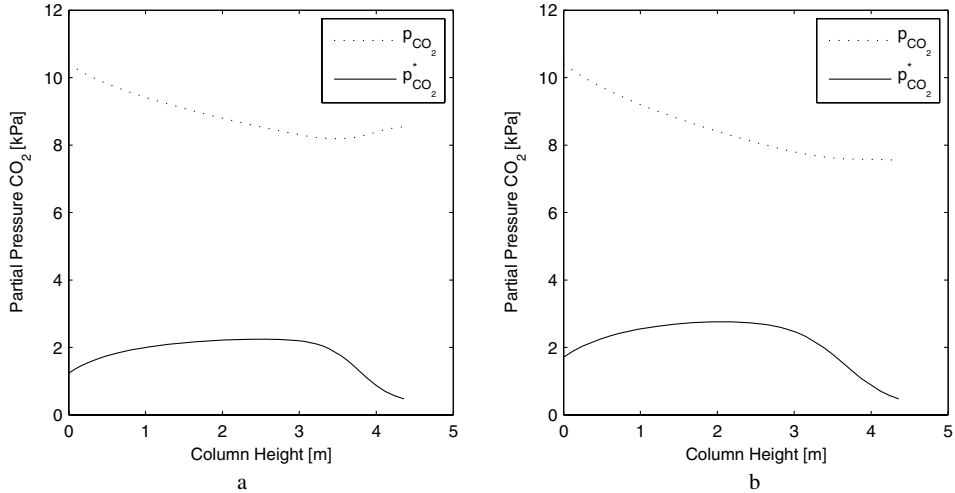

Figure 7-15. Partial pressure of CO2 (solid line) and partial pressure of CO2 that would have been in equilibrium with the liquid phase (dotted line) over the column as a function of column position from the bottom of the column for runs R11 using Billet and Schultes[7] (a) and Rocha et al.[8,9] (b).

7.1.2.1 Sensitivity Analysis of the Absorber Model when Using Structured Packing

A sensitivity analysis of the mass transfer based model was carried out under the conditions encountered during runs R7 and R11 using both of the earlier discussed mass-transfer correlations. The input parameters tested were the same as described for the sensitivity test carried out for the randomly packed absorber. The results are reported in Table 7-6. It is clear that compared to the sensitivity test of the randomly packed absorber presented in Table 7-2 the equilibrium partial pressure of CO_2 is of higher importance, as expected, since the column is run at conditions closer to equilibrium. Other than that, one can see that the same parameters are important as in the randomly packed column. One clear difference between the two different mass-transfer correlations is the sensitivity towards the surface tension of the solution. The

Billet and Schultes[7] correlation is clearly more sensitive with respect to surface tension than the Rocha et al.[8,9] correlation. This is due to the different expressions for the interfacial mass-transfer area used in the two different mass-transfer correlations, in the Billet and Schultes[7] correlation the surface tension is in a group which is raised to the power of 0.75 whereas in the Rocha et al.[8,9] correlation the surface tension is in a group that is raised to the power of 0.15. Other than that the other parameters are of similar relative importance when comparing the two different mass-transfer correlations.

Table 7-6. Parameter sensitivity test for runs R7 and R11 using two different mass transfer correlations. The sensitivity is tabulated with respect to loading change over the column.

Input Parameter	Percent Deviation Loading Change			
	Rocha		Billet and Shultes	
	R7	R11	R7	R11
Calculated equilibrium partial pressure of CO_2	-1.7	-3.0	-1.1	-2.7
Diffusivity of CO_2 in the liquid solution	1.7	1.9	2.8	2.7
Diffusivity of AMP in the liquid solution	0.4	0.3	0.3	0.2
Surface tension of the liquid solution	-0.7	-0.4	-4.8	-3.8
Viscosity of the liquid solution	0.8	0.6	1.2	0.9
Henry's Law Const. for CO_2 in the liquid solution	-4.0	-4.1	-5.9	-5.8
Reaction rate constant	1.9	2.0	3.0	2.8

Seeing the importance of the mass transfer correlations and effective interfacial mass transfer area, calculations were carried out using the Rocha et al.[8,9] correlations for the mass transfer coefficients but the effective interfacial mass transfer area from de Brito et al. [21] to check if that would improve the results. The results were almost identical to the results found using the correlation found in refs.[8,9]. Furthermore, calculations were carried out with interfacial mass transfer area decreased by 20% compared to the value obtained using Rocha et al.[8,9] and excellent results were achieved for both temperature profiles and amount of CO_2 absorbed. The results for runs R7 and R11 are presented in Figure 7-16 and Figure 7-17 respectively.

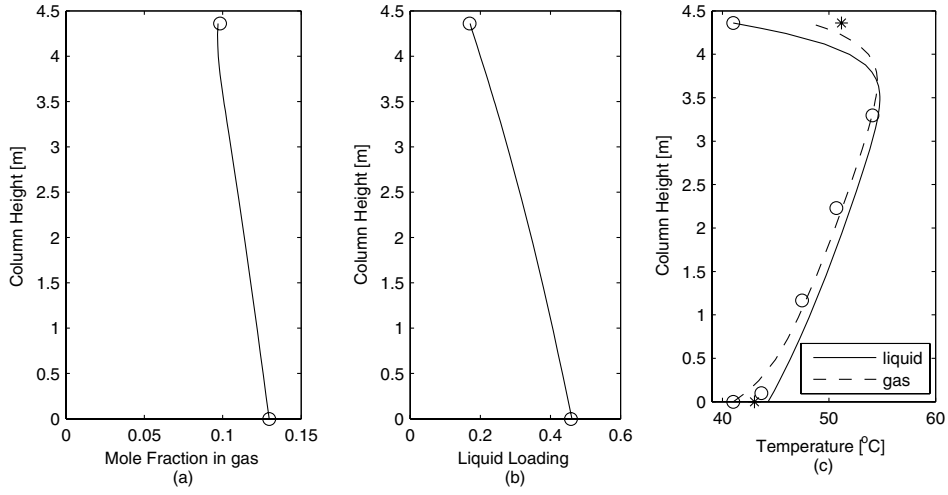

Figure 7-16. Modeled (lines) results and experimental data (circles and stars) for the AMP-CO2 system (run R7): (a) concentration profiles, (b) liquid loading, (c) liquid and gas temperature profiles using Rocha et al.[8,9] with a reduction in interfacial mass transfer area of 20%.

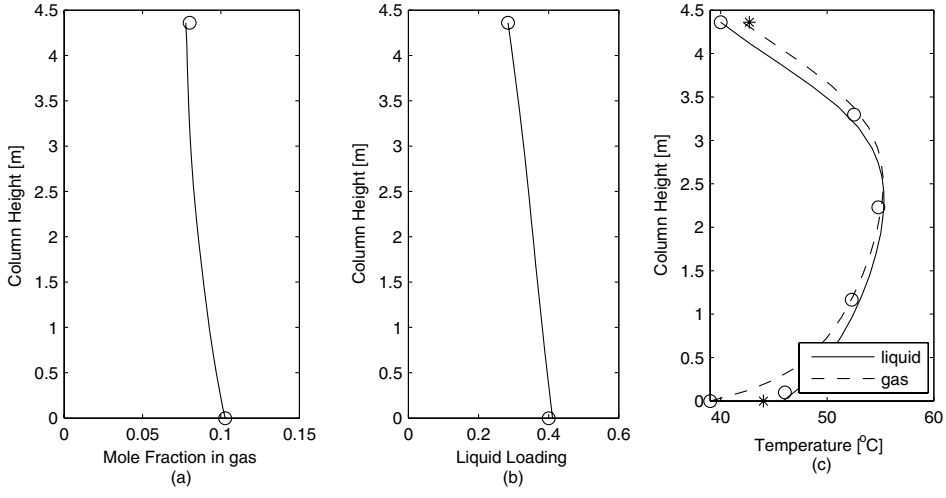

Figure 7-17. Modeled (lines) results and experimental data (circles and stars) for the AMP-CO2 system (run R11): (a) concentration profiles, (b) liquid loading, (c) liquid and gas temperature profiles using Rocha et al.[8,9] with a reduction in interfacial mass transfer area of 20%.

The value of the effective mass transfer area is then between the values found using Billet and Schultes[7] and Rocha et al.[8,9]. A fitting like this unfortunately decreases the predictive capabilities of the model, but it does show that the absorber model is based on sound physical principles. The temperature profile is heavily influenced by water mass transfer and could be captured correctly by just changing the mass transfer of water, as described earlier, but that did not change the absorption of CO_2 significantly. When changing the effective mass transfer area

both the water and CO_2 mass transfer was changed in a consistent way and excellent results were obtained for both temperature and CO_2 absorption.

7.1.3 Conclusions for Validation of the AMP Packed Column Model

The rate-based absorber model proposed in Chapter 3 has been validated for CO_2 absorption in an aqueous AMP solution using both a structured and a randomly packed tower. The model has been tested for two different AMP concentrations, 2.0 and 2.9 M, and for two different temperature ranges. Furthermore, for the column with structured packing two different mass-transfer correlations were evaluated, and one was found more appropriate for chemical absorption models due to a more accurate description of the wetting of the packing material. Sensitivity analysis of the model under the different conditions encountered was carried out and the most important parameters were identified. When using the mass-transfer model form Billet and Schultes[7] the most important parameters were the Henry's law coefficient of CO_2, the surface tension of the solution and at the highest temperatures and loadings encountered, the equilibrium partial pressure of CO_2. When using the mass-transfer correlation form Rocha et al.[8,9] the most important parameters were the Henry's law coefficient of CO_2 and at the highest temperatures and loadings encountered, the equilibrium partial pressure of CO_2. It would have been of interest to validate the model at even higher temperatures in order to verify the model under pinch conditions in order to check the accuracy of the thermodynamic model used.

7.2 MEA

As discussed in section 3.2.1 most models published in the literature have only been validated against data from pilot plants using aqueous MEA as the absorbent, and with pilot plant data from Tontiwachwuthikul et al.[1]. This was also done for the model proposed in this work. In Table 7-7 the physical properties implemented in the model in this work are presented with references. The second order chemical reaction rate constant used was calculated using an Arrhenius equation found in Versteeg et al.[22]. The mass-transfer correlation used was obtained from Billet and Schultes[7].

Table 7-7. Physical and Chemical properties used in the absorber model for MEA.

Property	Source	Comment
Liquid Density	Cheng et al.[13]	Linear mixing
Specific heat of gas components	Reid et al.[11]	
Specific heat of liquid solution	Cheng et al. [13]	Linear mixing
Diffusivity of CO_2 in the liquid solution	Ko et al.[14]	Based on the N_2O analogy
Viscosity of the gas	Reid et al.[11]	Method of Wilke
Thermal conductivity of the gas	Reid et al.[11]	Eucken for pure compounds, Mason and Saxena for mixture
Diffusivity of CO_2 and water in the gas phase	Reid et al.[11]	Fuller equation
Surface tension of the liquid solution	Vazquez et al.[15]	
Viscosity of the liquid solution	Cheng et al.[13]	
Henry's Law Constant of CO_2 in the liquid solution	Wang et al.[23] and Browning et al.[18]	Based on the N_2O analogy and using an expression to account for the salting out effect with increased CO_2 loading
Diffusivity of AMP in the liquid solution	Snijder et al.[24]	

7.2.1 Model Validation MEA

The validation of the proposed model when using a tower with random packing is done by comparison of simulation results with experimental data. The experimental data is taken from Tontiwachwuthikul et al.[1] where results for ten runs of CO_2 absorption into an aqueous MEA solution in a packed column are reported. The concentration of the MEA solution used in the experimental work is ranging from 2 to 3.8 M. According to the mass-transfer correlation the column was found to run at approximately 60 % of flooding. The interfacial mass-transfer area was estimated to 75 m^2/m^3, a surprisingly low value since the surface area of the packing is 545 m^2/m^3. In Figure 7-18 and Figure 7-19 comparison between experimental data and simulated results for runs T14 and T17 are presented respectively. The reason why these experimental runs were chosen is that these are the two runs which most closely resemble the rich and lean loading conditions most likely to be encountered in flue gas cleaning. Furthermore, the two different runs represent two different concentrations of MEA namely 2.0 M in run T14 and 3.8 M in run T17.

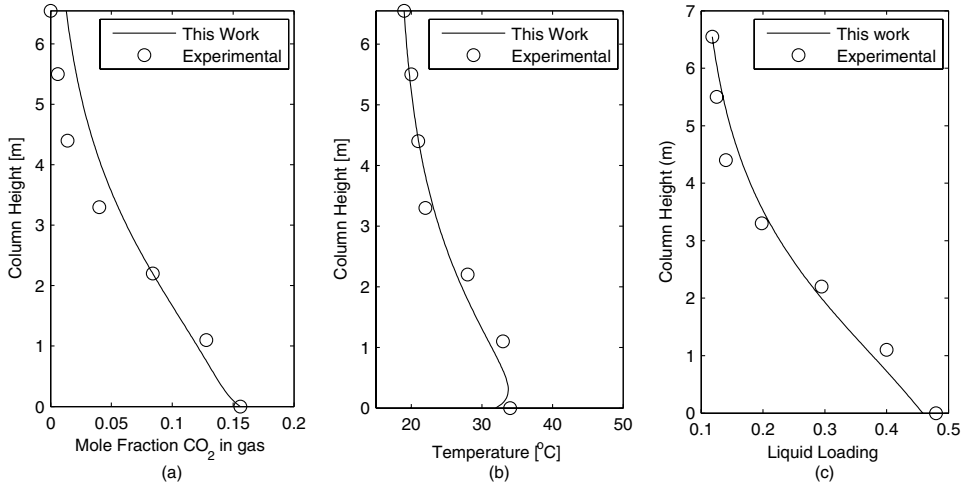

Figure 7-18. Modeled (lines) results and experimental data (circles) for the MEA-CO2 system (run T14): (a) concentration profiles, (b) liquid loading, (c) liquid temperature profiles.

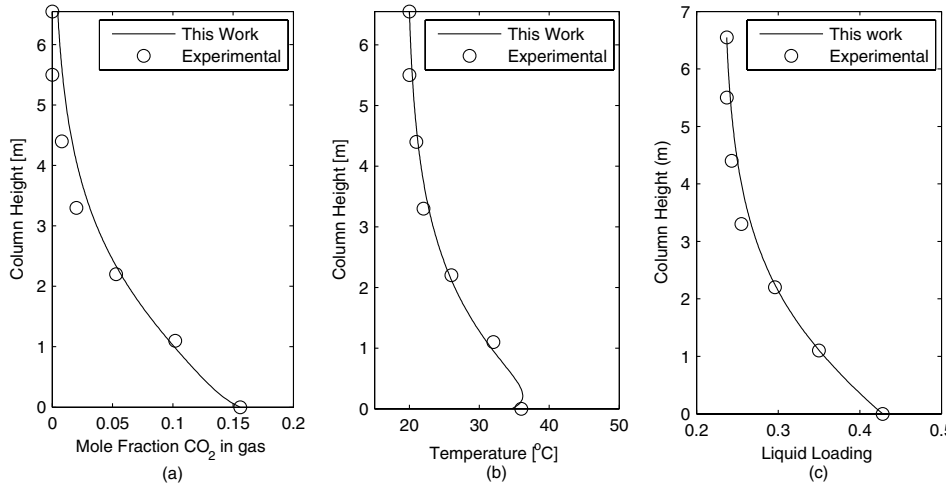

Figure 7-19. Modeled (lines) results and experimental data (circles) for the MEA-CO2 system (run T17): (a) concentration profiles, (b) liquid loading, (c) liquid temperature profiles.

It is clear form Figure 7-18 and Figure 7-19 that the temperature profile of the column is accurately captured for both runs. It is also clear that for run T14 the CO_2 absorption is slightly under predicted, but for run T17 the liquid loading profile is accurately captured. The amount of CO_2 in the clean gas is over predicted in both runs. For run T17 this is unexpected since the liquid loading is correct and the experimental mass balance error for the experimental run is reported to be only 0.89 %.

7.2.2 Parameter Sensitivity MEA

A parameter sensitivity test including several of the physicochemical properties was carried out for the mass transfer based model run T17 and is presented in Table 7-8. The sensitivity of the output of the model was checked by increasing the parameter with ten percent and calculating how this change affected the two important variables, rich liquid loading and mole fraction of CO_2 in the clean gas. It is clear that the two parameters the model is most sensitive to are the liquid surface tension and Henry's Law constant for CO_2 in the liquid solution.

Table 7-8. Parameter sensitivity tabulating percent deviation in both loading rich solution and mole fraction CO2 in the clean gas when the input parameter is increased with 10 percent using run T17 as a base case.

Input Parameter	Percent Deviation (T17)	
	Rich Loading	y_{CO2} out
Calculated equilibrium partial pressure of CO_2	0.00	0.00
Diffusivity of CO_2 in the liquid solution	0.28	-12.66
Diffusivity of MEA in the liquid solution	0.02	-1.27
Surface tension of the liquid solution	-0.52	25.32
Viscosity of the liquid solution	0.14	-6.33
Henry's Law Const. for CO_2 in the liquid solution	-0.61	30.38
Reaction rate constant	0.28	-13.92

7.2.3 Conclusion from MEA Model

A simple rate based model for CO_2 absorption in a packed column using aqueous MEA, utilizing a simple thermodynamic model, has been developed. A parameter sensitivity test for different physicochemical properties has been carried out and the model is clearly most sensitive to the surface tension of the liquid solution and the Henry's Law constant for CO_2 in the solution for an absorber under the conditions considered in this work. Other important parameters are the diffusivity of CO_2 in the liquid solution and the reaction rate constant.

7.3 Conclusion

The developed adiabatic absorber model combined with the simple thermodynamic model developed in this work has been applied to CO_2 absorption using two different aqueous alkanolamine solutions, MEA and AMP, of varying concentrations. For the AMP solution two different columns using both randomly and structured packing were used for verification, as well as two different temperature ranges. It is clear that the mass-transfer correlation used is of very high importance when modeling absorption towers; one should especially check that the interfacial mass-transfer area is in a range that is feasible. The most important physicochemical input parameters in the model have been identified.

1. The Henry's law coefficient for CO_2 in the liquid solution.

2. Depending on the temperature and the loading of the liquid solution, the equilibrium partial pressure of CO_2 is of high importance.
3. The diffusivity of CO_2 in the liquid solution and the chemical rate constant are also of high importance. When using the mass-transfer correlation from Billet and Schultes[7] the surface tension of the solution is of high importance since it has a large influence on the calculated interfacial mass-transfer area.

The other tested physicochemical properties such as viscosity and diffusivity of alkanolamine in the liquid solution are of less importance under the conditions tested in this work. In order to predict the correct temperature profile over the column at higher temperatures the gas side mass-transfer coefficient of water is essential. Since the condition of all the experimental data treated in this work was close to the pseudo first-order regime, the value of the liquid side mass-transfer coefficient for CO_2 is not of high significance.

References

[1] Tontiwachwuthikul P, Meisen A, Lim CJ. CO_2 Absorption by NaOH, Monoethanolamine and 2-Amino-2-Methyl-1-Propanol Solutions in a Packed Column. Chem Eng Sci. 1992;47:381-390.

[2] Alatiqi I, Sabri MF, Bouhamra W, Alper E. Steady-State Rate-Based Modelling for CO_2/Amine Absorption-Desorption Systems. Gas. Sep. Purif. 1993;8:3-11.

[3] Weiland RH, Rawal M, Rice RG. Stripping of Carbon Dioxide from Monoethanolamine Solutions in a Packed Column, AIChE Journal. 1982: 28; 963-973.

[4] Aboudheir A, Tontiwachwuthikul P, Idem R. Rigorous model for predicting the behavior of CO-2/ absorption into AMP in packed-bed absorption columns. Ind. Eng. Chem. Res. 2006;45: 2553-2557.

[5] Pandya, JD. Adiabatic Gas Absorption and Stripping with Chemical Reaction in Packed Towers. Chem. Eng. Comm. 1983; 19: 343-361.

[6] Aroonwilas A. High Efficiency Structured Packing for CO_2 Absorption using 2-Amino-2-methyl-1-propanol (AMP). M.Sc. Thesis, University of Regina, Regina, Canada, 1996.

[7] Billet R, Schultes M. Prediction of Mass Transfer Columns With Dumped and Arranged Packings Updated Summary of the Calulation method of Billet and Schultes. Trans IChemE. 1999;77:498 -504.

[8] Rocha JA, Bravo JL, Fair JR. Distillation columns containing structured packings: A comprehensive model for their performance. 1. Hydraulic models, Ind. Eng. Chem. Res. 1993;32:641-651.

[9] Rocha JA, Bravo JL, Fair JR. Distillation columns containing structured packings: A comprehensive model for their performance. Mass-Transfer Model, Ind. Eng. Chem. Res. 1996;35:1660-1667.

[10] Xu S, Otto FD, Mather AE. Physical Properties of Aqueous AMP Solutions, J. Chem. Eng. Data. 1991;36:71-75.

[11] Reid RC, Prausnitz JM, Poling BE. The Properties of Gases and Liquids (4th edition). New York: McGraw-Hill, 1987

[12] Chiu L-F, Liu H-F, Li M-H. Heat Capacity of Alkanolamines by Differential Scanning Calorimetry. J. Chem. Eng. Data. 1999;44:631-636.

[13] Cheng S, Meisen A, Chakma A. Predict Amine Solution Properties Accurately. Hydrocarbon Process. 1996;75: 81-84.

[14] Ko J-J, Tsai T-C, Lin C-Y, Wang H-M, Li M-H. Diffusivity of Nitrous Oxide in Aqueous Alkanolamine Solutions. J. Chem. Eng. Data. 2001;46:160-165.

[15] Vazquez G, Alvarez E, Navaza, JM, Rendo R, Romero E. Surface tension of binary mixtures of water + monoethanolamine and water + 2-amino-2-methyl-1-propanol and tertiary mixtures of these amines with water from 25°C to 50°C. J. Chem. Eng. Data. 1997;42: 57- 59.

[16] Henni A, Hromek JJ, Tontiwachwuthikul P, Chakma A. Volumetric Properties and Viscosities for Aqueous AMP Solutions from 25 °C to 70 °C. J. Chem. Eng. Data. 2003;48:551-556.

[17] Saha AK, Bandyopadhyay S S, Biswas AK. Solubility and Diffusivity of N_2O and CO_2 in Aqueous Solutions of 2-Amino-2-Methyl-1-Propanol. J. Chem. Eng. Data. 1993; 38: 78-82.

[18] Browning GJ, Weiland RH. Physical Solubility of Carbon Dioxide in Aqueous Alkanolamines via Nitrous Oxide Analogy. J. Chem. Eng. Data. 1994;39:817-822

[19] Chang L-C, Lin T-I, Li M-H. Mutual Diffusion Coefficients of Some Aqueous Alkanolamines Solutions. J. Chem. Eng. Data. 2005;50:77-84.

[20] Saha AK, Bandyopadhyay SS, Biswas AK. Kinetics of Absorption of CO_2 into Aqueous Solutions of 2-amino-2-methyl-1-propanol. Chem. Eng. Sci. 1995;50: 3587-3598.

[21]de Brito MH, Von Stockar U, Bangerter AM, Bomio P, Laso M. Effective Mass-Transfer Area in a Pilot Plant Column Equipped with Structured Packings and with Ceramic Rings. Ind. Eng. Chem. Res. 1994; 33:647-656.

[22] Versteeg, G.F.; Van Dijck, L.A.J.; Van Swaaij, W.P.M. On the kineticks Between CO_2 and Alkanolamines both in Aqueous and non-Aqueous Solutions. An Overwiew. Chem. Eng. Comm. 1996;144:113-158.

[23] Wang, Y.W. and Xu, S. and Otto, F.D. and Mather, A.E. Solubility of N_2O in alkanolamines and in mixed solvents, Chemical Engineering Journal and the Biochemical Engineering Journal, 1992;48:31-40.

[24] Snijder, E. D.; te Riele, M. J. M.; Versteeg, G. F.; van Swaaij, W. P. M. Diffusion Coefficients of Several Aqueous Alkanolamine Solutions. J. Chem. Eng Data. 1993;*38*:475-480.

8 Conclusions and Future Challenges

8.1 Conclusions

The main conclusions that can be derived from this thesis are:

Partial pressures of CO_2 over aqueous solutions of MEA, DEA, MDEA, AMP, PZ and PZ/MDEA can be correlated, given certain conditions, using a simple approach where only one chemical equilibrium reaction is taken into account, and assuming ideal gas and ideal liquid properties. The approach combines the Henry's law constant and the chemical reaction equilibrium constant for the formation of carbamate for primary and secondary alkanolamines (MEA,DEA) or bicarbonate for sterically hindered and tertiary alkanolamines (AMP,MDEA), resulting in an explicit expression for calculating the partial pressure of CO_2 over an aqueous alkanolamine solution. The diamine PZ has been treated in a similar way as the sterically hindered and tertiary alkanolamines. The deviations from experimental data are similar to deviations reported by other authors using models where the non-idealities are accounted for through activity coefficient models or equations of state. Heat of absorption values derived from the model agree with experimental data from the literature.

Work has been carried out in order to verify an experimental set-up and method for determining chemical rate constants in reactive gas liquid systems using a string of discs absorber. Furthermore, experimental work has been carried out in order to determine the effective mass transfer area for the string of discs absorber. It has been shown that the value found for the mass transfer area is strongly dependent on the liquid rate as well as the physicochemical properties used in the calculation. Validation of the experimental set-up and method was done using a system with a well defined chemical rate constant, the results show promise but are not conclusive. Efforts have been made to find an Arrhenius expression for the chemical rate constant for the reaction of CO_2 with AMP in an aqueous solution, but the experimental data are inconclusive. But the experiments confirmed which Arrhenius expression, found in the literature, which is the most reliable one. A parameter sensitivity test was carried out and addressed possible difficulties with using the experimental set-up and the method for determination of chemical rate constants in reactive gas-liquid systems. Especially the concentration of CO_2 in the bleed gas and the Henry's Law constant for CO_2 in the solution were of high significance.

A simple rate-based absorber model, utilizing the simple thermodynamic model developed, has been validated for CO_2 absorption in an aqueous AMP solution using both a structured and a randomly packed tower and aqueous solutions of MEA in a randomly packed tower. Using AMP the model was validated for two different concentrations, 2.0 and 2.9 M, and for two

different temperature ranges. Furthermore, for the column with structured packing two different mass-transfer correlations were evaluated, and one was found more appropriate for chemical absorption models due to a more accurate description of the wetting of the packing material. Sensitivity analysis of the model under the different conditions encountered was carried out and the most important parameters were identified. The most important parameters were the Henry's law coefficient of CO_2, the surface tension of the solution and, at the highest temperatures and loadings encountered, the equilibrium partial pressure of CO_2.

8.2 Future Challenges

Future challenges based on this work could be to further develop the thermodynamic model in order to account for the vapor pressure of the alkanolamine and to include two chemical equilibrium reactions. A first step should be to gather and critically evaluate all experimental data available and establish a comprehensive data base. Other relevant data than the VLE of the systems, such as heat of absorption of CO_2 found through calorimetry and speciation of the solution found through NMR, should be used to verify the thermodynamic model.

Include the volatility of the alkanolamine in the absorber model, to be able to predict the alkanolamine slip, for environmental and economical reasons. Further extend the absorber model to include other alkanolamines and mixed alkanolamines. It would also be of interest to include a term in the model to account for the degradation of the alkanolamine.

Furthermore, it would be of interest to carry out experiments to find the necessary physicochemical properties, needed for column design, that are valid at the temperatures encountered in the desorber and the warmest part of the absorber.

Develop a desorber model based on the absorber model and the experimental pilot plant data presented in this work and new data from the literature. And finally use the developed tools to design optimal solutions for CO_2 capture including solvent selection and operating conditions.

Appendices

Appendix A. Chemical Structures and Abbreviations

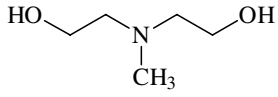

MDEA
methyldiethanolamine

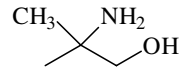

AMP
2-amino-2-methyl-propanol

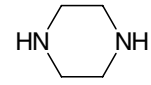

Piperazine

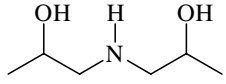

DIPA
diisopropanolamine

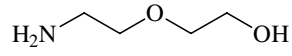

DGA
diglycolamine

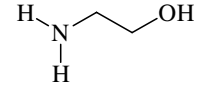

MEA
monoethanolamine

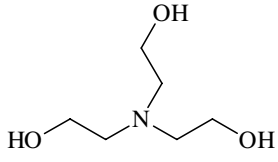

TEA
triethanolamine

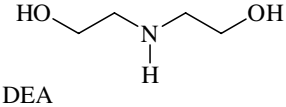

DEA
diethanolamine

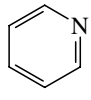

Pyridine

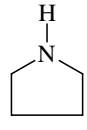

Pyrrolidine

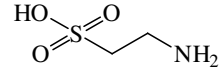

Taurine
2-amino-ethanesulfonic acid

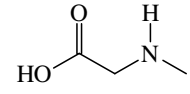

Sarcosine
N-methyl-glycine

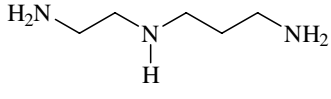

AEPDNH$_2$
N-(2-aminoethyl)-1,3-propandiamine

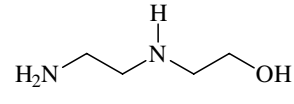

AEE
2-(2-aminoethylamino)ethanol

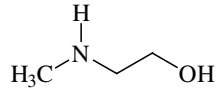

MAE
2-(methylamino)-ethanol

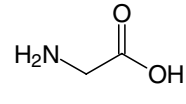

Glycine
2-aminoacetic acid

Appendix B. Derivation of the Rate-Based Model

Using Figure 3-4 the following mass and heat balances can be set up.

Gas Phase Mass and Heat Balances

Total mole balance for the gas phase assuming that no chemical reactions take place in the gas phase:

$$\left(G+dG\right)+N_{CO_2}aA_c dz+N_{H_2O}aA_c dz-G=0$$

$$\Downarrow$$

$$\frac{dG}{dz}=-\left(N_{CO_2}+N_{H_2O}\right)aA_c$$

Component mole balance for CO_2:

$$\left(G+dG\right)\left(y_{CO_2}+dy_{CO_2}\right)-Gy_{CO_2}+N_{CO_2}aA_c dz=0$$

$$Gdy_{CO_2}+dGdy_{CO_2}=-N_{CO_2}aA_c dz-dGy_{CO_2}$$

using the total mole balance for the gas phase and inserting for dG

$$Gdy_{CO_2}+dGdy_{CO_2}=-N_{CO_2}aA_c dz+y_{CO_2}\left(N_{CO_2}+N_{H_2O}\right)aA_c dz$$

and neglecting the product $dGdy_{CO_2}$ gives

$$\frac{dy_{CO_2}}{dz}=\frac{N_{CO_2}aA_C\left(y_{CO_2}-1\right)+N_{H_2O}y_{CO_2}aA_c}{G}$$

Following the same procedure for water gives:

$$\frac{dy_{H_2O}}{dz}=\frac{N_{H_2O}aA_C\left(y_{H_2O}-1\right)+N_{CO_2}y_{H_2O}aA_c}{G}$$

The energy balance of the gas phase, neglecting the product, $dGdT$ and assuming that the heat capacity is constant in the temperature range covered, can be written:

$$\left(G+dG\right)\left(T_G+dT_G\right)c_{p,G}+N_{CO_2}c_{p,CO_2}aA_cT_G dz+N_{H_2O}c_{p,H_2O}aA_cT_G dz+qdz-GT_Gc_{p,G}=0$$

$$dGT_Gc_{p,G}+GdT_Gc_{p,G}+N_{CO_2}c_{p,CO_2}aA_cT_G dz+N_{H_2O}c_{p,H_2O}aA_cT_G dz+qdz=0$$

$$-\left(N_{CO_2}c_{p,CO_2}+N_{H_2O}c_{p,H_2O}\right)aA_cT_G dz+GdT_Gc_{p,G}+\left(N_{CO_2}c_{p,CO_2}+N_{H_2O}c_{p,H_2O}\right)aA_cT_G dz+qdz=0$$

Resulting in the expression

$$\frac{dT_G}{dz}=-\frac{q}{Gc_{p,G}}$$

Where q is the heat transfer between the gas and the liquid phase and is given by:

$$q=haA_c\left(T_G-T_L\right)$$

Liquid Phase Mass and Heat Balances

Carbamate forming reaction

$$CO_2 + 2R_2NH \rightleftarrows R_2H_2^+ + RCOO^-$$

Carbamate formation is the main reaction of CO_2 and a primary or secondary alkanolamine when loading is less than approximately 0.48. As it can be seen in the reaction CO_2 and an alkanolamine are the only reactants, and there are only two products which both are ionic. The changes in concentration of reactants and products can be related to the rate of absorption of CO_2, N_{CO2}, by stoichiometry as shown in equation (3.28) where the mole fraction of chemically bound CO_2 in the bulk of the liquid phase is X_{CO_2} $(= x_{RCOO^-})$. Total mole balance for the liquid phase taking account of the chemical reaction and assuming that no CO_2 exists in molecular form in the bulk of the liquid:

$$L + \left(N_{CO_2}(2-1-1) - N_{H_2O}\right) aA_c dz - (L + dL) = 0$$

$$\Downarrow$$

$$\frac{dL}{dz} = -N_{H_2O} aA_c$$

Due to the fact that there is no net increase in total moles in the liquid phase when CO_2 is transferred over the phase boundary where it reacts and forms a new compound, only vaporization or evaporation of water contributes to the change in total liquid flow in moles. Component mole balances for the liquid phase carried out in the same fashion as the gas phase. The mole fraction of chemically bound CO_2 is equal to the mole fraction of carbamate:

$$\frac{dX_{CO_2}}{dz} = \frac{\left(N_{H_2O} x_{CO_2} - N_{CO_2}\right) aA_C}{L + dL}$$

$$\frac{dx_{H_2O}}{dz} = \frac{N_{H_2O}\left(x_{H_2O} - 1\right) aA_C}{L + dL}$$

Bicarbonate forming reaction

$$CO_2 + R_3N + H_2O \rightleftarrows R_3NH^+ + HCO_3^-$$

As it can be seen in the reaction CO_2 and an alkanolamine are reactants, and there are only two products. The changes in concentration of reactants and products can be related to the rate of absorption of CO_2, N_{CO2}, by stoichiometry as shown in equation (3.29) where the mole fraction of chemically bound CO_2 in the bulk of the liquid phase is X_{CO_2} $(= x_{HCO_3^-})$.

Total mole balance for the liquid phase taking account of the chemical reaction and assuming that no CO_2 exists in gas form in the bulk of the liquid:

$$L+\left(N_{CO_2}\left(1+1-1-1\right)-N_{H_2O}\right)aA_c dz-(L+dL)=0$$

$$\Downarrow$$

$$\frac{dL}{dz}=-N_{H_2O}aA_c$$

As seen in the overall reaction water is a reactant, thus the absorption of CO_2 plays part in the change of the mole fraction of water.

$$\frac{dX_{CO_2}}{dz}=\frac{\left(N_{H_2O}x_{CO_2}-N_{CO_2}\right)aA_C}{L+dL}$$

$$\frac{dx_{H_2O}}{dz}=\frac{\left(N_{H_2O}\left(x_{H_2O}-1\right)+N_{CO_2}\right)aA_C}{L+dL}$$

The energy balance including absorption for CO_2 in the liquid, ΔH_{CO_2}, as well as the heat of condensation of water, ΔH_{H_2O}, is included, the product *dLdt* is neglected and assuming that the heat capacity is constant in the temperature range covered, Furthermore assuming that water and CO_2 leaves the gas at T_G:

$$LT_L c_{p,L}-\left(L+dL\right)\left(T_L+dT_L\right)c_{p,L}-N_{CO_2}c_{p,CO_2}aA_c T_G dz-N_{H_2O}c_{p,H_2O}aA_c T_G dz$$
$$-qdz+N_{CO_2}\Delta H_{CO_2}+N_{H_2O}\Delta H_{H_2O}=0$$

$$-dLT_L c_{p,L}-LdT_L c_{p,L}-N_{CO_2}c_{p,CO_2}aA_c T_G dz-N_{H_2O}c_{p,H_2O}aA_c T_G dz-qdz$$
$$+\left(N_{CO_2}\Delta H_{CO_2}+N_{H_2O}\Delta H_{H_2O}\right)=0$$

$$-\left(-\left(N_{CO_2}c_{p,CO_2}+N_{H_2O}c_{p,H_2O}\right)\right)aAcT_L dz-LdT_L c_{p,L}-\left(N_{CO_2}c_{p,CO_2}+N_{H_2O}c_{p,H_2O}\right)aA_c T_G dz-qdz$$
$$+\left(N_{CO_2}\Delta H_{CO_2}+N_{H_2O}\Delta H_{H_2O}\right)=0$$

$$\left(N_{CO_2}c_{p,CO_2}+N_{H_2O}c_{p,H_2O}\right)aAcT_L dz-LdT_L c_{p,L}-\left(N_{CO_2}c_{p,CO_2}+N_{H_2O}c_{p,H_2O}\right)aA_c T_G dz-qdz$$
$$+\left(N_{CO_2}\Delta H_{CO_2}+N_{H_2O}\Delta H_{H_2O}\right)=0$$

$$-LdT_L c_{p,L}+\left(N_{CO_2}c_{p,CO_2}+N_{H_2O}c_{p,H_2O}\right)\left(T_L-T_G\right)aA_c dz-qdz+\left(N_{CO_2}\Delta H_{CO_2}+N_{H_2O}\Delta H_{H_2O}\right)=0$$

$$\frac{dT_L}{dz}=\frac{\left(N_{CO_2}c_{p,CO_2}+N_{H_2O}c_{p,H_2O}\right)aA_c\left(T_L-T_G\right)}{Lc_{p,L}}-\frac{q}{Lc_{p,l}}+\frac{\left(N_{CO_2}\Delta H_{CO_2}+N_{H_2O}\Delta H_{H_2O}\right)}{Lc_{p,l}}$$

Appendix C. Density of a Loaded AMP Solution

When analyzing the loaded AMP solutions from the pilot plant experiments, the densities at room temperature were measured using a scale and an automatic pipette. The results are presented in Table C-1.

Table C-1. Experimental data for the density of a loaded 2.9 M AMP solution at 20°C.

Loading	Density (kg/m^3)
0.072	998
0.084	1000
0.096	1001
0.116	1005
0.121	1003
0.133	1009
0.136	1004
0.141	1009
0.147	1005
0.151	1005
0.169	1005
0.171	1011
0.178	1012
0.210	1019
0.219	1016
0.226	1020
0.233	1019
0.246	1019
0.272	1030
0.283	1021
0.284	1030
0.302	1032
0.309	1030
0.326	1037
0.347	1035
0.367	1035
0.376	1043
0.398	1044
0.399	1044
0.407	1038
0.425	1043
0.459	1051
0.479	1051

In Figure C-1 the experimental density data are plotted as a function of liquid CO_2 loading and a straight line is fitted to the data using a least squares regression. As expected the liquid density increases with increasing loading. From the equation for the straight line the density of an unloaded 2.9 M AMP solution is found to be approximately 988 kg/m^3. This is slightly lower compared to the value found, 996 kg/m^3, when using the expression for the density of aqueous

solutions of AMP found in Xu et al.[1]. But the result of the extrapolation to zero loading is satisfying.

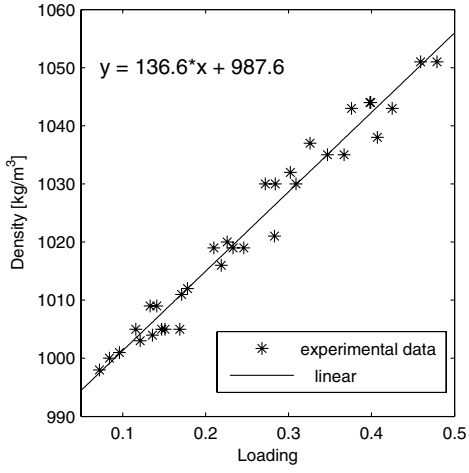

Figure C-1. Density of a 2.9 M AMP solution as a function of liquid loading at 20°C.

[1] Xu S, Otto FD, Mather AE. Physical Properties of Aqueous AMP Solutions, J. Chem. Eng. Data. 1991;36:71-75.

Appendix D. Experimental Data for the Desorber Heat Loss

Table D-1. Experimental data used for the calculation of the heat loss from the desorber.

	1	**2**	**3**	**4**
Flow Rate (l/min)	4	4	4	4
Reboiler duty (kW)	10.0	10.0	4.0	4.0
Pressure reboiler (bar)	1.81	1.61	1.29	1.27
Flow condensate stripper to reboiler (kg/h)	~9	10.5	2.2	2.1
Temperature TI-06 (°C)	108	107	101	101
Temperature TI-08 (°C)	12	13	14	14
Temperature TI-11 (°C)	117	113	106	106
Temperature TI-12 (°C)	115.6	112.3	105.7	105.4

Appendix E. List of Publications

International Peer-Reviewed Journals

1. Gabrielsen J., Svendsen H.F., Michelsen M.L., Stenby E.H., Kontogeorgis G.M., Experimental Validation of a Rate-Based Model for CO_2 Capture using an AMP Solution, Accepted for publication in *Chem. Eng. Sci.* (Available online)
2. Gabrielsen J., Michelsen M.L., Stenby E.H., Kontogeorgis G.M., Modeling of CO_2 Absorber Using an AMP Solution. AIChE J. 2006; 52:3443-3451.
3. G.K. Folas, J. Gabrielsen, M.L. Michelsen, E.H. Stenby, G.M. Kontogeorgis, Application of the Cubic-Plus-Association (CPA) Equation of State to Cross-Associating Systems. Ind. Eng. Chem. Res. 2005;44:3823-3833.
4. Gabrielsen J., Michelsen M.L., Stenby E.H., Kontogeorgis G.M., A Model for Estimating CO_2 Solubility in Aqueous Alkanolamines. Ind. Eng. Chem. Res. 2005;44:3348-3354.

International Conferences Oral Presentations

1. Gabrielsen J., Svendsen H.F., Michelsen M.L., Stenby E.H., Kontogeorgis G.M., Pilot Plant Studies and Modeling of CO_2 Capture Using an AMP Solution, Proceedings of AIChE Annual Meeting, San Francisco, USA, 12th-17th November, 2006.
2. Gabrielsen J., Michelsen M.L., Stenby E.H., Kontogeorgis G.M., CO_2 capture from coal fired power plants, Proceedings of 1st Symposium MT0EP, Leptokarya Pieria, Greece, 20th – 22nd June, 2005.

International and National Conferences Poster Presentations

1. Gabrielsen J., Michelsen M.L., Stenby E.H., Kontogeorgis G.M., Modeling of Randomly Packed CO_2 Absorber Using an Alkanolamine Solution, Proceedings of 22nd ESAT 2006, Elsinore, Denmark, June 28- July 1 2006.
2. Gabrielsen J., Michelsen M.L., Stenby E.H., Kontogeorgis G.M., Modeling of Randomly Packed CO_2 Absorber Using an Alkanolamine Solution, Proceedings of GHGT-8, Trondhiem, Norway, 12th-22nd June, 2006.
3. Gabrielsen J., Michelsen M.L., Kontogeorgis G.M., and Stenby E.H., Modelling of Randomly Packed CO_2 Absorber Using an Alkanolamine Solution, Proceedings of Dansk Kemiingeniør Konference, Kgs. Lyngby, Denmark, 31st May -2th June 2006.

4. Gabrielsen J., Michelsen M.L., Stenby E.H., Kontogeorgis G.M., Modelling of CO_2 Absorption with Chemical Reaction in Packed Columns, presented at the 4th Nordic Mini-symposium on CO2 Capture and Storage, Espoo, Finland, Sept. 8-9, 2005.
5. Gabrielsen J., Michelsen M.L., Stenby E.H., Kontogeorgis G.M., A model for estimating CO_2 in aqueous alkanolamines, Proceedings of 21st ESAT 2005, Jurata, Poland, June 1-5 2005.
6. Gabrielsen J., Michelsen M.L., Kontogeorgis G.M., and Stenby E.H., CO_2 Capture from Coal Fired Power Plants, Proceedings of Dansk Kemiingeniør Konference, Kgs. Lyngby, Denmark, 24th-26th May 2004